2008:38

DOCTORAL THESIS

Wet clutch tribological performance optimization methods

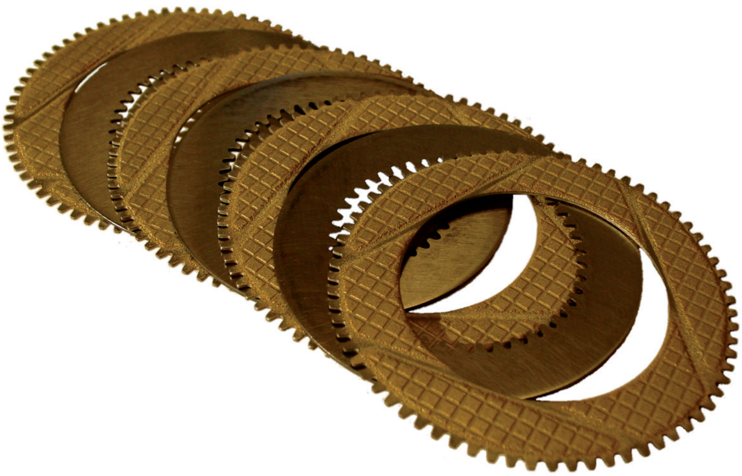

Pär Marklund

Luleå University of Technology
Department of Applied Physics and Mechanical Engineering
Division of Machine Elements

2008:38 | ISSN: 1402-1544 | ISRN: LTU-DT -- 08/38 -- SE

2008:38

WET CLUTCH TRIBOLOGICAL PERFORMANCE OPTIMIZATION METHODS

PÄR MARKLUND

Luleå University of Technology
Department of Applied Physics and Mechanical Engineering,
Division of Machine Elements

2008 : 38 | ISSN : 1402 – 1544 |ISRN:LTU-DT--08/38--SE

Cover figure:	Wet clutch friction discs and separator discs from a Limited Slip Differential.
Title page figure:	All Wheel Drive unit for cars. - Limited Slip Differential mounted in the rear axle of a vehicle.

WET CLUTCH TRIBOLOGICAL PERFORMANCE OPTIMIZATION METHODS

ISSN: 1402-1544
ISRN: LTU-DT--08/38--SE

This document was typeset in LaTeX 2_ε

.

Preface

This thesis comprises my research carried out at the Division of Machine Elements, Luleå University of Technology. Now that this thesis is presented I hope it will be of interest. Carrying out postgraduate research is interesting and inspirational, yet involves setbacks and late working hours. The research has, however, mostly provided favorable experience because of all my colleagues at the Division of Machine Elements and I would like to thank all of them for the time we have been working together.

I would like to thank my supervisors, Professor Roland Larsson and Professor Erik Höglund, for their guidance and encouragement in my work. Their knowledge and experience in the field have been very helpful in the discussion and planning of my research as well as in its execution. I would also like to thank my co-worker in the ProViking Interface program, Dr Fredrik Sahlin, for his technical and moral support and for collaboration in many graduate courses.

This research has been carried out in collaboration with the companies Haldex Traction Systems and Statoil Lubricants. I thank my colleagues at these companies for guidance regarding the industrial relevance of my work as well as for our technical discussions. I am also grateful to the Swedish Foundation for Strategic Research (SSF) and the Program Board for Automotive Research (PFF) for financial support.

Finally, this work has only been possible with the support and encouragement from my family and friends: I thank them all for having made this thesis possible.

Pär Marklund

Pär Marklund

Luleå, September 2008

Abstract

Wet clutches are used in a variety of machinery such as in vehicles where they are used to distribute torque in the drivetrains. Clutches can be located in automatic transmissions or in limited slip differentials. The frictional behavior of a clutch is of great importance for overall vehicle behavior and has to be thoroughly investigated when designing new wet clutch applications. Frictional behavior is normally studied in test rigs where whole friction discs or complete clutches are tested under similar working conditions to those pertaining to the clutches in the drivetrain of the vehicle. However, today clutch behavior may be simulated with regard to some clutch applications and design of the clutch system is not limited to testing. This is an advantage as it is possible to simulate behavior that may not be possible or suitable to study in a test rig. Another advantage is that the design process is faster and more cost efficient than that which is possible when all tests are carried out in a laboratory.

The torque transferred by the clutch during engagement can roughly be divided into full film torque and boundary lubrication torque. Full film torque originates from the part of the engagement where the clutch discs are completely separated by a lubricant film and the friction surfaces are not in contact, whereas boundary lubrication torque occurs when the lubricant film is so thin that the surfaces of the clutch discs are in direct contact, only separated by a thin additive film. The distribution between full film torque transfer and boundary lubrication torque transfer differs for different types of wet clutch and for differing operating conditions. When the clutch works in full film regime it is possible to simulate the friction quite well. However, the friction in the boundary lubrication regime is much more difficult to model and simulate since it is very dependent on the additives.

Wet clutches are most commonly used in automatic transmissions for vehicles. As a result, most research into wet clutch testing and most simulations concerns wet clutches suitable for such applications. In an automatic transmission the wet clutch is often used to brake a rotating shaft to stand still relative to

another shaft and the total engagement has a duration of fractions of a second. During most of the engagement the clutch is working in full film lubrication.

In this thesis the focus is on wet clutches working under limited slip conditions: in other words this thesis studies clutches that are working with a small amount of slip over a long period without reaching a state of lock-up. These clutch types can be found, for example, in limited slip differentials. During this type of engagement the clutch mainly works under boundary lubrication conditions and much heat can be generated.

The optimum method of designing a new wet clutch would be to simulate the clutch performance without having to do any measurements in the laboratory. This, however, is not yet possible, but an efficient way to design clutches can be achieved by combining simple measurements with efficient computer simulations.

In this thesis, simple measurement techniques for wet clutch materials are developed and combined with a temperature simulation of a wet clutch, where the lubricant cooling flow, which is dependent on the surface roughness and groove pattern, is simulated. This method makes it possible to optimize a wet clutch for given working conditions with regard to lubricant, friction material, surface roughness and groove pattern. The simulations are validated to measured data from a test rig in which torque behavior from whole friction discs are investigated. Good agreement between simulations and measurements is achieved.

Contents

Appended Papers

[A] **P. Marklund, R. Mäki, J. Jang, M. M. Khonsari, R. Larsson and E. Höglund.**
Thermal influence on torque transfer of wet clutches in limited slip differential applications.
Tribology International, 2007 May; vol. 40, no. 5, p. 876-884.
This paper describes a simulation model of a wet clutch working under boundary lubrication conditions. The friction coefficient used was measured in a wet clutch test rig and was dependent on sliding velocity, temperature and nominal surface pressure. The simulation model was developed by Pär Marklund and the experimental work and development of the boundary lubrication friction model was carried out by Rikard Mäki. The paper was written jointly by Pär Marklund and Rikard Mäki.

[B] **P. Marklund and R. Larsson.**
Wet clutch friction characteristics obtained from simplified Pin on Disc test.
Tribology International, 2008; vol 41, issues 9-10, Nordtrib 2006, p. 824-830.
In this paper a simplified method to measure the boundary lubrication friction coefficient of friction materials used in wet clutches was developed. The friction coefficient was measured on a small test specimen mounted in a pin on disc set-up. The small test specimens imply small variations regarding sliding velocity and contact temperature, which makes the measured friction coefficient suitable to use as input data in simulation models. The development of the measurement method and all experimental work was carried out by Pär Marklund who also wrote the paper. Roland Larsson was involved in the discussion and evaluation of the method.

[C] **P. Marklund, R. Larsson and T. S Lundström.**
Permeability of sinter bronze friction material for wet clutches.
Tribology Transactions, 2008 May; vol. 51, Issue 3, p. 303-309.
The permeability of wet clutch friction materials of sintered bronze was measured in this paper. The method and test rig was developed by Staffan Lundström and all experimental work was carried out by Pär Marklund. All authors were involved in the discussion of the results from the measurements and in some extent in the writing of the paper. The paper was mainly written by Pär Marklund.

[D] **P. Marklund, K. Berglund and R. Larsson.**
The influence on boundary friction of the permeability of sintered bronze.
Tribology Letters, 2008 July; vol. 31, no. 1, p. 1-8.
The boundary lubrication friction coefficient was measured with the test method developed in Paper B for the friction materials tested in the permeability measurement in Paper C. The original idea for this investigation was formulated by Pär Marklund. Most of the experimental work was carried out by Kim Berglund and the analyze of the results and writing of the paper was carried out mainly by Pär Marklund. All authors were in some extent involved in the writing of the paper.

[E] **P. Marklund, F. Sahlin and R. Larsson.**
Modeling and simulation of thermal effects in wet clutches operating under boundary lubrication conditions.
To be submitted for publication in a journal.
All results from paper A-D were used to create the simulation model developed in this paper. The model includes temperature simulation in 3D and boundary lubrication friction coefficient measured in a pin on disc set-up according to Paper B. Permeability for the friction material were accounted for in the boundary lubrication friction measurement. Flow simulations with a homogenized Reynolds equation with a flow factor approach were used in the model. This paper shows a possible way to optimize a wet clutch system with simulation models and simplified general measurements. The research and writing of the paper was mainly carried out by Pär Marklund. The model used for solving the homogenized Reynolds equation was developed by Fredrik Sahlin in cooperation with colleagues from the Division of Machine Elements and the Division of Mathematics at Luleå University of Technology. Roland Larsson contributed to the discussions of the model and to the writing of the paper.

Additional publications not included in the thesis

[1] **A. Almqvist, S. Glavatskih, R. Larsson, P. Marklund, F. Sahlin, J. Dasht, L-E. Persson, P. Wall.**
Homogenization of Reynolds equation.
Research report / Department of Mathematics, Luleå University of Technology, 2005; vol. 2005:03 Luleå. 20 pages.
This research report investigates the applicability of homogenization as a tool to study the influence of surface topography on liquid film formation and pressure build up in hydrodynamically lubricated bearings. The theory was mainly developed by Andreas Almqvist, Johan Dasht and Peter Wall. Most of the work in the section about numerical results and grid convergence was carried out by Fredrik Sahlin and Pär Marklund. Other authors contributed to the work with discussions about the content and to the writing of the report.

[2] **P. Marklund and R. Larsson.**
Wet clutch at limited slip conditions -Simplified testing and simulation.
Proceedings of the Institution of Mechanical Engineers, Part J: Journal of Engineering Tribology, 2007; vol. 221, no. 5, p. 545-551.
This paper is a development of the earlier work in Paper A. The difference is that the boundary lubrication friction model from Paper B was used in the simulation model and the cooling flow in the clutch was simulated. The development of the simulation model was carried out by Pär Marklund. Roland Larsson was involved in discussions about the model. The paper was mainly written by Pär Marklund.

[3] **F. Sahlin, R. Larsson, P. Marklund, P. Lugt and A. Almqvist.**
A mixed lubrication flow factor model treating measured surface roughness.
To be submitted for publication in journal; Enclosed as paper E in Fredrik Sahlin's thesis: "Lubrication, contact mechanics and leakage between rough surfaces", Luleå University of Technology, Sweden, 2008, ISSN:1402-1544 ; 2008:26, p. 131-188.
This paper presents a simulation model for mixed lubrication in the interface between three-dimensional measured surface roughness. The model is based on an approach of using a homogenized Reynolds equation. The model considers linear elastic perfectly plastic surface displacement and is based on computing flow factors that incorporate the effects of the surface topography in all lubrication regimes. Fredrik Sahlin carried out the numerical analysis and simulations and wrote most of the paper. Pär Marklund and Fredrik Sahlin carried out the flow measurements used in the validation of the simulation model. Pär Marklund wrote the section about the experimental setup for the flow measurements.

Nomenclature

Variables

A	Area	$[m^2]$
α	Heat transfer coefficient	$[W/m^2K]$
δ	Displacement	$[m]$
ε	Thermal expansion coefficient	$[1/K]$
η	Dynamic viscosity	$[Pas]$
μ	Friction coefficient	$[-]$
ν	Poisson ratio	$[-]$
ω	Rotational speed	$[rad/s]$
ω_1	Rotational speed of friction disc	$[rad/s]$
ω_2	Rotational speed of separator disc	$[rad/s]$
ρ	Density	$[kg/m^3]$
θ	Angle	$[rad]$
c_p	Specific heat capacity	$[J/kgK]$
E	Young's modulus	$[Pa]$
E'	Composite Young's modulus	$[Pa]$
F	Force	$[N]$
G	Convolution kernel	$[m/N]$

h	Film thickness	$[m]$
K	Permeability	$[m^2]$
k	Thermal conductivity	$[W/mK]$
L	Load	$[N]$
m	Mass	$[kg]$
n	Revolutions per minute	$[rpm]$
p	Pressure	$[Pa]$
Q	Flow	$[m^3/s]$
q	Mass flow	$[kg/s]$
Qe	Heat flux	$[W/m^2]$
r	Radius	$[m]$
T	Temperature	$[^\circ C]$
t	Time	$[s]$
Tq	Torque	$[Nm]$
u	Velocity in r-direction	$[m/s]$
V	Volume	$[m^3]$
v	Velocity in θ-direction	$[m/s]$
W	Energy	$[J]$
w	Velocity in z-direction	$[m/s]$
w	Width	$[m]$
x	Cartesian spatial coordinate	$[m]$
y	Local coordinate	
z	Thickness	$[m]$

Superscripts

$\bar{}$	Mean value

Subscripts

abs	Absorbed
amb	Ambient
ax	Axial direction
bl	Boundary lubrication
cs	Cross section
c	Contact
cd	Core disc
d	Disc
e	Elastic
f	flow direction
fl	Friction lining
$fluid$	Lubricant film
$fric$	Friction
gen	Generated
hyd	Hydrodynamic
i	Node number in r-direction
in	Inner
int	Interface
l	Node number in z-direction
max	Maximum value
min	Minimum value

n	Normal direction
oil	Oil (Lubricant)
out	Outer
p	Plastic
p	Plastic
r	Radial direction
sd	Separator disc
$sump$	Oil sump
z	Thickness direction

Acronyms

AT	Automatic Transmission
ATF	Automatic Transmission Fluid
HLSC	Haldex Limited Slip Coupling
LS	Limited Slip
LSC	Limited Slip Coupling
LSD	Limited Slip Differential

Part I

Comprehensive Summary

Chapter 1

Introduction

The world, as we know it, is governed by a large number of natural laws which we take for granted every day. These can be obvious, such as gravity or the friction force between the shoe and the ground. The same rules also influence the performance of complex machine components as the rest of this thesis will demonstrate.

If an ordinary car is analyzed the complexity of a modern standard vehicle will soon become apparent. When considered, it is almost a wonder that it starts every morning and transports people to work without having to undergo service more often than once every ten thousands kilometers or so. The service interval has been extended during the development of the modern car and many services almost merely include a change of motor oil. This is quite a difference compared to cars fifty years ago which had to have the motor oil changed and have joints, hinges, wheel suspensions, etc. greased every couple of thousands kilometers or so. The cars also had to undergo different mechanical adjustments frequently.

Even so, a modern car is not optimized with regard to every tiny detail. Cars today are of course much safer when involved in collisions, have better performance and handling, and the driver's environment is much better, yet no revolutionary changes in fuel consumption, or in how the driver manoeuvres the vehicle, have been developed over the past 50 years. Newly developed cars today also often suffer from various malfunctioning components, both mechanical and electrical, because the rapid design process often forces the engineers to leave problems that are unresolved in order to start the production of a new model. New, higher demands on the appearance of vehicles and the fact that new models last for a shorter and shorter time before they are considered out of fashion imply increasing demands on efficient methods for designing vehicles. At the same time demands on the environmental friendliness, handling and comfort further increase the demands on the technical development of the vehicles. These problems can be solved with more efficient methods for designing and optimizing the vehicle components.

When the first real cars were developed in the late 19th century many of the mechanical components were not optimized at all. The development process mostly involved the Edisonian approach, or trial and error as it is also called. This means that the components were first manufactured and then tested in order to see if they really worked as intended in the application. How much trial and error, *i.e.* how many malfunctions and re-designs that were necessary before the components had sufficient performance, depended a lot of the knowledge and mechanical skill of the designer. Often a solution which was proven to work in earlier applications was used again in new designs without knowing in detail *why* it had worked earlier.

During the development of the modern car it soon became important to also know *why* and *how* it worked and not only *that* it worked. This led to research within different areas, but over a long period of time the designers had to rely on much testing and trial and error which is an expensive and time consuming process. It also often does not give all the answers regarding the function of the components because of the complexity of the tests and the difficulty in imitating a real application.

Later, computers became useful when designing vehicles. They were a great help in the modeling of components and when making drawings. They also soon started to be useful in various kinds of simulations, such as crash impact simulations and Multi Body Analysis. Without these simulations the cars would not have been as safe and maneuverable as they are today. These simulations made it possible to reduce trial and error to some extent and to reduce the testing of the vehicles, and made remaining testing more fruitful. It is important to note that a simulation can be very useful even if it does not give a 100% correct answer, precisely as is the case with laboratory testing. As long as the models show the same trends as the real applications they can be used in the product development process to increase the performance of the components. One great advantage with simulations is that parameter studies can be easily carried out because one parameter can be changed without changing the others. This can be very difficult to achieve in test rigs since different parameters often are coupled which makes it difficult to change only one property of the total system.

However, there are areas where simulations are still on the starting block. One of these areas is tribology, *i.e.* the science of wear, friction and lubrication.

When designing mechanical components involving tribological phenomena, which nearly all mechanical components do involve, traditionally almost all investigations have been experimental and often based on trial-and-error. This have made the tribological development slower than in many other fields. In the last couple of years, however, more and more simulation models have been developed and used in the field of tribology, but there is still much more to do. Tribology is a complicated field because it consists of several other sciences such as solid mechanics, contact mechanics, fluid mechanics, thermodynamics, chemistry, material science and physics. This makes tribology simulations extremely complicated and the tribological contact difficult to model. Simulation in combination with simple standardized measurement methods can, however, lead to satisfying results and a higher level of understanding than tribological modeling and measurements can on their own.

The different ways in which a modern car usually fails can be divided into solid mechanical, electrical, corrosive, and tribological ways, of which the latter is one of the most common. Certainly, as mentioned earlier, service intervals have been extended and more lubricated contacts are made filled-for-life, *i.e.* the components are lubricated when manufactured and then supposed to work during the entire lifetime of the vehicle. However, there remain problems with *e.g.* non-working steering knuckles and front suspensions, etc., so there is still much to improve. Recent demands on more fuel efficient, lighter and more durable vehicles have further increased the need for tribological research. One important step here would be to work with a combination of theoretical investigations, such as computer simulations, and experimental investigations to reduce the need of trial-and-error to a minimum. This would lead to better, more environmentally friendly and safer vehicles in a foreseeable future.

In this work the combination of computer simulation models and simplified tribological measurements are used to describe a possible effective design and optimization method for one type of machine component, a wet clutch. The function of the wet clutch is very interesting from a tribologist's point of view and more details of wet clutches are shown in the short introduction in section 3. The lack of simulation models for boundary lubrication contacts makes simulations of wet clutches difficult since wet clutches often work under both full film, mixed and boundary lubrication conditions. Here a systematic method for designing and optimizing a wet clutch system for Limited Slip applications is developed. A wet clutch in a Limited Slip application is working fully engaged for a long time with a low relative sliding speed between the friction surfaces. Good agreement with results from other more common wet clutch measurement methods is achieved.

Chapter 2

Tribology

The first time the expression "Tribology"' was mentioned was in the "Jost Report" [1] published by the UK's Department of Education and Science in 1966. Tribology was defined as "the science and technology of interacting surfaces in relative motion and of the practices related thereto". In other terms, tribology is the science of friction, wear and lubrication. Tribology has always been an important field of research, but it was after the "Jost Report" that tribology started to be recognized as a separate science, even though tribology is an interdisciplinary science in which materials science, chemistry, physics, fluid dynamics, solid mechanics, etc., are important components. The importance of the field of tribology can be illustrated by the fact that tribologically induced losses are of the order of 5 % of GNP [2] as several surveys in industrialised countries have indicated, implying that even small advances in tribology can lead to very large total savings if applied around the world.

There are several ways to distinguish between different branches of tribology, one of them being between dry and lubricated tribology.

Dry contacts are used where the use of lubricants due to high temperatures, or a vacuum is not possible. It is also used where contamination by a lubricant is not acceptable, such as in machines used in the food or fabric industry. Another area where dry contacts are common is in applications where a large friction coefficient is desired, such as in a disc brake or a friction clutch.

In lubricated contacts some kind of lubricant is used in the sliding interfaces to reduce friction and wear and to keep the tribological interface cool. The lubricated contact is often sealed to prevent lubricant leakage, hence reducing consumption of lubricants and preventing contamination of the surroundings. Lubricated interfaces can operate in various tribological regimes depending on the working conditions, such as load, L, sliding velocity, v, and other system parameters, such as fluid viscosity, η. Different lubrication regimes are often distinguished by analyzing the contact with the help of a Stribeckcurve, named after R. Stribeck who is the author of the classic papers [3] about properties of different types of bearings. A schematic Stribeck curve is shown in Fig. 2.1. At low speeds and high loads the friction coef-

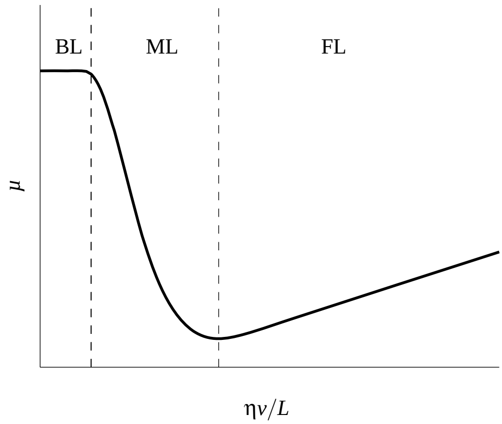

Figure 2.1: Schematic Stribeck curve

ficient, μ, is very dependent on the additives in the lubricant and is normally relatively high and does not vary much. This tribological regime is called boundary lubrication and is marked with "BL" in Fig. 2.1. In the mixed lubrication regime, marked with "ML" in Fig. 2.1, the hydrodynamic pressure starts to build up a lubricant film between the sliding surfaces and in full film lubrication, "FL", the lubricant film is so thick that the surfaces are completely separated. It is often possible to model the tribological behavior for a system working in full film lubrication rather well by solving the Reynolds equation, derived by Osborne Reynolds [4] in 1886. This is a thin film approximation of the more general Navier Stokes equations [5, 6]. The Reynolds equation is not applicable in mixed or boundary lubrication, where the fluid flows are much more complicated and the behavior is much dependent on asperity contacts and lubricant additives.

2.1 Interface

The word "Interface" can have many different meanings, depending on in which area it is mentioned. One explanation of the word is "A means or place of interaction between two systems, organizations, etc." according to the Oxford English Dictionary [7]. In this thesis interface refers to the tribological interface between two solids which are sliding against each other in relative motion. Depending on which tribological problem is being studied there are varying requirements with regard to the complexity of the description of the interface. The problem can be of such simplification that a constant friction coefficient may be applied between the two surfaces. In other cases description of the interface may require thermal or wear effects, etc.

If the interface is simulated the description of the interface should not be of greater complexity than that required for the simulation since the complexity of the interface has a major impact on the time required for computation. This induces the same problems in tribological simulations as in other simulations, such as those in solid mechanics and computational fluid dynamics. The simulation models ideally should be fast, stable, easy to use and at the same time be accurate enough to provide reliable solutions.

Many tribological simulations still today have to rely on input data from measurements. The friction coefficient for a system working in boundary or mixed lubrication, see Fig. 2.1, is especially difficult to simulate and is often necessary to measure in a test rig. However, in order to make the most use out of a friction coefficient measurement it is important to make the measurement as general as possible so it can be used in a variety of simulations. If the friction measurement is made to only correspond to a certain geometry or shape of the interacting solids it limits the areas in which it can be used in simulations.

Chapter 3

Wet clutch technology

This chapter is a brief introduction to the subject of wet clutches and comprises information from paper A - E and other publications. It can be a good help for the reader who is not experienced in the field to utilize the content in the rest of this thesis.

A clutch is a machine component used to transfer torque in different types of machinery. The clutch transfers torque when it is engaged; when disengaged it transfers no torque. When the clutch is engaged, torque is transferred by the frictional forces in the sliding interfaces in the clutch. The clutch can, therefore, transfer torque when the in shaft and the out shaft of the clutch rotate at different speeds. The frictional behavior of the clutch is of great importance with regard to clutch performance.

The principal difference between a clutch and a brake is that both surfaces in a clutch are moving and one of them is driven by the other, whilst in a brake one of the surfaces is stationary, which creates a braking torque.

In most clutch applications high torque transfer is favored. Torque behavior is also extremely important since it influence the behavior of the entire machine of which it is a part. To be able to transfer as much torque as possible and build small clutch units with high power density it is essential to have a high friction coefficient in the sliding interface. However, a high power density can lead to a high wear-rate in the sliding interface, hence decreasing the service life of the clutch. The change in surface roughness due to wear can also influence the frictional forces and make the clutch more difficult to control. Therefore the main research areas regarding clutches focus on the frictional behavior and wear of the sliding interfaces in the clutch.

Depending on the working conditions of the clutch, it can be designed as a wet or dry clutch. A dry clutch works in the surrounding air and a wet clutch works in a lubricant. For applications with much slippage over a long period a wet clutch is preferable since the lubricant in which the clutch is immersed cools the clutch. Since the friction coefficient in the sliding interface is lower for a wet clutch than for a dry clutch, a wet clutch is often built of several clutch discs in a "clutch pack" as shown in Fig. 3.1. The many discs imply many sliding interfaces and high torque transfer is therefore attainable. In

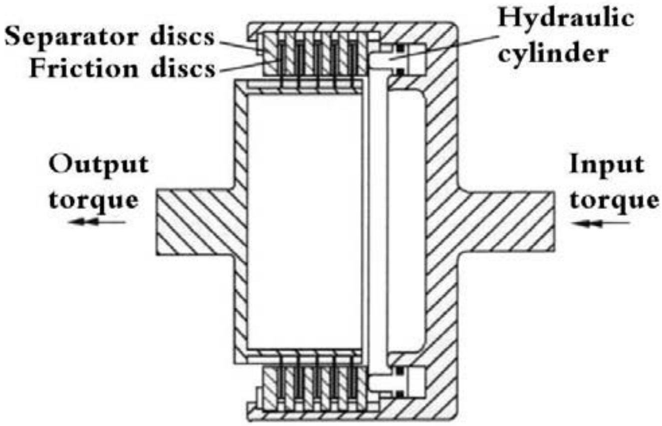

Figure 3.1: Schematic Wet Clutch

the clutch in Fig. 3.1 there are two kinds of discs: friction discs attached to the inner shaft by splines; and separator discs connected to the outer shaft by splines. The friction discs are made of a steel core discs with a friction material attached on both sides, and the separator discs are made of plain steel. The clutch is engaged by applying a normal force on the sliding interfaces from the hydraulic cylinder. This normal force is often referred to as axial force, or load, due to the common disc layout of the wet clutch such as shown in Fig. 3.1. When the friction discs and separator discs are pressed together the clutch transfers torque from the input shaft to the output shaft. The normal load applied by the hydraulic cylinder in Fig. 3.1 can be applied from various types of actuators in different clutch applications such as mechanical or electromechanical actuators. When the clutch is disengaged, the shafts are free to rotate independently apart from a slight drag torque due to viscous shear forces in the lubricant between the discs.

An advantage with a wet clutch over a dry clutch is that it works in a well-defined and relatively clean environment. This makes the clutch easier to control with an automatic control system, which is often the case in most wet clutch applications.

3.1 Applications

Wet clutches are used in a variety of machines and especially to distribute torque in vehicle drive-trains. The frictional behavior of wet clutches in the drive-trains of vehicles greatly influence the overall behavior of the vehicle and should therefore be studied in depth when designing new wet clutch systems. Wet clutches are often used in Automatic Transmissions (ATs) where they are used to shift gear ratios in the transmission. During the engagement of an AT clutch, the difference in rotational speed between the discs is normally quite high, and the clutch is thus working during quite a large part of the engagement in full film lubrication, see Fig. 2.1. At the end of the engagement, when the working conditions of the clutch change to mixed and boundary lubrication, it is important that the lock up of the clutch is smooth and without vibrations. When the clutch is fully engaged and has reached a state of lock-up no difference in rotational speed between the discs is allowed. The manufacturers of todays ATs are increasing the number of clutches in the transmission since more gears can reduce the fuel consumption of the vehicle and smoothen the ride for the driver. The increasing number of clutches used in the AT introduce new problems since the increased drag torque will create more frictional losses, warm up the AT-system and increase the fuel consumption of the car. More detailed information concerning the working principles of ATs is written in an introduction to automatic transmissions by Y. Kato and T. Shibayama [8].

Wet clutches are often used in motorcycles where engine, clutch and transmission are built together as one complete unit which gives a more compact engine-drive train. The working conditions of a motorcycle clutch is similar to a clutch in an AT. The time of engagement is short and no slippage is allowed when fully engaged. The motorcycle clutch is an application where the driver operates the wet clutch directly with a mechanical or hydraulic system without the use of an automatic control system.

Wet clutches can in some applications have much longer engagement time and work mainly in the boundary lubrication regime. This is normally the case for Limited Slip Differentials (LSDs). One such application is the Haldex Limited Slip Coupling (HLSC), see chapter 3.1.1. The measurement techniques and simulation models developed in this thesis have been applied to the HLSC as a control to check that the developed methods work in reality.

3.1.1 Haldex Limited Slip Coupling (HLSC)

The Haldex LSC [9, 10] is the main component in an All Wheel Drive system (AWD) for vehicles. The HLSC features an electronically controlled, disc-type wet clutch mounted between the propeller shaft and the rear differential of the vehicle. The torque transfer to the rear axle of the vehicle is controlled with a wet clutch. The clutch is actuated by an axial hydraulic engagement force generated from a hydraulic pump driven by the speed difference between the front and rear axles of the vehicle; see the schematic figure of the HLSC in Fig.3.2. The axial force is controlled with the throttle valve shown in Fig.3.2.

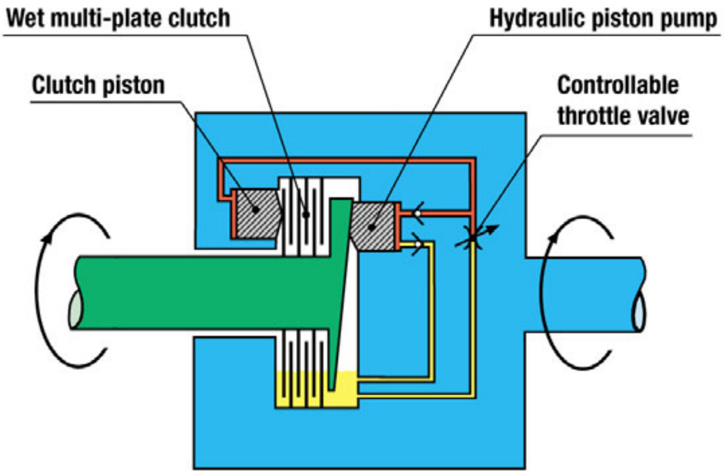

Figure 3.2: Schematic figure of the Haldex Limited Slip Coupling, generation 1-3.

Since the torque to the rear axle is controllable, this type of AWD system has several advantages over traditional transmission systems. The activation and deactivation of torque transfer to the rear axle is very fast, allowing the system to work in cooperation with other vehicle control systems, such as the Anti-lock Braking Systems (ABS) and the Electronic Stability Program (ESP). The system is also insensitive to differences in wheel size of the vehicle due to tire dimensions or air pressure, which can make other AWD systems malfunction.

To obtain a high power density while still keeping the cost down, a sintered bronze friction material is used in combination with separator discs made of hardened steel, see Fig. 3.3.

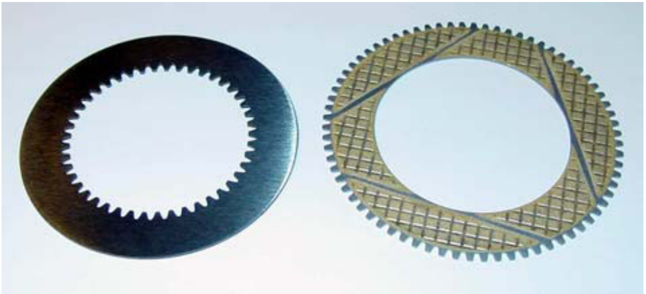

Figure 3.3: Separator- and friction disc.

The lubricant used in this application is a tailor-made semisynthetic fluid with a special additive formulation suitable for limited slip wet clutches with a friction material made of sintered bronze. More information about this lubricant is found in [11](fluid C).

Typical operating conditions for this clutch is a sliding velocity lower than 0.5 m/s and a mean surface pressure exceeding 4 MPa.

3.2 Lubricants for wet clutches

Lubricants for wet clutches are very complex products and since the boundary lubrication friction behavior is of great importance the additive formulation of the lubricant can be complicated. The complexity of a lubricant suitable for a wet clutch depends on the high demands on the frictional behavior of the clutch. Many applications where a wet clutch lubricant is used not only consist of the clutch itself, but often in addition a variety of different gears, bearings and seals, which further complicates the fluid formulation. A lubricant used in wet clutches also need to have high shear stability due to the constant shear stress between the clutch discs. The working conditions and frictional behavior vary for different types of wet clutch applications. Hence wet clutch lubricant standards are developed for different types of applications, see section 3.2.1 to 3.2.3.

3.2.1 Automatic Transmission Fluid (ATF)

ATFs are some of the most complex standardized lubricants in the automotive industry. The ATF is normally the only lubricant present in the AT and has a variety of tasks to cope with. An AT is often filled for life so the ATF has to work during the whole service life of the transmission. This demands both high oxidation stability and shear stability. The fluid also has to minimize the friction in bearings and gears and reduce drag torque in the clutch, see section 3.6, and also give a high and stable friction coefficient in the wet clutch. In some ATs the ATF also has to act as hydraulic fluid. To cope with all these tasks the additivation of the ATF is very important and an example of additives used in an ATF is shown in Table 3.1 [12, 13].

Table 3.1: Examples of additives for ATF's

Additive	*Representative Compounds*	*Influence on friction*
Anti-oxidant	Alkyl phenol, aromatic amine *	
Dispersant	Metal sulfonate, alkenyl succinic acid amide, organic boron compounds	Significant
Detergent	Phenate, sulfonate	Significant
VI improver	Poly-methacrylate, poly-isobutylene, poly-alkylstyrene	
Friction modifier	Fatty acid, amide, amine, polymerized phosphoric acid ester	Significant
Anti-wear agent	Phosphate, acid phosphate, sulfidized oil fat, organic sulfur or chlorine compounds *	Significant
Metallic deactivator	Organic sulfur compounds, organic nitrogen compounds *	
Rust preventer	Metal sulfonate, fatty acid, amine	Significant
Corrosion inhibitor	Perchlorinated metal sulfonate *	
Seal swelling agent	Phosphate, aromatic compounds, chlorinated hydrocarbon	
Anti-foaming agent	Silicone oil	
Coloring agent	Azo-compounds	

** ZDTP was often used in earlier fluid formulations but not in modern formulations since it is known to cause blockage trouble in the pores of the friction material, hence reducing its permeability [12].*

The special properties of the lubricants developed for ATFs have resulted in a variety of standards for wet clutch lubricants. Different manufacturers have different standards such as Dexron (General Motors), Mercon (Ford) and JASO (Japan Automobile Service Organisation). The Dexron standard is the oldest and was introduced by GM in 1967 while Ford introduced the Mercon standard in 1987 [14]. This was, however, quite long after the first Automatic Transmission Fluid (ATF) was introduced (General Motors 1949) and was a response to the higher demands on the Automatic Transmissions compared to the manual transmission at that time. Newer developed variants of these standards are still used today for ATFs but the newer JASO standard was developed in the mid-nineties [13].

Different ATF standards complicate the handling of lubricants in different applications and there is an obvious benefit if these standards could be united. It has been shown that it is possible to formulate lubricants which follow both Japanese and American standards [15]. The international Lubricant Standardization and Approval Committee (ILSAC) ATF subcommittee have initiated an effort to reconcile different standards [16].

3.2.2 Motorcycle lubricants

Many motorcycles have the engine, transmission and clutch built together as one compact unit. Hence the lubricant used in the motorcycle has to work as a lubricant for both the engine, the transmission and the wet clutch. This creates a requirement for a lubricant with special properties. It is important that the clutch has good friction performance for easy and smooth clutch control by the driver. The lubricant formulation should also prevent the clutch discs from sticking together when not used for a longer period of time while still transfer enough torque, *i.e.* have a high enough friction coefficient, when the clutch is in use.

Motor cycle lubricant is standardized according to a JASO standard regarding the motorcycle engine/transmission oil.

3.2.3 Fluids for Limited Slip Differentials

Wet clutches in Limited Slip Differentials (LSDs) often work with high surface pressures and low sliding speeds during long engagement times. Such working conditions are quite different from those that apply for an ATF or motorcycle lubricant and they demand a different kind of fluid. The fluids developed for LSDs can also, if mounted in the rear axle of a vehicle, be required to lubricate hypoid gears which demand a transmission fluid of API-grade GL 5.

Today it is quite common to use tailor made lubricants for LS clutches instead of standardized LS lubricants. One example where the standardized fluids do not work satisfying is the Haldex Limited Slip Coupling described in section 3.1.1 and further explained in [9, 10].

3.3 Friction discs and separator discs

The use of separate friction discs and separator discs in the clutch pack, as shown in Fig. 3.1, is the most common configuration. In such a configuration the friction disc is built up of a core disc made of hardened carbon steel with a friction material attached on both sides, and it is thus called a double-sided friction disc. The separator discs in such a wet clutch are often made of hardened carbon steel similar to the core disc. One example of a friction disc and a separator disc from a double-sided wet clutch is shown in Fig. 3.3. The friction material is essential for the frictional behavior of the clutch and is described in more detail in section 3.4.

Another configuration of the clutch discs is single-sided friction discs. In a clutch with single-sided friction discs all discs have friction material attached on one side of the core discs. Hence, one side of the core disc is working as separator disc surface in contact with the friction material of the neighboring friction disc. No separator discs are therefore needed in the clutch. Every other disc has an inner or outer spline in a similar arrangement as in the double-sided configuration to be able to transfer torque between two connecting shafts. One disadvantage with the single-sided configuration is that the difference in heat conduction ability and heat expansion of the core disc and friction material can lead to serious thermal issues such as coning of the friction discs. This is one reason why double sided friction discs are favored in wet clutch applications.

In some applications there is no need for special friction materials and the clutch pack is built up of simple steel discs without friction material attached. This is the case in some Limited slip differentials with low power density.

3.4 Friction materials

A variety of friction materials are used in wet clutch applications. The most important property for the friction material is the frictional behavior together with a suitable lubricant.

3.4.1 Material groups

The largest group of friction materials for wet clutches comprise paper-based materials. Paper-based materials are frequently used and especially in Automatic Transmissions for vehicles. The low cost of these friction materials is one important factor in their popularity. Paper-based friction materials have been used since the late 1950s and work well under low load conditions. The first materials all contained asbestos, but in the 1970s the use of asbestos became strictly regulated and the asbestos fiber was replaced by pulp or organic synthetic fiber. The increasing demand of smaller and more efficient ATs with higher power density later on led to the replacement of paper materials with natural pulp fiber and phenol resin by more heat resistant paper made of organic synthetic fiber and some more heat resistant resin [17].

Other friction materials for wet clutches are sintered bronze, carbon fiber, aramid fiber and cork (aramid is commonly known by its trademark Kevlar®). Also, new types of hybrid materials have been developed which are processed in similar ways as paper-based materials, but reinforced with carbon or aramid fibers in combination with organic or synthetic fibers. SEM pictures of a hybrid friction material reinforced by carbon fiber and a friction material of sintered bronze are shown in Fig. 3.4. The reinforcement carbon fibers of the hybrid material are the straight clear lines in the otherwise irregular paper structure. In more heavy duty applications materials such as sintered bronze, carbon fiber and hybrid materials are most common.

3.4.2 Mechanical properties

The mechanical properties of the friction materials, such as the Young's modulus, influence the behavior of the clutch. A lower Young's modulus can give a higher friction coefficient and higher power capacity according to Ohkawa [18].

3.4.3 Permeability

The permeability of the friction material or the ability for a lubricant flow inside the friction material can influence the engagement time of the clutch. The pores which make the friction materials permeable are visible in Fig. 3.4. The permeability is often used as input data in wet clutch simulation models where clutch engagements are investigated [19–24]. However, according to paper C the fluid flow inside the material can probably not have any significant effects regarding the temperature of the clutch. Paper C also shows that the groove

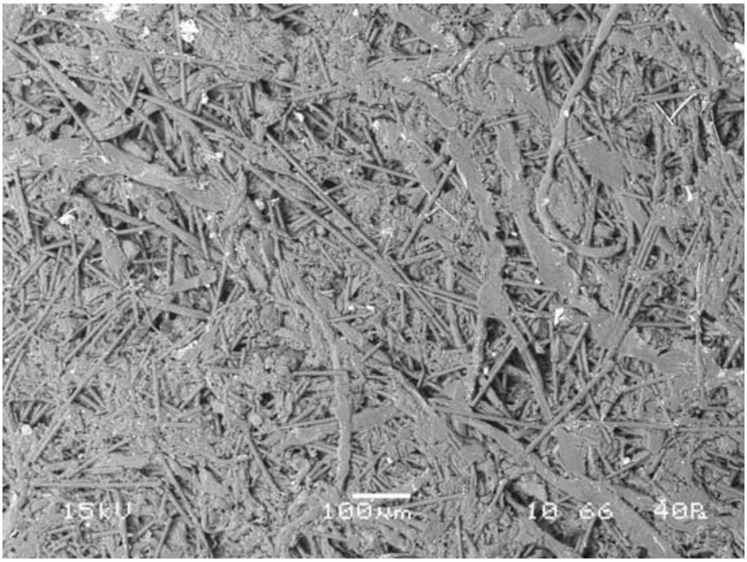

(a) Hybrid material reinforced with carbon fiber.

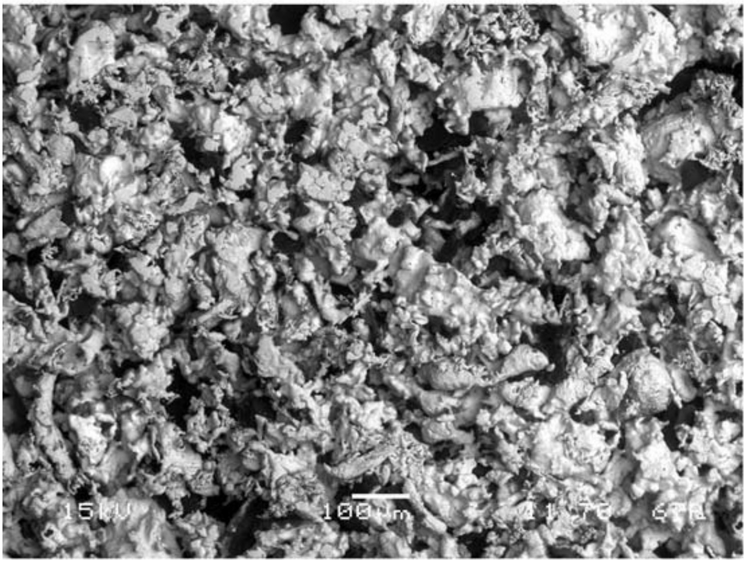

(b) Sintered bronze friction material.

Figure 3.4: SEM pictures of two different wet clutch friction materials. Magnification: 100X

patterns used on many friction discs, such as the groove pattern shown in Fig. 3.3, can seal off the friction material with almost non-permeable edges around the contact areas. This limits the lubricant flow inside the permeable material since no lubricant can flow through the groove edges. The investigation made in paper D showed that the boundary lubrication friction coefficient can be influenced by the permeability of the friction material. It also showed that the permeability strongly influences the ability of the clutch to work under starved lubrication conditions without suffering any damage by wear or undergoing a major change in frictional behavior.

3.4.4 Groove pattern

The friction lining surface often has some kind of groove pattern. One example of a groove pattern shaped like a "waffle-pattern" is shown in Fig. 3.3. The groove pattern has several functions. When the clutch is engaging, the grooves lead the fluid away from the sliding interface which decreases the time of engagement. When the clutch is engaged the grooves act as reservoirs for the lubricant and can supply the contact areas of the friction lining with lubricant, which is especially important in a limited slip application where the sliding contacts have to withstand continuous sliding for longer periods of time. The grooves also cool down the clutch since lubricant can flow through the grooves and transport heat away out of the sliding interface between the friction disc and separator disc.

3.4.5 Thermal conductivity

Thermal conductivity differs much between the various types of friction material. This influences the temperature in the clutch pack. A friction material with low thermal conductivity means that much of the generated heat increases the temperature in the separator disc and not in the friction disc. The behavior is the reverse for a friction material with high thermal conductivity. An example of a friction material with low thermal conductivity is a paper-based material and one example of a material with high thermal conductivity is a material made of sintered bronze.

3.5 Shudder and stick-slip in wet clutch systems

Shudder in wet clutch systems is friction induced torque variations similar to stick slip phenomenas for low sliding velocities. Shudder leads to noise and vibrations and decreased accuracy of the torque transfer, and can in some cases cause vibrations of such magnitude that the clutch system suffers permanent damage. Anti-shudder properties are generally examined with the friction-velocity relationship [25, 26]. The vibrations can be damped if a higher sliding velocity gives a higher friction coefficient, *i.e.* a positive slope on a friction-velocity curve. Three schematic friction-velocity curves are shown in Fig. 3.5. Here the frictional behavior given by Oil C is least likely to cause shudder since

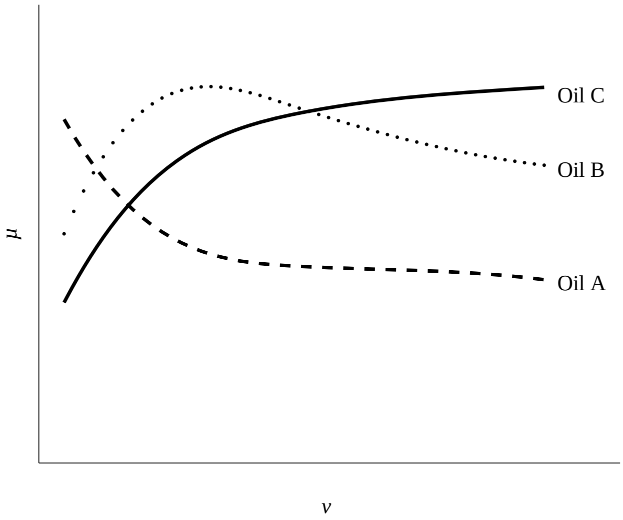

Figure 3.5: Schematic picture of the frictional behavior of three different wet clutch fluids.

the friction-velocity curve show a positive slope for all sliding velocities. Oil A shows a behavior which is likely to induce shudder for all sliding velocities, while Oil B can work properly for low sliding velocities, but not for high.

3.6 Drag torque

Drag torque is torque due to shear stress in the lubrication film between the clutch discs in a disengaged wet clutch. The torque transfer due to drag torque occurs when the clutch is disengaged and when torque transfer is not desirable. The aim is, therefore, to reduce drag torque as much as possible.

Drag torque is greatest at low temperatures when the viscosity of the fluid between the friction discs is high. Measurements [27] and simulations [28, 29] have been made to see which parameters affect the drag torque in a wet clutch. It is shown by Yuan et al. [29] that it is important that surface tension effects are included in simulation models for the simulations to agree with drag torque measurements. The reason for this is that the surface tension and capillary forces are important in retaining an oil film between discs in the clutch.

3.7 Wet clutch measurement methods and simulations

This section is a brief introduction to measurement methods and to simulation models for wet clutches.

3.7.1 Measurement methods

The frictional behavior of wet clutches is normally investigated in test rigs where complete friction discs are tested under similar working conditions as a clutch in an actual application.

A test rig frequently used to imitate the working conditions of an engagement clutch such as a clutch in an AT is the SAE II test rig, described in [30]. In the SAE II test rig a flywheel is accelerated to 3600 rpm and then a full clutch pack is used to brake the flywheel to stand still. This test is repeated several times a minute for as much as 100 hours to investigate the durability of the fluid. A low speed mode is also possible in a SAE II test rig. The low speed mode investigates the breakaway friction and the friction coefficient after a couple of seconds of continuous slip with 0.72 or 4.37 rpm difference in rotational speed between the shafts [16]. Other similar test rigs with a flywheel retardation are also used in laboratory tests.

For LS differentials other types of test rigs are usually suitable, such as the LS wet clutch test rig described by Mäki et al. [10]. In the LS wet clutch test rig the rotational speed and axial force are varied independently and the transfered torque can be investigated for a variety of axial loads and rotational speeds during a longer time of engagement.

Other more general and simplified friction measurements are made with smaller sections of a friction disc made in a pin on disc apparatus as in paper B and [30]. More about pin on disc measurements is found in section 7.

3.7.2 Simulation models

Testing is today not the only method available for investigating the behavior of a wet clutch as several simulation models have been developed to simulate wet clutches running under various working conditions. Simulations are advantageous as behavior may be simulated that cannot be measured in test rigs. Another advantage is that simulations can lead to a faster and less expensive design process than if all investigations are carried out in test rigs in a laboratory.

The most usual simulation approach is to study an engagement from a state of high rotational speed to a state of lock-up which corresponds to the working conditions of a clutch in an AT. Many simulation models have been developed to simulate the AT wet clutch engagement and good agreement with experimental data can be achieved [19–24]. During a clutch engagement the transmitted torque is a combination of viscous shear forces between the discs and contact friction forces.

Typically, the Reynolds equation is used to model the viscous torque and film thickness at the beginning of the engagement, followed by the application of a measured boundary lubrication friction behavior at the latter part of the engagement. To obtain satisfactory agreement with experimental data, it can be necessary to include an appropriate thermal model to take account of the change of fluid viscosity during engagement. Boundary lubrication friction, however, is often not compensated for temperature [22, 31–33].

These traditional clutch engagement models are generally not suitable for wet clutches in limited slip differentials, such as the HLSC. Since the wet clutch in a limited slip differential is often engaged at a rather low velocity, the torque computed with the full-film Reynolds equation is less relevant. In addition, it is not always desirable to reach a state of lock-up for a LSD, but rather to allow a controlled limited slip, thus transferring only a certain controlled torque. Since this limited slip time period can be long, a significant amount of heat might be generated, making it important that a boundary lubrication friction coefficient model that is temperature dependent is used. In papers A and E and [34] the temperature distribution in a LSD wet clutch is simulated. The simulated temperature in the sliding interface is used with the temperature dependent boundary lubrication friction coefficient to compute the boundary lubrication torque transfer of the clutch.

Chapter 4

Objectives

Wet clutches are important for the total performance of many modern vehicles. The clutches are located in many automatic or semi-automatic transmissions and can also be found in other parts of the drive-train such as limited slip differentials. In many types of construction equipment, such as wheel loaders, wet clutches are also frequently used along with wet brakes.

Demands from the vehicle industry force the manufacturers of wet clutch systems to continuously develop products more rapidly that are cheaper and more functional: thus increases the requirements for more efficient tools and methods regarding the development of new clutch systems.

"Classic" wet clutch test rigs, in which more complete clutch systems are tested, should be used as a complement to these tools as validation before the clutch is tested in an actual application. The aim of this thesis is, however, to minimize the need for time-consuming and expensive testing of complete wet clutch systems, and to make the required testing as well-planned and informative as possible.

The objective of this thesis is, therefore, to develop a systematic method which decreases the time needed for the design and optimization of a wet clutch application, as well as to expand knowledge of the working principles of a wet clutch. The method consists of simple tools such as simplified measurement techniques and simulation models which can increase the knowledge regarding the behavior of the clutch. The wet clutch design and optimization method is described in section 5 and the following sections 6 to 9.

The appended papers A to E describe the steps of the design and optimization method in more detail.

- Paper A shows how a measured boundary lubrication friction coefficient which is temperature dependent can be used in combination with a temperature simulation model of the clutch, in order to simulate the torque transfer of the clutch.

- Paper B describes a simple method to measure the friction coefficient for wet clutch friction materials using a pin on disc test rig.

- Paper C describes a method to measure the permeability of wet clutch friction materials.

- Paper D investigates how the boundary lubrication friction coefficient of wet clutch friction materials of sintered bronze is influenced by the permeability of the material.

- Paper E is a development of paper A where results and findings from paper A to D are used in combination with a developed 3D temperature simulation model of a wet clutch. The developed models simulates the temperature and the torque transfer of a wet clutch working under limited slip conditions.

Chapter 5

The design and optimization method

The usual approach when developing wet clutches is to perform a series of tests in test rigs using whole clutch discs or complete clutches. The advantage with these methods is that the test, if properly designed, will give a good indication of how the clutch system will work in an actual application. One major disadvantage with this approach is the expense incurred when tested disc geometry or material is changed, since new complete friction discs have to be manufactured in a small series before further tests can be conducted. This is time-consuming and expensive. The vast number of variables in such tests also makes it complicated, if at all possible, to reach an optimal design of the clutch.

It is unfortunately not possible today to omit all the testing of these components, nor will it be in the foreseeable future. The goal of this thesis is to reduce testing as far as possible. If simplified testing and simulations can be used to gain increased knowledge of the clutches, and to find the most suitable combination of materials, lubricants and clutch disc geometry, the testing needed in test rigs with whole clutch discs or complete clutches can be more efficient, hence reducing both time and expense. With simplified measurement methods the number of variables in the test is reduced which makes the methods suitable for optimization of the clutch. In combination with simulations the simplified measurement method makes it easier to isolate the effects of one variable, thus facilitating parameter studies.

The systematic method developed here to be followed when designing a wet clutch is divided into 5 steps:

1. Mapping system parameters. In this step all necessary data regarding material and working conditions needed for simulations and analysis of measurements are gathered.

2. Measurements of boundary lubrication friction coefficient. The velocity and temperature dependent friction coefficient is measured for a small sample of the friction lining in a pin on disc apparatus according to the method described in paper B.

3. Tribological simulations of a wet clutch. The type of simulation model used is dependent on the working conditions of the clutch and in what kind of application it is used.

4. Validation with measurements in wet clutch test rigs. The investigations are planned with the help of information from steps 1- 3 to be as efficient and fruitful as possible.

5. Implementation in full scale applications. Final testing of the wet clutch system before the product is released on the market.

In industry today steps number 2 to 3 are usually skipped, but if the design process is complemented with an extension of step 1 and expanded with step 2 to 3 more knowledge regarding the investigated clutch system is gained. A screening process of different materials, lubricants and disc geometries can also be carried out very quickly and more carefully prepared experiments can be carried out in steps 4 to 5. This makes final testing faster and more fruitful than if the design process starts at the more complicated tests of step 4.

This thesis focuses on the first steps in this design process, step 1, 2 and 3, and they are described in detail in following sections and papers. The clutch design process was applied to a wet clutch working under limited slip conditions. These working conditions require that different simulation models are used than the simulation models suitable for automatic transmission clutch types.

Chapter 6

Mapping system parameters

The gathering of data regarding all components in the investigated clutch may seem as an obvious step. However, when performing simulations of the system the importance of correct input data is far more important than if only measurements are conducted. The properties of the components in the clutch can be used for two reasons;

- To evaluate a certain property of the measured system when analyzing measurement data.
- To use as input data for simulation models.

A behavior of a measured system is of course the same whether the properties of the system are known or not. However, the system properties are important in order to evaluate different parameters and to be able to draw any well-founded conclusions regarding the behavior of the system. It is therefore up to the persons who are doing the measurements to decide how many of the system parameters they need to map to be able to make well-grounded conclusions. With a scientific approach where the focus is on reaching a higher level of understanding of the function of the system, an extensive investigation of the system parameters is needed. This differs from a trial and error investigation where the main focus is to see *if* the system works without needing to understand in detail *how* it works.

If simulation models are used to describe the behavior of the system it is very important to know all system parameters. A deterministic model gives one answer for each data set for which the model is used. All important properties, used in the model, have to be decided in advance for the model to work. This often leads to a more thorough investigation of the properties of the system if they are used as input to a simulation model compared to if the system is measured in a test rig.

However, the more extensive investigation of the system properties is also beneficial when conducting measurements since the system is better described, with the result that the analysis of the measured system can be better and there is less risk of forgetting important parameters in the analysis.

6.1 Young's modulus of the friction material

The Young's modulus of the friction material is needed mainly for the contact mechanics calculations involved in the flow calculations in paper E. Measurements of the Young's modulus of the friction material can be complicated. A compressive test is the most suitable test for measuring this property since the material behaves completely different under tensile stress than under compressive stress.

The friction lining on a friction disc is also often made with groove patterns which can increase or decrease the total stiffness of the friction lining depending on how the groove pattern is manufactured. Measurements on the friction discs used in the HLSC have shown that the groove type used makes the friction lining stiffer than the original lining. The groove pattern is pressed into the friction material which is made of sintered bronze, Fig. 3.3. To get an idea of the stiffness of the friction lining a small circular test specimen is cut out of a steel sheet covered with friction material, similar to the method used in paper B. The diameter of this specimen was, however, larger to be able to increase the load and reduce the influence of the resolution in the measurements.

6.1.1 Results from the Young's modulus measurements

The test specimen was loaded with a compressive load up to 1 kN in a tensile test machine . The presicion of the tensile stress machine used (Dartec 100) was ± 0.5 N and ± 4 μm. One calibration measurement was first performed with an empty machine without the test specimen. This made it possible to calculate the load-displacement curve for the test specimen alone and disregard the stiffness of the machine when measuring the stiffness of the test specimen. The measurements for one of the test specimens are shown in Fig. 6.1. The test specimen is compressed and released two times before the measurement series shown in Fig. 6.1 in order to eliminate the influence from a permanent plastic deformation of the friction material.

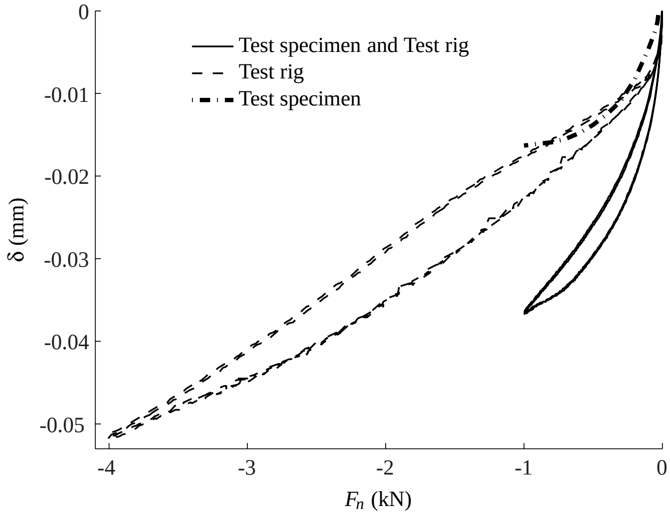

Figure 6.1: Stiffness of friction material measured in tension test rig. The measurement is shown with solid lines, a calibration measurement without a test specimen is shown with dashed lines and the stiffness of the test specimen compensated for the stiffness of the test rig is shown with a dash-dotted line.

The measurement shows a relatively large hysteresis in the deformation behavior. This behavior is also obvious when no test specimen is present, shown by the dashed line in Fig. 6.1. From the mean displacement from both the loading and unloading of both measurements the load-displacement curve for the test specimen alone is calculated, see the dash-dotted line in Fig. 6.1. This is used to calculate the Young's modulus for the friction lining. The Young's modulus is higher the more the test specimen is compressed. The highest load used in the measurement on the test specimens is 1 kN which corresponds to a nominal surface pressure of 5.7 MPa with the area of the test specimen used. At this maximum load the calculated Young's modulus is 6.1 GPa. A constant Young's modulus of 5.0 GPa is used as approximation of the Young's modulus in the simulation model in paper E where the nominal surface pressure varies between 3.9 and 9.7 MPa.

6.2 Permeability of the friction material

A permeability measurement method for wet clutch friction materials is developed in paper C. The test rig used in the measurements is originally designed by Lundström et al. [35] to measure permeability in various textile materials such as press fabric used in paper machines. The test cell in which the permeability is measured is shown in Fig. 6.2. This test cell is suitable for measuring

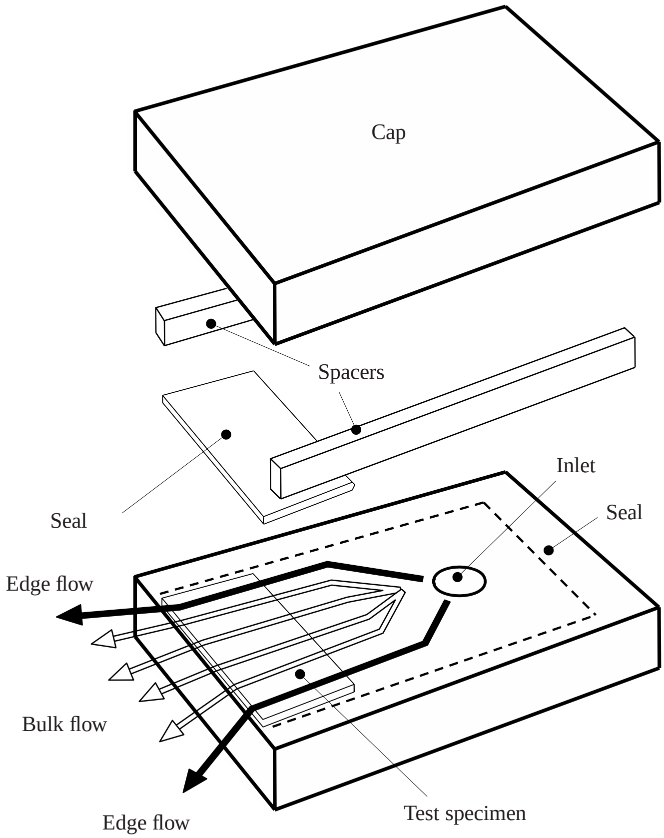

Figure 6.2: Schematic sketch of in-plane parallel flow test cell used to measure permeability in rectangular shaped test specimens.

permeability in wet clutch friction materials since the correct thickness and density of the material can be used. A drawback is that special test specimens have to be manufactured since it is not possible to use pieces from existing friction discs. This is a further disadvantage as it makes it impossible to measure permeability on a used friction material. In used friction materials the pores can be clogged by wear particles, contaminants and lubricant additives which can change the permeability of the material.

The mass flow through the material is measured by weighing the lubricant which passes through the material on a scale. To make sure that no possible leakage on the side of the test specimen is influencing the measurement, the edge flow is separated from the bulk flow. The bulk flow measurement is used when calculating the permeability of the material.

The configuration in Fig. 6.2 is designed so that only the flow inside the material is measured since the test specimen is completely sealed off between the holder and the cap. It is also possible to measure a combination of both the flow inside the material and in the interface between the friction material and the counter surface if the upper seal is changed to a smooth steel specimen. This flow can be of interest since it corresponds quite well with that of a wet clutch where the rough friction material surface is facing the smooth steel separator disc.

Results from permeability measurements are shown in Fig. 6.3. The per-

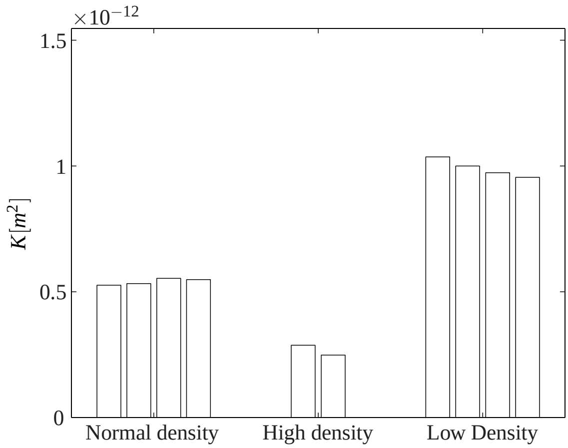

Figure 6.3: Permeability for friction material of sintered bronze with three different densities. (Paper C, Fig. C.8(a))

meability for friction materials with three different densities was measured. A friction material with high density is more compact and has less pores than a material with low density, which results in a lower permeability. Results from the permeability measurements are shown in detail in paper C.

6.3 Geometrical properties

Geometrical data are very important when describing a system. For wet clutches important geometrical data are, for example, the radius and the thickness of the discs, the thickness of the friction lining, the width and depth of the grooves, and the contact surface area without grooves. These data are easily measured on the clutch discs and can often be supplied by the manufacturer of the discs.

6.4 Thermal constants for the disc materials

It is important that all the material parameters used in the temperature simulations, such as specific heat capacity and thermal conductivity, are known. These material constants are often not easily measured and we often have to rely on the data presented by the manufacturer of the discs.

6.5 Fluid properties

The properties of the lubricant comprise bulk properties and additive properties. The bulk properties are viscosity, density, specific heat capacity, heat conduction and thermal expansion coefficient. Density and viscosity are especially temperature dependent and should therefore be described as a function of temperature. Some values of the fluid used throughout the experiments in this thesis are shown in Table 6.1.

Table 6.1: Fluid parameters

Parameter	**Value**
Viscosity, η	0.0296 Pas (at 40°C)
Density, ρ	855 kg/m^3 (at 40°C)
Specific heat capacity, c_p	2190 J/kgK
Heat conduction coefficient, k	0.131 W/mK
Thermal expansion coefficient, ε	$6.5 \cdot 10^{-4}$ 1/K;

Most additives are active when the clutch is working in boundary lubrication and the additives which influence the boundary lubrication friction coefficient are therefore of most interest. The measurement of the boundary lubrication friction coefficient is described in section 7.

6.6 Surface topography

In some tribological investigations it can be sufficient to describe the surface topography with basic surface parameters. However, often a more complex description of the surface is required. A good surface topography measurement in 3D is necessary in many simulation models such as the models used in paper E. This facilitates the use of the measurement in contact mechanics and flow dynamics simulations. Since the surfaces of the friction materials used in wet clutches normally have a high surface roughness width deep valleys and are rather soft an optical measurement method is preferable. For the work in this thesis, an optical profiler (WYCO NT1100) fulfills all requirements. The surface measurement may easily be exported as raw data to other softwares and may therefore easily be used in flow and contact mechanics calculations. An example of a surface measurement of a wet clutch friction material is shown in Fig. 6.4.

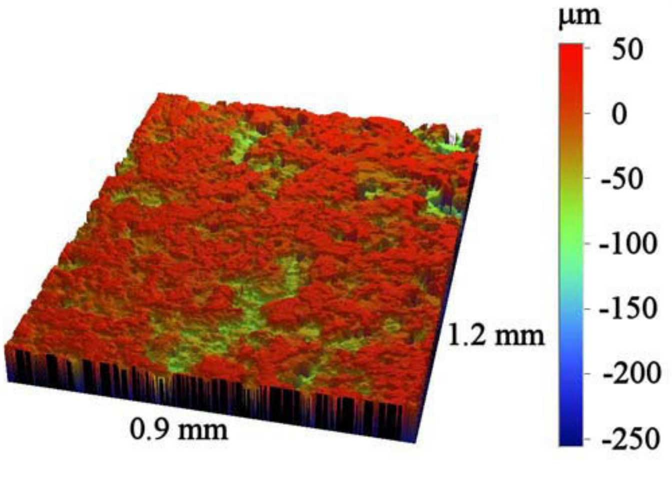

Figure 6.4: Surface roughness measurement of friction material of sintered bronze. Ra= 18.7 μm, Rt= 308 μm, Rsk= -1.26

Chapter 7

Measurements of the boundary lubrication friction coefficient for wet clutch friction materials

The aim of the measurement of the boundary lubrication friction coefficient is to measure the friction coefficient as a function of both sliding velocity and temperature. The friction coefficient should be measured for a tribological system that is as well-definedand simple as possible. In many measurement methods for wet clutches the friction coefficient is measured in test rigs in which whole friction discs or complete clutches are mounted. The friction coefficient is calculated from the measured transfered torque. This friction coefficient is thereby a mean friction coefficient since the temperature and sliding velocity in the sliding interface between the clutch discs is not constant. If the boundary lubrication friction coefficient is to be used in a simulation model of the clutch a more exact measurement is required. To meet these demands a measurement method was developed in paper B where the boundary lubrication friction coefficient was measured in a pin on disc apparatus on a small test specimen cut out from the original friction disc. A short summary of the measurement method based on paper B and paper D is given in this chapter together with the results obtained in these papers.

7.1 Pin on disc test

A pin on disc machine comprises a stationary pin which is facing a rotating disc according to the schematic sketch in Fig. 7.1. The machine used in these measurements was a Phoenix Tribology TE67. In paper B a method was de-

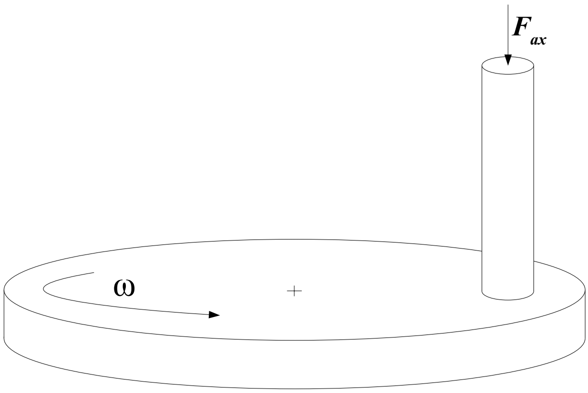

Figure 7.1: Schematic sketch of a pin on disc machine. With the method developed in paper B a small test specimen is mounted in the pin in contact with the rotating disc.

veloped to mount a small test specimen made from a wet clutch friction disc in the pin. The temperature was measured with a thermocouple mounted about 0.3 mm from the sliding interface through a hole in the back of the test specimen. The counter surface was made of the steel material used in the separator discs in the clutch. This gives a pin on disc setup with all the properties of an actual wet clutch.

7.2 Test specimens

The test specimens are cut out from a real friction disc using electrical spark-erosion. Spark-erosion is a good method for a material that conducts electricity since the method implies good tolerances and a small heat affected zone. A picture of the cut out test specimens is shown in Fig. 7.2 and part of the the original disc is shown in Fig. 7.3.

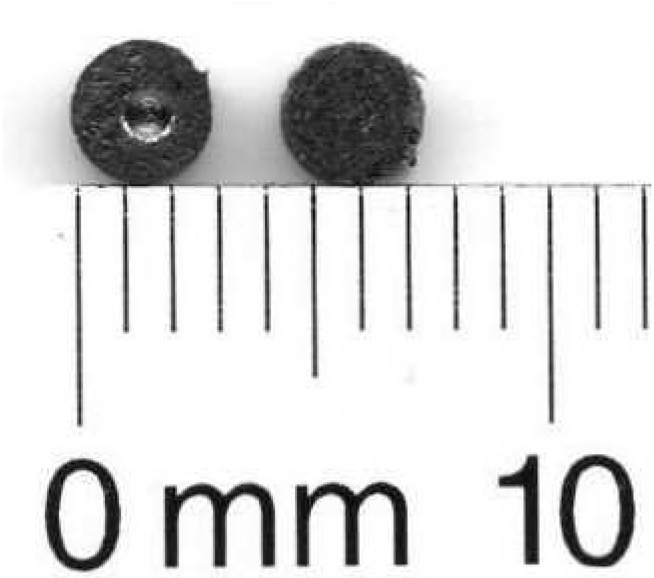

Figure 7.2: Test specimens from friction disc with a friction material of sintered bronze. Specimen to the left shown from the back where the hole for mounting the thermocouple is visible. (Paper B, Fig. B.3)

In paper D one part of the study was to investigate the influence of the permeability of the groove edge on the boundary lubrication friction behavior. To investigate this a new type of test specimen was manufactured where the edges were sealed off by pressing a groove pattern around the test specimen. This method was used since it was shown in paper C that pressed groove patterns in a friction material made of sintered bronze led to non-permeable groove edges. One test specimen with sealed edges and one with porous edges is shown in Fig. 7.4.

In paper D test specimens with differing permeability were also investigated to see the influence of the permeability on the boundary lubrication frictional behavior. These test specimens were cut out from the the test specimens used in the permeability investigation in paper C.

Figure 7.3: Friction disc from which the test specimens are cut out with spark-erosion.

Figure 7.4: Test specimens used in pin on disc tests in paper D . Left hand side: The edges of the test specimens are sealed by pressing a groove around the test specimen. The groove walls are non-permeable because the pores of the original material are compressed so no fluid can pass through the wall. Right hand side: porous edges. The contact area of both test specimens is circular with a diameter of 3.0 mm.

7.3 Test sequence

The investigations in papers B and D can be divided into two main groups depending on the lubrication conditions during the measurements, flooded lubricated running conditions and starved running conditions.

7.3.1 Flooded lubrication condition

In the tests with a flooded lubricated contact the disc and test specimen were completely submerged in lubricant. The boundary lubrication friction coefficient was measured at a sliding velocity that varied between 0-0.5 m/s, a temperature that varied between 22- 100°C and a nominal contact pressure that varied between 4.0- 8.0 MPa. The total test sequence consists of a number of measurements with differing initial temperatures during which the sliding velocity is increased from 0 m/s to 0.5 m/s, followed by a decrease in sliding velocity to standstill. Every measurement last for about 30 seconds. The first measurement starts at the ambient temperature. The difference in the initial temperature of the measurements is 5°C. The complete test series consists of 16 different measurements with different initial temperatures. After each measurement a heater is engaged to warm up the test equipment to the next required temperature level.

Measurements with flooded lubricated contacts were made in papers B and D and more detailed information concerning the measurement method, and the results from the measurements are shown in those papers.

7.3.2 Starved lubrication conditions

In paper D the tribological behavior of the friction material when running under starved lubricated conditions was investigated. Before the measurements the test specimens were impregnated with lubricant and no further lubricant was added during the measurements. To impregnate the test specimens they were put into lubricant and the surrounding pressure was decreased to an absolute pressure of about 10^4 Pa with a vacuum pump, making the air inside the pores exit the material. When the surrounding pressure was restored to normal atmospheric pressure the lubricant filled the pores of the friction material.

The measurements were divided into two separate tests. One test was similar to the test when the system was working under flooded lubricated running conditions, section 7.3.1, except from the lubrication conditions. The other test comprised a constant sliding velocity of 0.2 m/s for a period of 3 hours. More detailed information about these tests is given in paper D.

7.4 Results and discussion

One example of the boundary lubrication frictional behavior measured in the pin on disc is shown in Fig. 7.5. The friction coefficient increases with in-

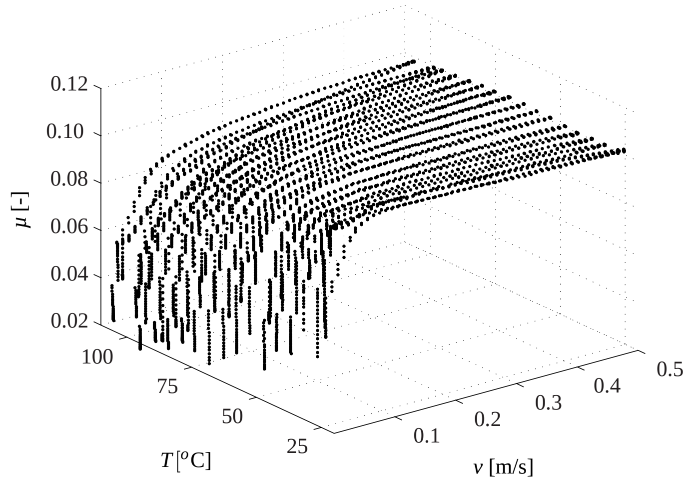

Figure 7.5: Friction coefficient as a function of the sliding velocity and the interface temperature. Nominal pressure = 8.0 MPa.

creased sliding velocity and decreasing temperature. To simplify the use of the measured friction coefficient in simulation models, a mathematical expression can be fitted to the measured data. Such an expression is developed in paper B,

$$\mu = a_1 + a_2 \cdot tanh(v \cdot a_3) + a_4 \cdot T + a_5 \cdot T^2 + a_6 \cdot T^3 + a_7 \cdot v + a_8 \cdot vT + a_9 \cdot (vT)^2. \tag{7.1}$$

In this equation μ is the friction coefficient, v is the sliding velocity and T is the interface temperature. The influence of the nominal surface pressure on the friction coefficient is not included in this equation since it was shown in paper B that influence is not large regarding the loading conditions studied. The friction coefficient according to this expression is shown with the mesh in Fig. 7.6, and as a function of sliding velocity for four different temperatures in Fig. 7.7.

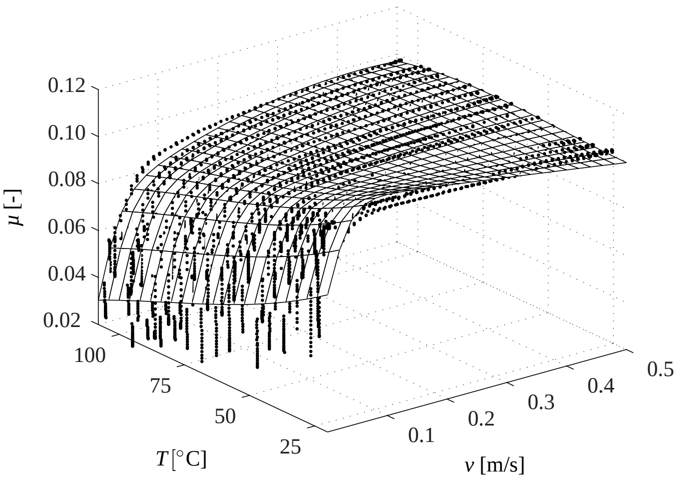

Figure 7.6: Friction coefficient as function of the sliding velocity and the interface temperature. Measured data and mesh according to Eq. 7.1. Nominal pressure = 8.0 MPa.(Paper B, Fig. B.6)

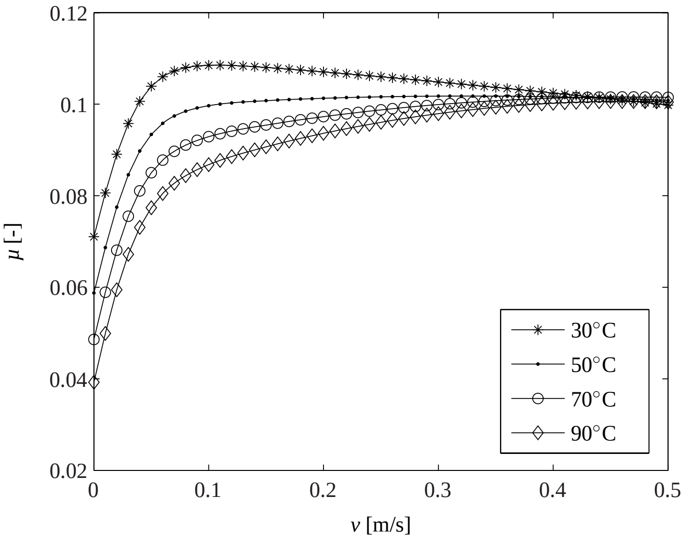

Figure 7.7: Friction coefficient as a function of the the sliding velocity at different interface temperatures. Based on Eq. 7.1. Nominal pressure = 8.0 MPa. (Paper B, Fig. B.7)

Since the friction coefficient for a wet clutch is usually measured in test rigs with whole friction discs and separator disc [10, 36]: the pin on disc method was compared to such a measurement method to see whether there was agreement between the two methods. Figure 7.8 shows a comparison between friction coefficient measured in a wet clutch test rig [10] and friction coefficient measured in the pin on disc set-up, both with a nominal contact pressure of 8.0 MPa. The two measurement methods shown in Fig. 7.8 show

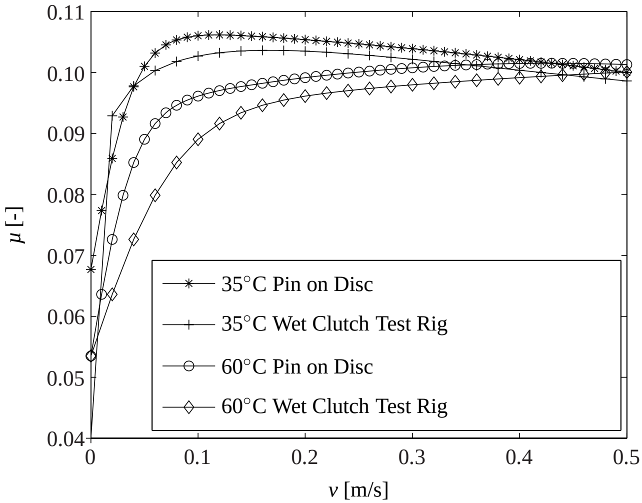

Figure 7.8: Comparison between friction measurements with a pin on disc set-up and with a wet clutch test rig [10]. Nominal pressure = 8.0 MPa. (Paper B, Fig. B.8)

similar frictional behavior throughout the whole range of sliding velocity and temperature. The friction coefficient is consistently slightly higher in the pin on disc measurements than in the wet clutch test rig measurements. The different measurement methods do, however, not measure exactly the same friction coefficient and might, therefore, well not give exactly the same friction coefficient characteristics. The friction coefficient from the wet clutch test rig is a mean friction coefficient calculated from the torque measurements in the test rig. The friction varies in the sliding interface between the friction disc and the separator disc due to differences in sliding velocity and temperature. In the pin on disc set-up both sliding velocity and temperature vary to a lesser degree, which means that the friction coefficient measured in the pin on disc is more suitable for use in simulation models than the friction coefficient measured in a wet clutch test rig.

7.4.1 Permeability influence on boundary lubrication frictional behavior

Paper D showed that the permeability of the test specimen influences the friction coefficient in boundary lubrication; Fig. 7.9. Higher permeability of the friction material implies a slightly lower boundary lubrication friction coefficient for a contact flooded with lubricant. The maximum standard deviation

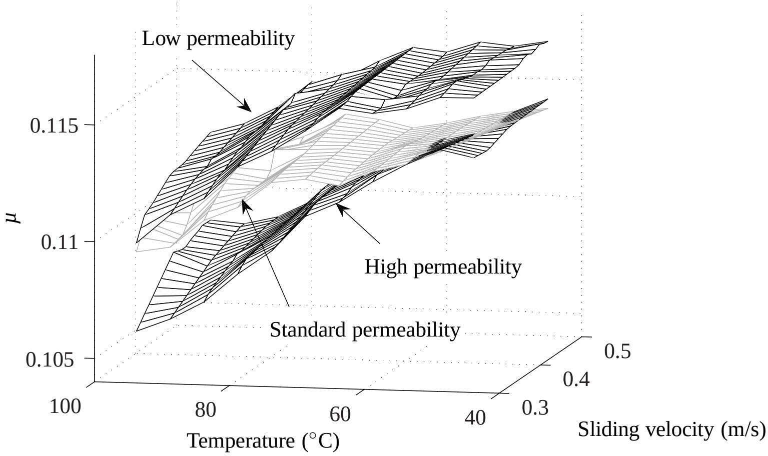

Figure 7.9: Frictional behavior of materials with different permeability for test specimens with porous edges. Each surface represents mean values calculated from two different measurements from test specimens with the same permeability. (Paper D, Fig. D.4)

for any value in the displayed area in Fig. 7.9 is 3.1%.

Paper D also showed an obvious influence of the permeability on the friction behavior when the test specimens were running under starved conditions for 3 hours. The most obvious difference in behavior occurs during the first ten minutes of the measurement, which is shown in Fig. 7.10. The figures show that pores influence the way a material of sintered bronze works under starved running conditions since the pores can act as reservoirs and supply lubricant to the otherwise dry contact. A material with high permeability is thus more durable and can work for a long time with an almost constant friction coefficient even though there is a shortage of lubricant. The friction coefficient increases when the lubricant from the pores is exhausted and no new lubricant is supplied to the contact. With all the lubricant exhausted from the pores the contact is working under dry conditions and the friction coefficient increases to a value between 0.15 and 0.2.

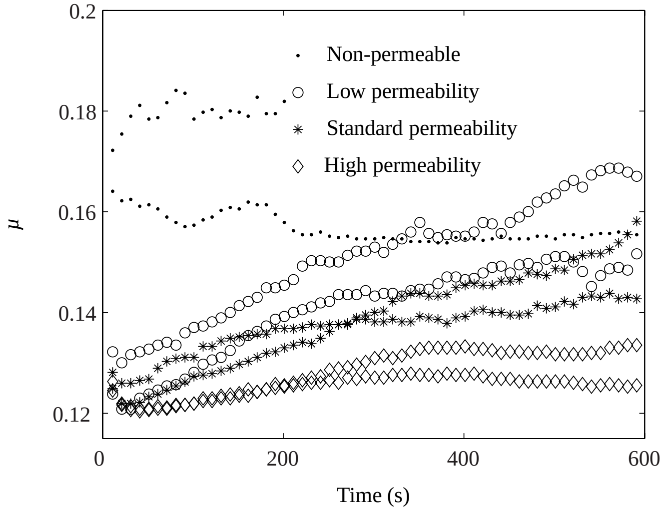

Figure 7.10: Comparison of the frictional behavior under starved conditions for test specimens with three different permeabilities and non-permeable test specimens. The first ten minutes of the 3h long measurements are shown. All test specimens have porous edges. (Paper D, Fig. D.6)

In paper D a similar 3h long starved investigation was also conducted for test specimens with sealed edges. A comparison of the frictional behavior for test specimens with sealed edges and test specimens with porous edges is shown in Fig. 7.11. Measurements on all test specimens with sealed edges except for one show that a constant friction coefficient when running under starved conditions is maintained. The friction coefficient for the test specimens with porous edges increases from the start of the test. The sealed edges of the test specimen facilitate the ability to retain the lubricant in the permeable material, which further improves performance when working under starved conditions. This shows that different manufacturing methods for the groove patterns on the friction disc can influence the behavior of the clutch when working under starved conditions since different ways of manufacturing the grooves causes the permeability of the groove walls to vary.

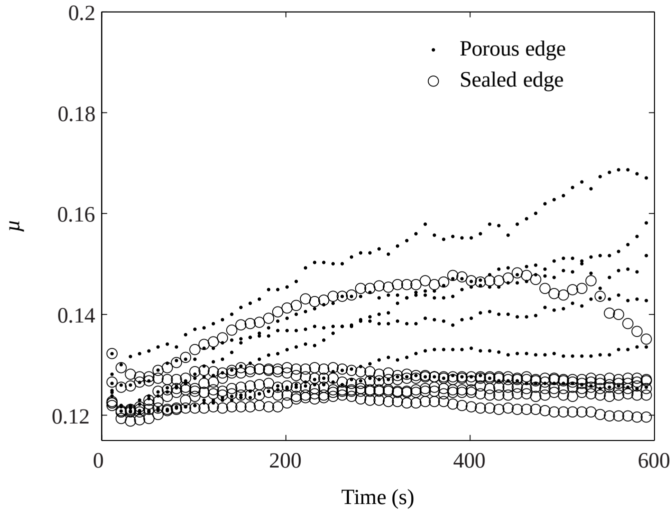

Figure 7.11: Comparison of the frictional behavior under starved conditions of test specimens with porous and with sealed edges. The first ten minutes of the measurement is shown. Test specimens with three different permeabilities are used. The measurements on test specimens with porous edges are the same measurements as in Fig 7.10. (Paper D, Fig. D.7)

7.5 Conclusions

It is possible to measure the boundary lubrication friction coefficient for a wet clutch friction material using a pin on disc apparatus.

The friction coefficient obtained is described with an mathematical equation dependent of sliding velocity and temperature. This equation is very suitable for use in wet clutch simulation models.

The boundary lubrication friction coefficient has been shown to be dependent on the permeability of the tested material.

The performance of a wet clutch working under starved conditions is very dependent on the permeability of the groove walls. The type of grooves used on a friction disc therefore influences the performance of the clutch when it is working with a shortage of lubricant.

Chapter 8

Tribological simulations of wet clutches

A common approach when developing wet clutches is to perform a series of tests in test rigs where whole clutch discs or complete clutches are investigated. Simulation models, such as the ones described in this chapter, give more information regarding the investigated clutch than what is possible with merely testing. The information revealed from the simulations can reduce the final testing needed before the clutch is used in an actual application.

A simulation model is never better than the input data and the procedure of gathering this data is described in chapter 6 and 7. The simulation models developed in this thesis are made to simulate the behavior of a wet clutch working under limited slip conditions, but simulations are important also for other types of wet clutches.

The simulation model used in papers A and E are used to estimate the temperature in a wet clutch during 10-30 s of engagement working under limited slip conditions. The boundary lubrication friction coefficient described in chapter 7 which is temperature and sliding velocity dependent is used to calculate the transferred torque in the clutch simulation. Included in the temperature simulation in paper E is a fluid film simulation which includes the fluid's cooling effect of the clutch. In paper A this is replaced by a simple empirical expression including the oil flow pumped through the clutch, rotational speed and temperature. The thermal model is an axisymmetric 2D model in paper A and a polar cylindrical 3D model in paper E. The main advantage of the latter model in paper E is that the empirical expression based on measurements in a wet clutch test rig is not required. Different geometries of the friction discs are easily modeled and simulated which makes this model suitable for optimization of the geometry of the disc.

The temperature, fluid film and torque simulations are described below and more detailed information is given in papers A and E.

8.1 Temperature model

The temperature model in paper A solves the energy equation in a 2D axisymmetric domain shown in Fig. 8.1. The advantage with this approach compared

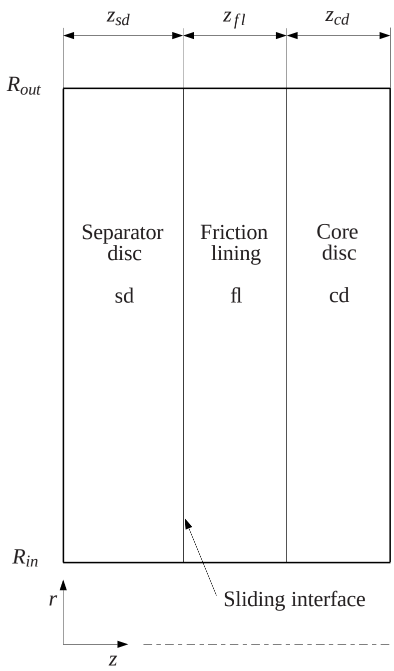

Figure 8.1: Schematic sketch of computation temperature domain in paper A.

to a 3D approach is that the simulation time is shorter. A disadvantage of this approach is that it is hard to take account of the effects of the groove patterns. The boundary lubrication torque is dependent on the temperature of the contact area and not the temperature in the grooves. The 3D simulation used in paper E, shown in Fig. 8.2, gives a better description of the temperature field in the friction disc and the separator disc. With the 3D geometry , it is possible to simulate the temperature of the contact areas. The contact areas are

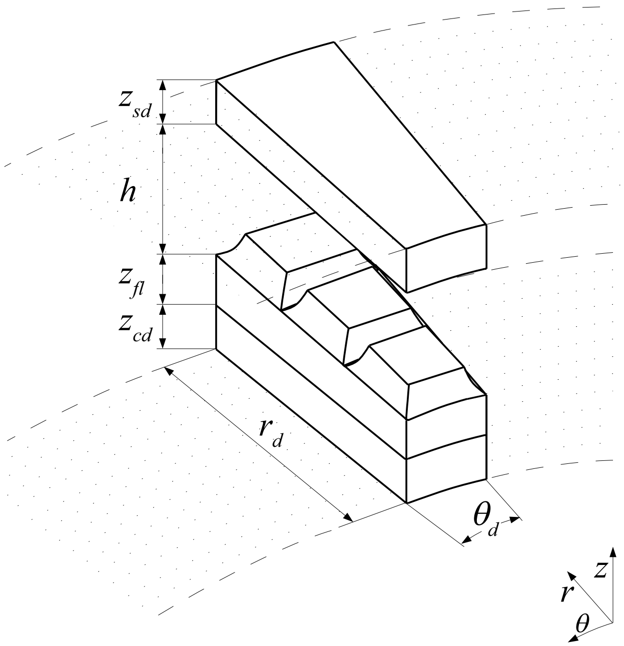

Figure 8.2: Computed temperature domain used in temperature simulations in paper E. 1/64th of one friction disc and 1/64th of one separator disc. (Paper E , Fig. E.1)

warmer than the rest of the friction disc because nearly all heat is generated in the sliding interface between the friction disc and separator disc. This gives a better prediction of the temperature dependent boundary lubrication friction coefficient, and thus a better torque simulation.

The separator disc temperature is, however, calculated as axisymmetric in paper E since the separator disc does not have any geometric variations in the angular direction and is considered to rotate fast enough for the temperature in the angular direction to be uniform. This gives faster simulations which demand less computer memory and the difference in the solution with regard to a full 3D simulation of the separator disc is negligible. Similar approximations can also be made in simulations of tilting pad thrust bearings where the temperature in the runner is calculated using an axisymmetric model [37].

8.2 Fluid film simulations

The fluid film model in paper E comprises both a fluid mechanics model and a thermal model. The temperature distribution across the film is approximated with a polynomial of second order. The pressure gradients in radial and angular directions are solved with a homogenized Reynolds equation including surface roughness effects. The details about the simulations with the homogenized Reynolds equation is described in [38]. In paper E all details concerning the temperature simulations is described and a brief description is given of the fluid flow model from [38]. In the grooves the thermal calculation comprises a simplified power equilibrium to ensure a numerically stable solution.

In paper A, the fluid film simulation comprises an empirical cooling flow equation, Eq. (A.12), based on measurements from a wet clutch test rig [10]. The disadvantage with this equation is that it is valid only for the system used in the test rig: it can not be used to investigate the behavior of a wet clutch in another system. The advantage is that it requires a short computing time and gives a very rapid simulation.

8.3 Torque simulations

The boundary lubrication torque is calculated by simply integrating the boundary lubrication friction force and radius over the disc contact area

$$Tq_{bl} = p_c \int_{\theta} \int_{r} \mu r^2 dr d\theta, \tag{8.1}$$

where the friction coefficient varies due to different temperature and sliding velocity in the sliding interface. The nominal contact pressure, p_c, is considered constant in paper A while in E it is calculated with a force balance between the axial force and the calculated hydrodynamic force and contact mechanics force. The working conditions simulated in paper A and E imply an almost negligible hydrodynamic force, hence almost all axial load is carried by the asperity contacts. In paper E the small hydrodynamic torque is also computed and the total transferred torque is computed as the sum of the boundary lubrication torque and the hydrodynamic torque.

8.4 Results and discussions

The results from the simple axisymmetric model used in paper A correspond well to the measurements made in the wet clutch test rig [10]. The simulated case is shown in Fig. 8.3 where the rotational speed during ten seconds of engagement with a constant axial load is shown. The measured and simulated torque and temperature during this test is also shown in Fig. 8.3. In this

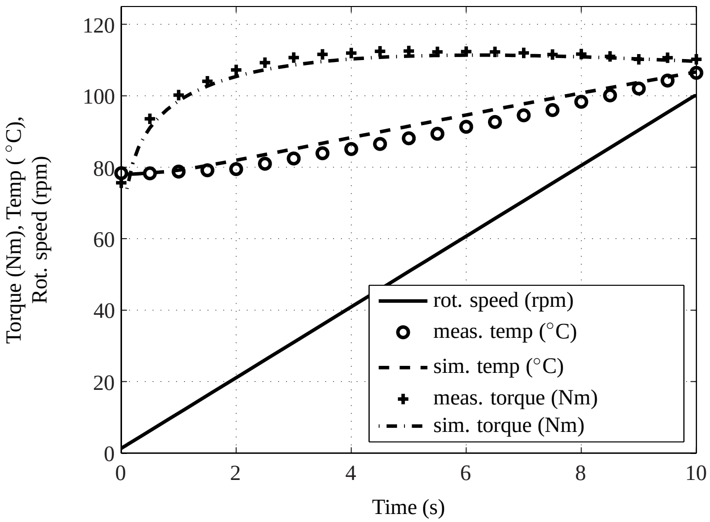

Figure 8.3: Comparison between measurements in wet clutch test rig and simulation with an axial force of 25.3 kN. (Paper A, Fig. A.12)

measurement the axial force is 25.3 kN, corresponding to a nominal surface pressure of 9.7 MPa.

The temperature distribution in the computed temperature domain, see Fig. 8.1, is shown in Fig. 8.4 after 9 seconds of engagement with an axial force of 10.3 kN or a nominal surface pressure of 3.9 MPa. The temperature shown in Fig. 8.3 is the temperature at the position of the black dot shown in Fig. 8.4.

The difference between using temperature and sliding velocity dependent friction coefficient and a friction which is only dependent of the sliding velocity is visualized in Fig. 8.5. The use of a non-temperature dependent boundary lubrication friction coefficient, which is the most common approach in wet clutch simulations, would give a fairly large error in the torque calculations, especially in the case with wet clutches working under limited slip conditions.

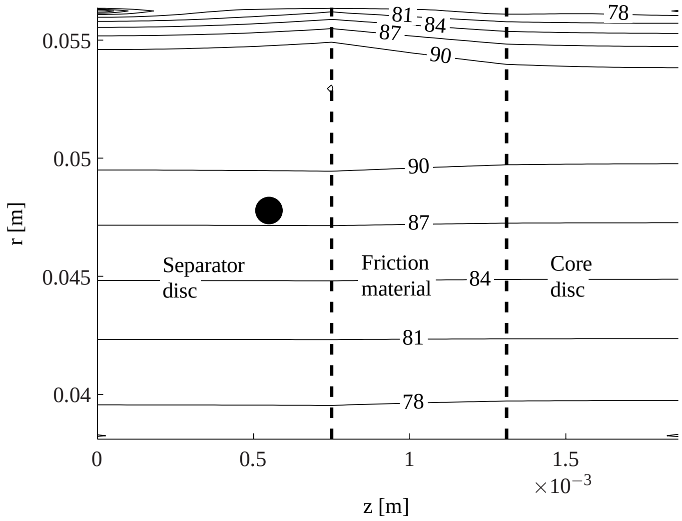

Figure 8.4: Simulated temperature for the rotational speed shown in Fig. 8.3 with an axial force of 10.3 kN after 9 seconds of engagement. (Paper A, Fig. A.11)

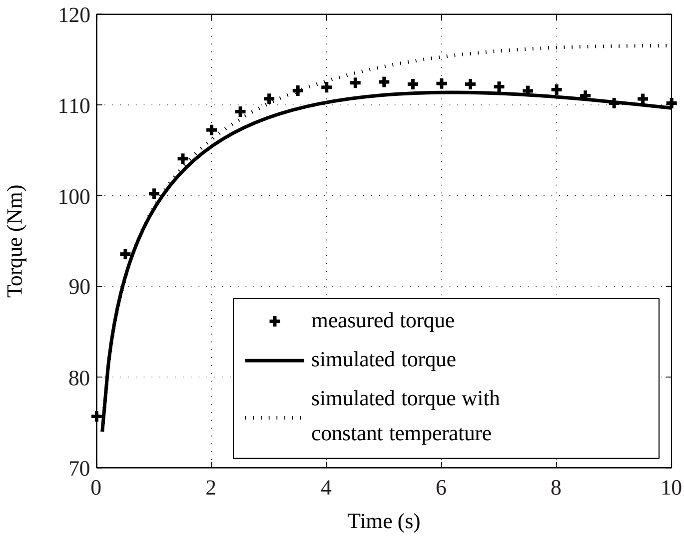

Figure 8.5: Comparison between torque for constant temperature vs. simulated temperature. Same running conditions as in Fig. 8.3. (Paper A, Fig. A.14)

Temperature and torque simulations with the 3D temperature model in paper E is shown in Fig. 8.6. The rotational speed is the same as in Fig. 8.3 and the axial force is 10 kN. The simulations agree well with measurements from a wet clutch test rig even though no friction measurement from the wet clutch test rig was used in the simulations. This shows that the model is suitable for simulating wet clutches that have not yet been built, and it is thus suitable for use in the design process of new wet clutch systems.

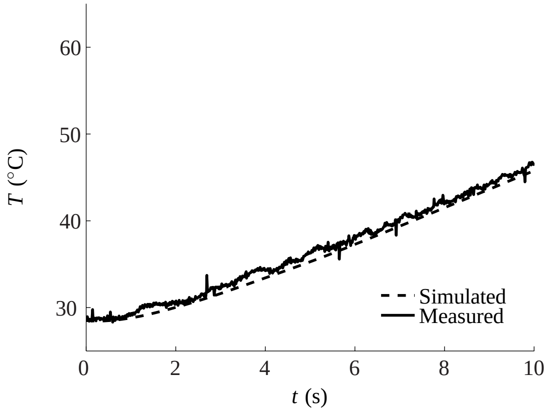

(a) Comparison between simulated and measured temperature. (Paper E, Fig. E.5(a))

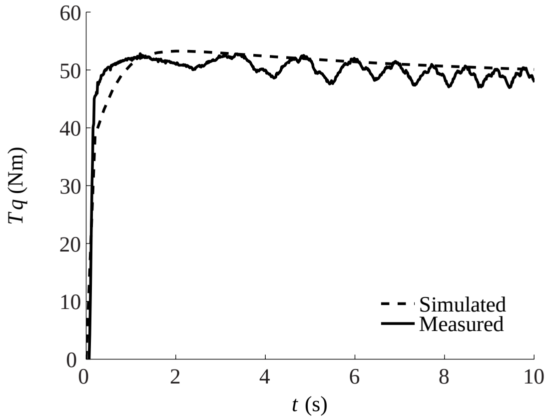

(b) Comparison between simulated and measured torque. (Paper E, Fig. E.7(a))

Figure 8.6: Temperature and torque simulations for an axial force of 10 kN.

A calculated temperature distribution is shown in Fig. 8.7. Here the temperature in the core disc is around 35°C while the highest temperature in the contact region is above 41°C. The temperature in the fluid film in the contact region is the temperature which governs the boundary lubrication friction coefficient in the model.

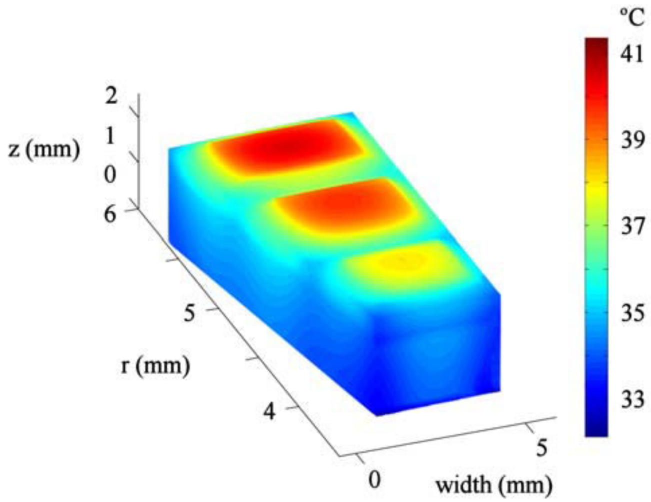

Figure 8.7: Temperature distribution in simulated friction disc domain after 4 seconds of engagement with an axial load of 20 kN. (Paper E, Fig. E.6)

8.5 Conclusions

The behavior of a wet clutch working under limited slip conditions may be simulated with good accuracy with the methods described in this chapter. Simple pin on disc boundary lubrication friction measurements in combination with temperature and torque simulations are shown to be effective ways to investigate the behavior of a wet clutch without the need for full-scale wet clutch measurements.

Chapter 9

Main Conclusions

The main conclusions of this doctoral thesis are:

- Boundary lubrication friction measurements in combination with simulation models are a good complement to "classic" wet clutch test methods where torque transfer is measured in test rigs where whole clutch discs or compete clutches are investigated, because:
  - More details concerning the function of the wet clutch can be investigated.
  - The temperature distribution and torque behavior for a clutch is easily described for clutches with different friction materials, lubricants and disc geometry, making the method suitable for use when optimizing a wet clutch system.
  - The use of simplified measurements and simulations to optimize a wet clutch can shorten the time needed to develop a wet clutch system, thus minimizing the development costs.
- The torque and temperature simulation models described in papers A and E can be used as optimization tools in the design process of new limited slip wet clutch systems.
- Boundary lubrication friction measurements made in a pin on disc apparatus as described in paper B are suitable for screening different material/fluid combinations when new wet clutch systems are developed.
- Permeability investigations in papers C and D show that permeability of the groove walls on friction discs used in wet clutches are much influenced by the way the grooves are manufactured. The permeability of

the friction material is also shown to influence the boundary lubrication friction behavior. The influence of permeability on friction behavior is very high when working under starved conditions.

Chapter 10

Future Work

In this work, a simulation model is developed which makes it possible to simulate the behavior of a wet clutch working under limited slip conditions. Future work should focus on:

- An extension of the model to include wet clutch engagements similar to the working conditions of a wet clutch mounted in an automatic transmission, hence make the developed wet clutch optimization method work for all types of wet clutches. This can be done by implementing a time dependent fluid film thickness governed by the force balance between the engagement force, the hydrodynamic force and the contact mechanics force. The engagement simulations also have to be validated with a suitable test rig in which torque and temperature can be measured during engagement of a complete wet clutch.

- More investigations of the boundary lubrication friction behavior and development of better simulation models of the boundary lubrication contact. A simulation model where no boundary lubrication friction measurements is needed to simulate the wet clutch behavior is the overall goal. This is, however, extremely difficult because of the complexity of the boundary lubrication contact, where the friction coefficient is governed by the chemical and physical reactions of the additives in the lubricant.

- An investigation of aging effects of the clutch system in order to simulate the torque behavior for an aged clutch. The degradation of the wet clutch can be dependent on, for example, wear, oxidation of friction material and fluid, clogging of pores in the friction materials, additive consumption and water contamination of the lubricant.

- An investigation of the possibility of using the model in the control software for a wet clutch system to improve the control of the clutch.

Part II

Appended Papers

Paper A

Thermal influence on torque transfer of wet clutches in limited slip differential applications

Tribology International, 2007 May; vol. 40, no. 5, p. 876-884.

Thermal influence on torque transfer of wet clutches in limited slip differential applications

P. Marklund*, R. Mäki, J. Jang, M. M. Khonsari, R. Larsson and E. Höglund

**Luleå University of Technology, Division of Machine Elements, Luleå, SE-971 87 Sweden*

Abstract

Wet clutches operating under low velocity and high load are studied with the aim of obtaining reliable models for the torque transfer during boundary lubrication conditions. A friction model which takes temperature, speed and nominal pressure into account is developed and used with temperature calculations to be able to simulate behavior of a wet clutch working in boundary lubrication regime. Predicted torque and temperatures from the model agree well with experimental data.

A.1 Introduction

Disk-type wet clutches are exceedingly important for controlling torque transfer in modern drive trains for both two- and four-wheel drive passenger cars. Modern drive trains are generally equipped with on-board computers that make it possible to predict the vehicle dynamics in real time and control vehicle handling by changes in the differential settings. Implementation of this system requires good theoretical or semi empirical models that are capable of accurately predicting torque transfer as a function of the actuator signal at any given operating condition. The common simulation approach is to study an engagement from a high velocity to a state of lock-up. Typically the Reynolds equation is used to predict the torque and film thickness at the beginning of the engagement and then a measured friction characteristic is applied to the boundary friction at the latter part of the engagement. In order to obtain good agreement with experimental data, it is necessary to include an appropriate thermal model to compensate the change of fluid viscosity during the engagement. The boundary friction, however, is generally not compensated for temperature [22, 31–33].

Traditional engagement models are generally not suitable for application to limited slip differential (LSD) applications. An LSD-clutch is generally engaged at a rather low velocity, making the contribution of the full-film Reynolds equation less important. The common approach of using flow factors in the model can not be applied since the oil film thickness is so small that the flow factors are not valid [39]. In addition, it is not always desired to reach a state of lock-up, but rather to allow a controlled limited slip, hence transferring only a certain given torque. Since this period of limited slip can be long, a significant amount of heat might be generated, making it important to use a temperature dependent model for the boundary, or asperity, friction.

The aim of this work is to develop a technique suitable for modeling thermal behavior and torque transfer for wet clutches in LSD-applications, in particular the Haldex LSC (Limited Slip Coupling) all-wheel drive system [9, 10] . The Haldex LSC features an electronically controlled disc-type wet clutch mounted between the propeller shaft and the rear differential. The clutch controls the torque transfer to the rear axle of the vehicle, and is actuated by hydraulic pressure generated by a hydraulic pump driven by the speed difference between the front and rear axles of the vehicle. In order to obtain a high power density while still keeping the cost down, a sintered bronze friction material is used in the friction discs in combination with separator discs made of hardened steel, see Figure A.1. The lubricant used in this application is a tailor made semi-synthetic fluid with a special additive formulation. Thermal data

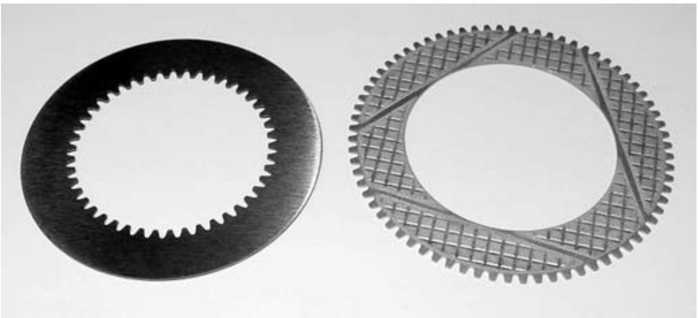

Figure A.1: Separator- and friction disc.

and geometries for the discs can be found in Table A.1 as well as data for the lubricant. Typical operating conditions are sliding velocity less than 0.5 m/s and mean surface pressure exceeding 5 MPa.

A.2 Approach

Initially the wet clutch model of Jang and Khonsari [32], with a somewhat modified boundary friction model, was applied to investigate an LSD clutch. The boundary friction model was,

$$\mu = 0.15 + 0.011 \cdot log\left(\frac{0.038+0.056}{2}\triangle\omega\right) \tag{A.1}$$

where $\triangle\omega$ is the difference in rotational speed between friction disc, ω_{fl}, and separator disc, ω_{sd}, respectively. The four constants in Equation (A.1) were obtained by curve-fitting experimental data from the Limited Slip Clutch Test Rig [10]. Input data were modified to represent the investigated clutch system, including the oil which was a Statoil LSC fluid. A drawback with this model is the values at very low velocities where the friction value will approach $-\infty$. However, at velocities of interest during engagement simulations (above $\sim 10^{-5}$ rad/s), this factor does not influence the results.

Figure A.2 shows resulting torque transmission obtained from a clutch engagement simulation, the respective contribution from full film , computed with Reynolds equation, and asperity friction is also displayed.

It was found that the contribution from the Reynolds equation to the transmitted torque is negligibly small at the end of the engagement. In limited slip

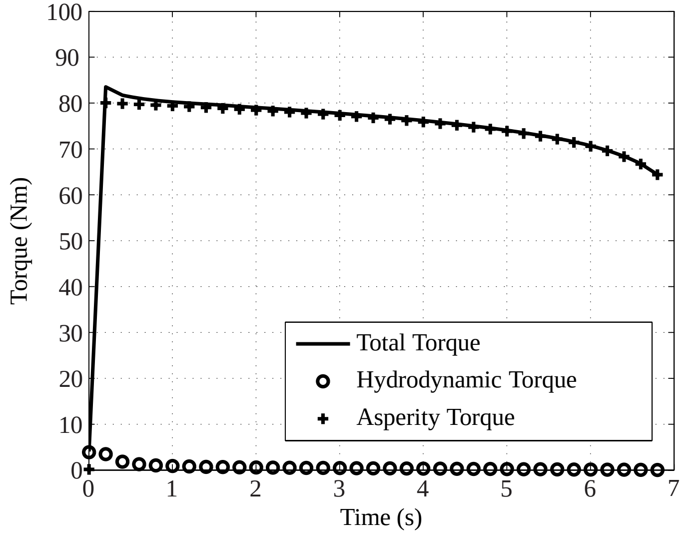

Figure A.2: Simulated torque response during engagement from 3000 rpm at 1.25 MPa surface pressure.

applications the system primarily operates in boundary lubrication regime with a corresponding time of 2-3 seconds and higher after the start of engagement in Figure A.2. Therefore the torque contribution from Reynolds equation can be neglected.

Figure A.3 shows measured friction data obtained at several different initial clutch temperatures obtained for the same fluid tested in the Limited Slip Clutch Test Rig [10]. As evident from Figure A.3, for the working conditions in an LSD application, a boundary friction model only depending on velocity is not sufficient because friction is significantly influenced by the heat generated in the clutch during operation. Therefore a better boundary friction model is needed.

Based on these findings a new approach was adopted. The suggested model features a semi-empirical boundary friction model that calculates the friction as a function of sliding velocity, temperature, and applied pressure. This friction model is connected to a thermal model that predicts the temperature in an LSD clutch based on current operating conditions and the temperature history of the clutch.

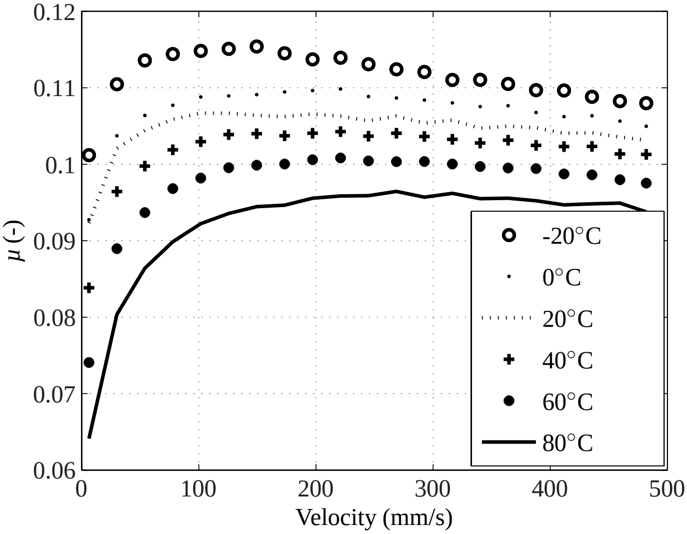

Figure A.3: Measured friction coefficient at different contact temperatures.

A.2.1 Thermal model

The thermal model considers heat dissipation in the fluid as well as heat conduction into the separator disc, friction lining, and core disc. The computation domain is the axisymmetric cross section presented in Figure A.4. In this figure, the separator and core disc are half the thickness of the discs used in the clutch. Since the simulated friction discs are considered to be located in a clutch consisting of several similar discs, the heat conduction over the edges in axial direction is neglected due to symmetry [40, 41]. This means that the outer edges in z-direction on the core and separator disc at z =0 and $z = Z_{sd} + Z_{fl} + Z_{cd}$ are considered as insulated and Neuman boundary conditions, can be applied:

$$\frac{dT}{dz} = 0. \tag{A.2}$$

The boundaries in radial direction at R_{in} and R_{out} will have Dirichlet boundary conditions with a constant temperature at Rin and an oil sump temperature, T_{sump}, at R_{out}. T_{sump} will change during engagement according to Equation (A.7).

A model was developed to simulate a wet clutch under limited slip conditions, i.e. when the surfaces of the friction lining and the separator disc are in contact with each other. The gap between the friction lining and the separator

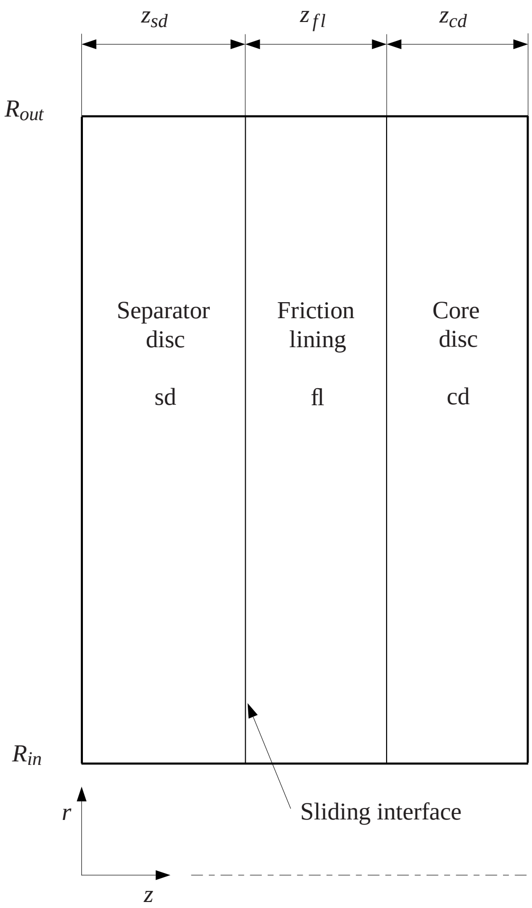

Figure A.4: Schematic sketch of computation domain.

disc is, therefore, very small during the simulations, and there will not be a large oil flow through the gap. However, even though the oil flow is small, it is not insignificant. Much of the generated heat in the interface between friction lining and separator disc is not absorbed in the materials but transferred out of the clutch by the oil flow. In the computations there is also a certain amount of oil along the outer circumference, see Figure A.4, which represents the oil sump. This absorbs the heat transferred by the oil and gives a better boundary condition on the outer edge of the clutch discs than a more simple constant temperature boundary condition. The oil in the oil sump is assumed to be perfectly stirred.

Temperature is solved in the clutch by taking advantage of the axisymmetric condition of the problem. In the separator disc, friction disc and core disc, respectively, the temperature is solved with the energy equation in polar coordinates,

$$\rho C_p \frac{dT}{dt} = k\left[\frac{1}{r}\frac{\partial}{\partial r}\left(r\frac{\partial T}{\partial r}\right) + \frac{\partial^2 T}{\partial z^2}\right], \tag{A.3}$$

where density ρ, specific heat capacity C_p and thermal conductivity k have different values for different parts of the clutch according to Table A.1. The friction lining, which is made of bronze, is considered as impermeable so there is no heat convection in the friction material.

Table A.1: Input data. Material constants, and geometry parameters. Subscripts according to Fig. A.4.

Variable	Value	Unit
ρ_{sd}	7600	kg/m^3
ρ_{fl}	5000	kg/m^3
ρ_{cd}	7600	kg/m^3
ρ_{oil} (40°C)	868	kg/m^3
C_{p-sd}	449	J/kgK
C_{p-fl}	471	J/kgK
C_{p-cd}	449	J/kgK
C_{p-oil}	2040	J/kgK
k_{sd}	46	W/mK
k_{fl}	15.7	W/mK
k_{cd}	46	W/mK
k_{oil}	0.131	W/mK
z_{sd}	$0.75{\cdot}10^{-3}$	m
z_{fl}	$0.56{\cdot}10^{-3}$	m
z_{cd}	$0.55{\cdot}10^{-3}$	m
R_{in}	0.0381	m
R_{out}	0.0564	m
h_{mean}	$1{\cdot}10^{-5}$	m
V_{sump}	$500{\cdot}10^{-6}$	m^3

For each time step, the temperature in the friction discs changes. The heat flux, Qe_{int} (W/m^2), generated in the interface between the friction lining and the separator disc at a given radius is

$$Qe_{int} = r\triangle\omega p\mu, \tag{A.4}$$

where r is radius to the contact, $\triangle\omega$ is difference in rotational speed between the two discs, p is nominal pressure in the interface and μ is friction coefficient in the contact. Qe_{int} is not constant for different values of the radius r. This is the case not only because of the difference in radius, but also the different friction coefficient because the temperature is not constant in radial direction. The total energy in interface for each time step is a summation of heat flux over the total contact area as

$$W_{gen} = \triangle t \int_{R_{in}}^{R_{out}} Qe_{int} dA, \tag{A.5}$$

where $\triangle t$ is the time for one time step. The absorbed energy in clutch discs for the same time is described by

$$W_{abs} = \int_0^z \int_{Rin}^{R_{out}} \triangle T \rho C_p 2\pi r dr dz, \tag{A.6}$$

where $\triangle T$ is difference in temperature in clutch discs for one time step. The difference between the energies described in Equation (A.5) and (A.6) is assumed to warm up the oil in the oil sump as

$$T_{sump} = T_{sump-old} + \frac{(W_{gen} - W_{abs})}{\rho_{oil} V_{sump} C_{p-oil}}, \tag{A.7}$$

which gives the boundary temperature, T_{sump}, at R_{out}.

The boundary conditions between the friction lining and core disc are

$$T_{fl} = T_{cd}; k_{fl}\frac{dT_{fl}}{dz} = k_{cd}\frac{dT_{cd}}{dz}, \tag{A.8}$$

which implies an energy equilibrium over the boundary.

The heat balance in the interface-layer between the friction lining and the separator disc is given by the following equation.

$$r\triangle\omega p\mu - k_{sd}\frac{dT}{dz_-} + k_{cd}\frac{dT}{dz_+} - \rho c_p u_{oil} r\frac{\partial T}{\partial r} = 0, \tag{A.9}$$

which is a combination of heat generation, Equation (A.4), conduction in materials, similar to Equation (A.8), and forced convection in fluid film,

$$\rho_{oil} \cdot C_{p-oil} \cdot u_{oil} \cdot r\frac{\partial T}{\partial r}, \tag{A.10}$$

The convection in the fluid film gives a cooling effect to the interface. Heat conduction in the fluid is much smaller than the conduction in the friction discs and can thus be neglected. The velocity of the oil, u_{oil}, is computed with a mean film thickness, h_{mean}, and an oil flow, Q_{oil}, in the interface as

$$u_{oil} = \frac{Q_{oil}}{h_{mean} 2\pi r}. \tag{A.11}$$

The energy equation (A.3) is solved with an explicit finite difference method of the first order. The transient frictional heat source is computed with a friction coefficient according to the boundary friction model described below. This means that the friction is varying during the whole engagement process since the temperature and rotational speed is changing. It is also possible to let the friction coefficient vary with radius r because temperature in radial direction in the interface will be computed. When comparing the simulations with the tests performed in the test rig, it was obvious that the cooling oil flow, needed to get a good correlation, was far less than the total flow through the clutch. Between the friction lining and the separator disc, see Fig. A.1, a forced oil flow, Q_{oiltot}, of 200 ml/min is pumped. The results indicate that some of this oil can pass through the clutch without being heated much and therefore not serve as a coolant. The heated oil, working as cooling flow, is probably flowing near the friction disc and separator disc surfaces. It was found in the simulations that the active cooling flow was dependent on $\Delta\omega$ and temperature and that a smaller amount of the total flow, Q_{oiltot}, were cooling the friction discs even with zero rotation. To get a cooling oil flow which gives a good correlation between simulations and test results, an empirical flow model depending on velocity and temperature is developed:

$$Q_{oil} = Q_{oiltot} \left(a \cdot (\triangle\omega + 1)^b + c \cdot T_{mean}^d + e \right) \tag{A.12}$$

This model is valid only for the geometry used in this application and has to be recalibrated for other geometries of the friction discs, meaning the values of $a - e$ is system dependent.

A.2.2 Boundary Friction Model

The boundary friction is modeled as a function of load, velocity and temperature based on an extensive amount of experimental data. The data is analyzed according to the method described in an earlier publication [26], generating friction-velocity profiles for different loads and temperatures. The following expression has been curve fitted to experimental data,

$$\mu = C_1 tanh(C_c \cdot v) + C_3 v^{0.1} + C_4 \tag{A.13}$$

where μ is friction and v is sliding velocity, similar models are commonly used as friction models for boundary and mixed lubrication [42]. C_1 is connected to the friction value at the point where the friction starts to level out. C_2 is used to adjust the curve with respect to the x-axis, i.e. velocity. C_3 governs the slope of the curve at higher velocities and C_4 is used in order to adjust the friction level, i.e. shift the friction curve up or down.

Figure A.5 shows measured data points and the resulting fitted curve for one load case, nominal pressure of 7.6 MPa and temperature 70 °C.

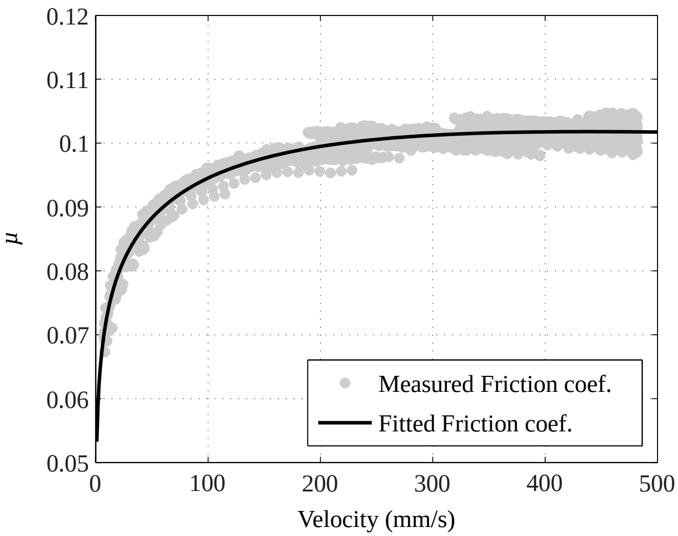

Figure A.5: Observed values of friction coefficient and the fitted friction model at nominal pressure 7.6 MPa and temperature 70°C.

The fitting parameters from Equation A.13, for different loads and temperatures, are stored in a matrix, Table A.2. The matrix spans loads from 3.8 MPa to 9.6 MPa and temperatures from -40°C to +200°C. The friction is calculated using a linear interpolation between the friction values generated by the parameter sets surrounding the current operating condition.

The different parameter sets are primarily based on a total of 1 750 friction measurements where the velocity is linearly increased from 1 rpm to 100 rpm (0.006 m/s to 0.59 m/s) in 10 s using the Limited Slip Clutch Test Rig [10].

Table A.2: Example of values from the data matrix containing information on boundary friction fitting parameters.

	10 kN 3.8 MPa	**15 kN 5.7 MPa**	**20 kN 7.6 MPa**	**25 kN 9.6 MPa**
-40°C	C1=-0.031 C2=0.0014 C3=0.057 C4=0.035	C1=-0.026 C2=0.0037 C3=0.035 C4=0.070	C1=-0.0025 C2=0.013 C3=0.012 C4=0.098	C1=-0.0024 C2=0.0098 C3=0.012 C4=0.101
⋮	⋮	⋮	⋮	⋮
70°C	C1=-0.024 C2=0.0024 C3=0.070 C4=-0.010	C1=-0.338 C2=0.0001 C3=0.077 C4=-0.025	C1=-0.039 C2=0.001 C3=0.077 C4=-0.024	C1=-0.038 C2=0.002 C3=0.089 C4=-0.036
⋮	⋮	⋮	⋮	⋮
200°C	C1=-0.024 C2=0.0024 C3=0.070 C4=0.038	C1=-0.027 C2=0.0021 C3=0.087 C4=-0.067	C1=-0.092 C2=0.0006 C3=0.097 C4=-0.082	C1=-0.038 C2=0.002 C3=0.089 C4=-0.063

This type of data is available from -20°C up to 90°C for all loads. At higher temperatures (above 90°C) the fitting parameters C_1, C_2 and C_3 are constant (the shape of the curve is constant and same as at 90°C), the parameter C_4 is however modified to adjust the friction level. This adjustment is based on friction measurements conducted at a constant velocity of 100 rpm where the temperature is increased up to 200°C under a constant load, yielding a friction-temperature dependence (the decrease in friction is $2.1 \cdot 10^{-4}$ per degree Celsius). These measurements were also conducted using the Limited Slip Clutch Test Rig. At low temperatures (below -20°C) the fitting parameters C_1, C_2 and C_3 are also constant (the shape of the curve is constant and same as at -20°C), the parameter C_4 is however modified to adjust the friction level. This adjustment is based on friction measurements conducted on an actual Haldex Coupling. Figure A.6 illustrates the friction-velocity output from the friction model for a case with load 20 kN ($\sim$7.6 MPa) and temperature 70°C.

The friction is assumed constant at velocities in excess of the measured 0.59 m/s and for velocities less than 0.006 m/s. The friction coefficient for a velocity of 0.59 m/s is used for velocities higher than 0.59 m/s and for velocities less than 0.006 m/s the friction coefficient for the velocity 0.006 m/s is used.

Figure A.7 shows an example of the friction as a function of temperature for an arbitrary case, load 20 kN (∼7.6 MPa) and velocity 0.05 m/s (∼8 rpm). Around 20°C an alteration in the curve can be observed, this is in agreement with experimental observations from a large series of tests and are believed to be caused by additive effects in the fluid. At temperatures below and in excess of the observed -40°C and 200°C friction is assumed constant and at the same value as at -40°C and 200°C respectively.

Between -40°C and -20°C and between 90°C and 200°C the friction characteristics (friction-velocity) have the same shape, but the friction curve is based on less measurements compared to the friction between -20°C and 90°C, respectively.

At normal loads under 3.8 MPa and above 9.6 MPa the friction function will return to the same value as at 3.8 MPa and 9.6 MPa, respectively.

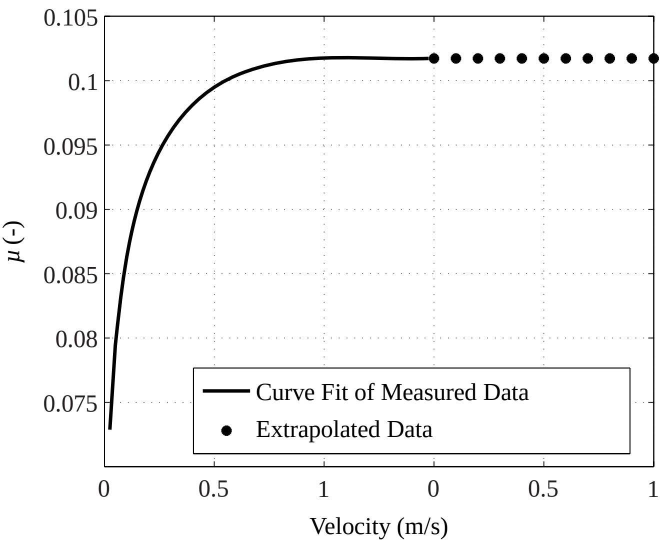

Figure A.6: Friction characteristics generated by the friction model at nominal pressure 7.6 MPa and temperature 70°C.

A.2.3 Solution Technique

Engagement force, sliding velocity, and initial temperature are assumed to be known parameters and are given as input to the model. These parameters can be easily measured on-board the vehicle.

The energy equation (A.3) is discretized on an axisymmetric grid.

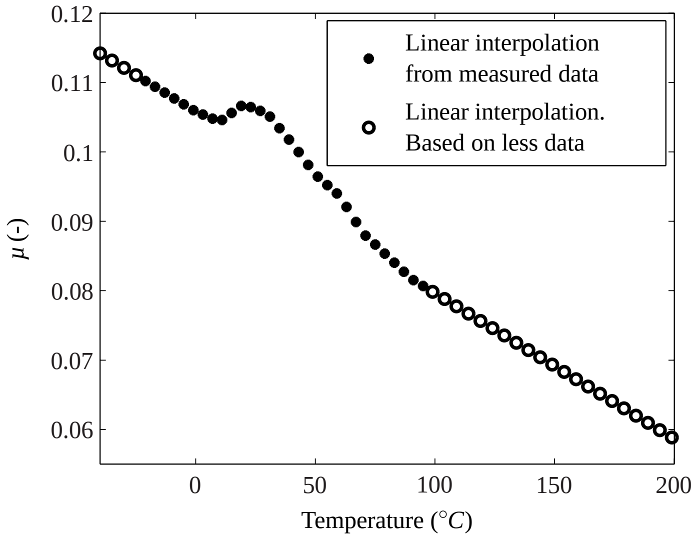

Figure A.7: Friction coefficient at different temperatures generated by the friction model at nominal pressure 7.6 MPa and velocity 0.05 m/s.

The friction in each sliding grid point is given by the boundary friction model at each time step based on velocity, pressure, and temperature. The generated heat is calculated based on the friction and velocity and is used in the thermal model to predict the temperature in the next time step. Based on this temperature, a new friction value is calculated. Finally, the transmitted torque is calculated by integration of the friction force over the clutch area.

A.3 Results

A wet clutch used in an LSD application is working with high applied force and low difference in rotational speed between separator disc and friction lining, . The behavior of a wet clutch in an LSD is tested in the test rig described in earlier publications [10]. Common tests for wet clutches used in LSD applications are carried out with a constant axial force during the whole experiment. During the tests, $\triangle\omega$ is often linearly increased from a rather low value during a couple of seconds or linearly decreased from a higher value. A combination of these tests can also be carried out, where first is linearly increasing from a low value, held constant a couple of seconds, followed by being linearly decreased to the lower start value. In this paper two cases with different loads are investigated.

- Case 1: $\triangle\omega$ is linearly increased from 1 to 100 rpm in 10 seconds.

- Case 2: $\triangle\omega$ is constant 1 rpm during 5 seconds, linearly increased from 1 to 100 rpm in 10 seconds, held constant at 100 rpm during 2 seconds, linearly decreased from 100 to 1 rpm in 10 seconds, and finally held constant at 1 rpm during 3 seconds.

The maximum difference in rotational speed in these cases, 100 rpm, gives a maximum surface velocity of 0.59 m/s. Temperature can increase up to 40°C in some cases. Start temperature in the clutch can vary from -25°C to 100°C, depending on the working temperature investigated. The investigations in Figures A.8 - A.13 describe the normal working conditions with temperatures during the tests between about 75°C to 110°C. Figure A.8 describes Case 1 with a relative small nominal pressure, 3.9 MPa. The start temperature in this test is 77°C and the small nominal pressure will lead to a quite low torque transfer, about 45 Nm, which gives a small heat generation. This gives a temperature of about 90°C in the warmest parts of the clutch after 10 seconds. In this figure the difference between the measured and simulated torque and temperature is very small.

The temperature in the computational domain described in Figure A.4 during engagement is shown as contour plots in Figure A.9 to Figure A.11. The temperature distribution is shown for 3, 6 and 9 seconds of engagement in Figures A.9-A.11, respectively. As expected, the temperature is rising during the whole engagement process. It is also shown that the maximum temperature is located in almost the same position in all figures and just slightly moves towards the outer radius when the oil sump is slowly heated. One more interesting observation in these figures is that the maximum temperature is not located where the temperature is measured in the test rig. The thermocouple is located in about z = 0.5 mm and r = 48 mm. This location is marked with a black point in the contour plots. The temperature, shown in Figure A.8, Figure A.12 and A.13 is the temperature in this location. As the contour plots show, the measured temperature in the test rig is not the maximum temperature in the clutch and the temperature in the sliding interface is non-uniform. This combined gives a small error for the temperature dependency in the boundary friction model. Since the measured temperature only can be regarded as a mean temperature in the wet clutch, also the friction coefficient can be regarded as a mean friction coefficient. However, in the temperature model, the friction coefficient is computed individually at each discrete node. Therefore,

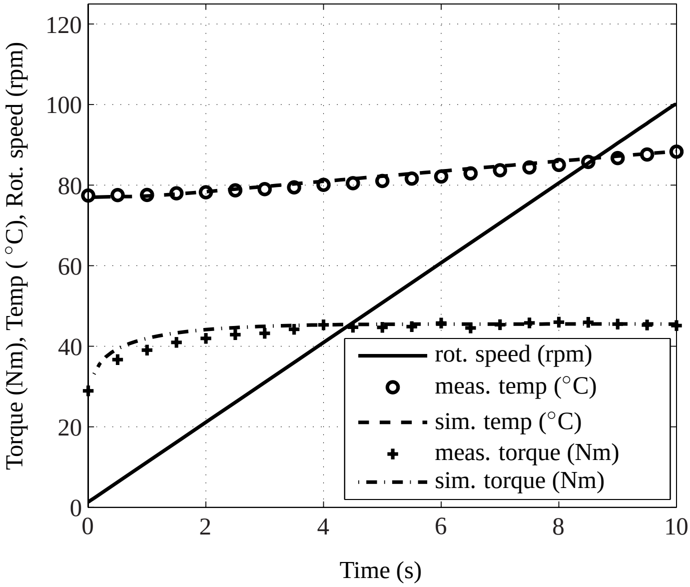

Figure A.8: Comparison between measurements and simulation of Case 1 with a nominal pressure of 3.9 MPa.

the knowledge of more local friction behavior would have been of great interest to achieve more accurate solutions.

Figure A.12 shows a comparison between simulated and measured data for Case 1 with a nominal pressure of 9.7 MPa. When comparing Figure A.12 with Figure A.8, it is obvious how the applied force affects the torque and therefore the heat generation in the sliding interface. In this case the transferred torque is over 110 Nm and the temperature will rise to almost 110 °C. Also in this case with much higher load, the difference in temperature and torque between simulations and measurements is not very large.

Figure A.13 shows a comparison between simulations and measurements for Case 2 with a nominal pressure of 5.7 MPa. In this case the difference between simulated and measured temperature and torque is larger than the simulations of Case 1. This gives a simulated torque which is lower than the measured torque in the part with increasing $\triangle\omega$ and higher torque than the measured torque in some parts with decreasing $\triangle\omega$.

All figures show a torque behavior which is rapidly changing with $\triangle\omega$ when $\triangle\omega$ is low. On the other hand, when $\triangle\omega$ is higher than about 40 rpm, the torque is not very sensitive for changes in $\triangle\omega$. Change in torque transfer during these conditions with $\triangle\omega > 40$ rpm is very much depended on the dif-

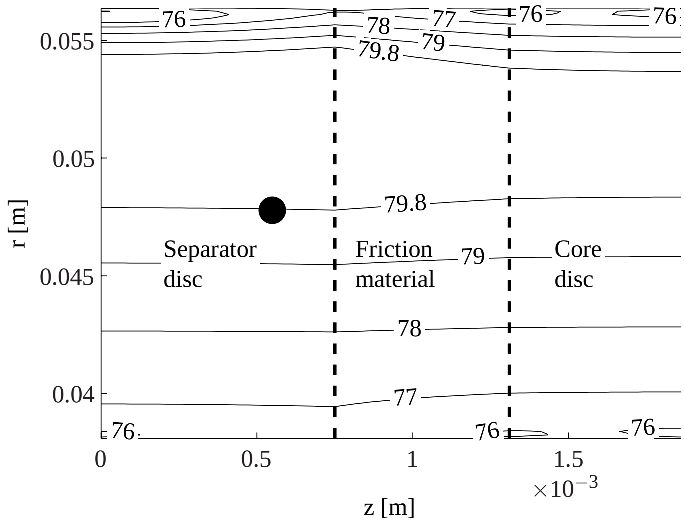

Figure A.9: Simulated temperature for Case 1 with a nominal pressure of 3.9 MPa after 3 seconds.

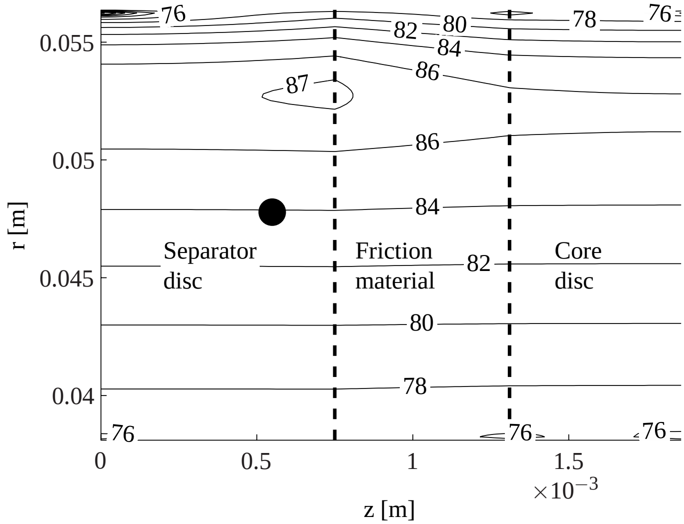

Figure A.10: Simulated temperature for Case 1 with a nominal pressure of 3.9 MPa after 6 seconds.

ference in temperature, and this makes it important to take temperature changes into account when simulating the torque transfer in wet clutches working un-

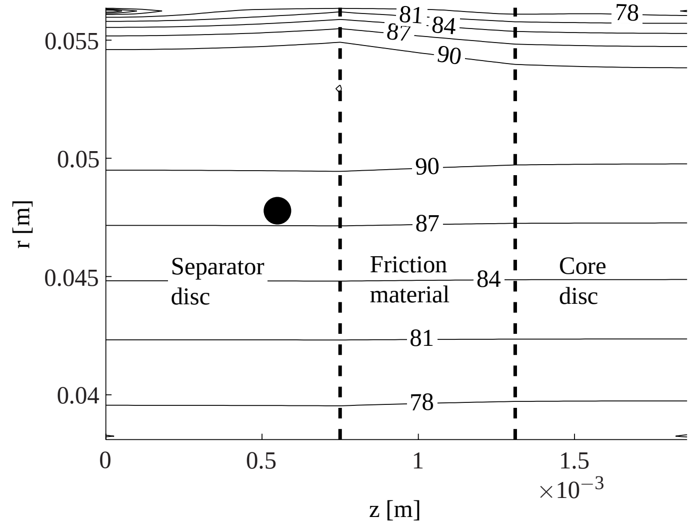

Figure A.11: Simulated temperature for Case 1 with a nominal pressure of 3.9 MPa after 9 seconds.

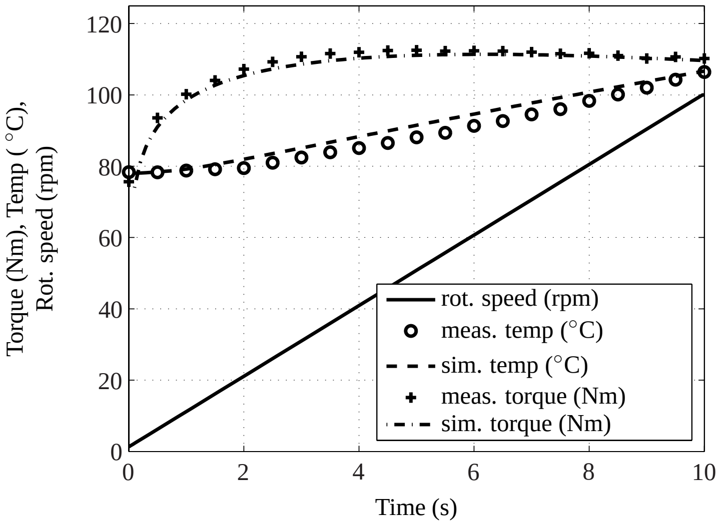

Figure A.12: Comparison between measurements and simulation of Case 1 with a nominal pressure of 9.7 MPa.

der boundary lubrication condition. Figure A.14 shows a comparison between the torque for a constant temperature and that for simulated temperature. Also

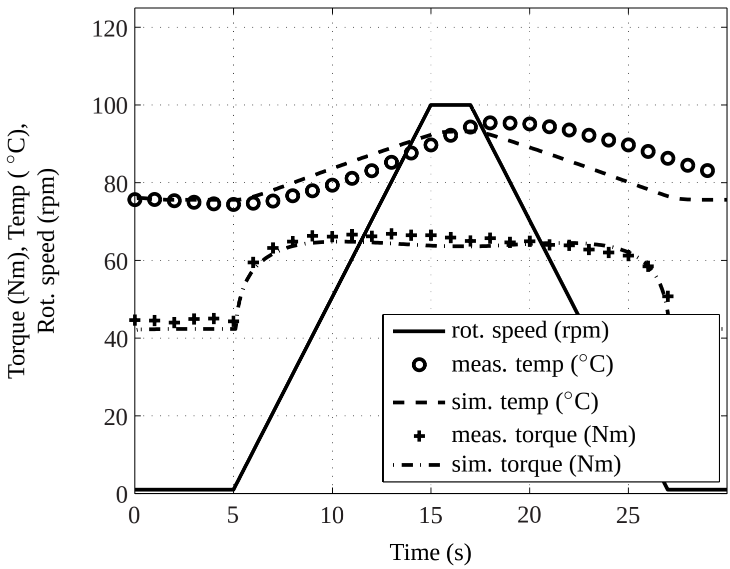

Figure A.13: Comparison between measurements and simulation of Case 2 with a nominal pressure of 5.7 MPa.

shown is the measured torque for Case 1 with a nominal pressure of 9.7 MPa. This is the same case as in Figure A.12. The difference in torque transfer in this clutch, consisting of just one sliding interface, is quite large. The torque for the case with constant temperature also shows a rather different behavior than the torque for the simulated temperature, which is decreasing when the temperature is rising. This can be very important to take into account when simulating vehicle dynamics, since it can change the behavior of the LSD and the whole vehicle drive train, when working under limited slip conditions.

A.4 Discussion

The presented model is valid at low velocities, i.e. the boundary lubrication regime. For applications where the velocity can be expected to be in excess of somewhere around 1 m/s, it should be combined with a model including hydrodynamic effects.

Temperature in the clutch is depending on the heat generation and the heat transfer as well as the boundary conditions. When working with the simulations it was clear that the cooling oil flow was of great significance. For instance, the temperature in the case described in Figure A.13 will rise to over

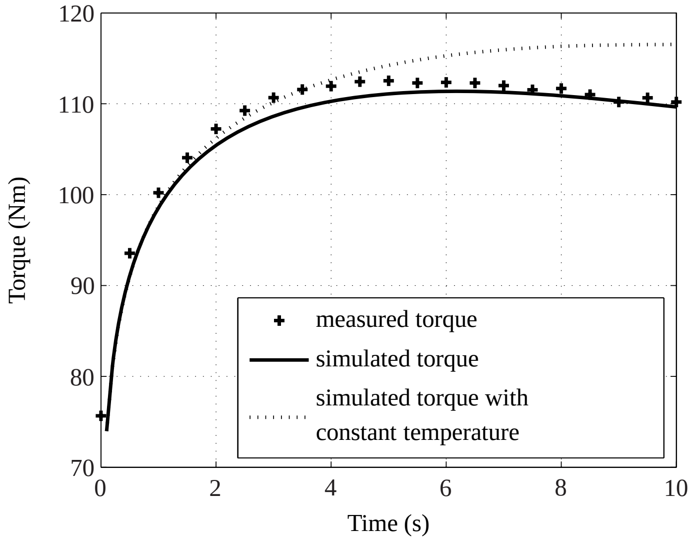

Figure A.14: Comparison between torque for constant temperature vs. simulated temperature.

160°C without any cooling oil flow. This gives a torque about 10% lower than the measured torque.

In this paper an empirical formula for the oil flow was adopted. The empirical formula was estimated for experiments according to Case 1. The assumption that there is no heat conduction over the edges in z-direction may be correct in a clutch with many friction discs. Nevertheless, in the test rig, which is testing just one friction disc, we will have a small heat transfer over the boundaries in z-direction. This heat will be transferred to other parts in the test rig, such as the hydraulic piston which gives the axial engagement force. The formula for the interface oil flow is adopted with the assumptions that the z-boundaries are insulated. To keep the right temperature in the simulations, the adopted oil flow therefore will not be the same as in the test rig. This can explain the temperature difference in the parts with decreasing $\triangle\omega$ in Figure A.13. When $\triangle\omega$ is decreasing, the temperature will also decrease. In the test rig, not only the friction discs have to decrease in temperature, but also the other parts of the test rig. This will give a slower decrease in temperature for the measurements in the test rig than in the simulation model.

To get better simulations in the future, the oil flow in the interface also has to be estimated by simulations. This will give better temperature prediction and will be more general and applicable on different geometries than the model used today.

This friction function is working for the system it is adopted to, but for other friction materials or transmission fluids it is still necessary to run a quite extensive experimental investigation in order to obtain new and accurate fitting parameters throughout the friction parameter matrix, Table A.2. A possible method to reduce this effort would be to assume that the friction-velocity curve is only influenced by temperature and not by normal load; this will significantly reduce the amount of testing necessary while still maintaining a decent accuracy in the prediction.

Torque transfer in wet clutches, working in boundary lubrication regime, is quite complicated to compute. The friction is depending on lubricant, friction material and geometries of friction discs as well as the environment the clutch is working in. The complicated models needed to describe these clutches have implied that most of the development of wet clutches for Limited Slip Differentials have been carried out in test rigs in laboratories and full scale testing in working vehicles. These testes are expensive and time consuming and the product development process would benefit significantly if some of these testes could be carried out as computer simulations instead. Since the clutches work in boundary lubrication, the friction is depending much on different additives in the lubricant. These additive reactions are difficult to simulate, and today the only way to get a reliable friction coefficient as function of temperature and sliding velocity is to measure the friction coefficient under working conditions. However, a simplified friction measurement in combinations with temperature and flow simulations can give good indications on how future wet clutches would perform. These simulation models can simplify the product development and lower the manufacturing costs, Full scale tests could primarily concentrate on fine calibration of products already tested in the simulation models.

A.5 Conclusions

Thermal effects have a significant influence on the torque transferred by the differential under limited slip conditions. It is therefore necessary to have a temperature dependant boundary friction model.

The contribution to the transferred torque from hydrodynamic effects are small under limited slip conditions and can be neglected without influencing the accuracy of the torque prediction.

It is possible to accurately determine the transferred torque knowing the current operating conditions and the thermal history of the clutch, given that the boundary friction model is taking clutch temperature into account.

A.6 Acknowledgements

The authors would like to express gratitude to The Swedish Agency for Innovation Systems and The Swedish Foundation for Strategic Research through the HiMeC and Interface research programs for financial support. Co-operation of all colleagues at Haldex Traction AB and Statoil Lubricants R&D are greatly acknowledged.

Paper B

Wet clutch friction characteristics obtained from simplified Pin on Disc test

Tribology International, 2008; vol 41, issues 9-10, Nordtrib 2006, p. 824-830.

Wet clutch friction characteristics obtained from simplified Pin on Disc test

P. Marklund and R. Larsson

Luleå University of Technology, Division of Machine Elements,
Luleå, SE-971 87 Sweden

Abstract

The frictional behavior of wet clutches in vehicle drivetrains is critical for their overall behavior. During the development of new wet clutch systems there is a need to know this friction behavior. The transferred torque is normally investigated in test rigs where the friction in a sliding interface between a friction disc and separator disc is investigated. These test rigs can be designed differently, depending on the working conditions of the investigated clutch. However, it is possible today to simulate the clutch behavior and not limit ourselfs to only using measurements from test rigs for the design of the wet clutch. The torque transferred by the clutch during engagement can be roughly divided into full film torque and boundary lubrication torque. The full film regime is possible to simulate quite well, whereas the friction in the boundary regime is much more difficult to simulate due to its strong additive dependency. To obtain a good prediction of the total engagement, friction measurements in the boundary lubrication regime are still needed. These measurements should be easy to perform and fast tests are preferable. Friction coefficients for the whole range of sliding speed, interface temperature and nominal surface pressure should be measured. To use these measurements in simulations and get a better understanding of the friction behavior, it is also preferable to conduct these measurements on a small test sample, for which the temperature and sliding speed can be regarded as constant.

Here, the friction of a small sample of a wet clutch friction disc is investigated in a pin on disc test and the temperature is measured in the sample during the tests. Measurements are compared with measurements from a test rig for whole friction discs. A good correspondence between the frictional behaviors of the different measurement methods is achieved.

B.1 Introduction

Wet clutches are often used in vehicle drivetrains. The working conditions of different clutches in the transmission greatly vary depending on the application. Wet clutches in automatic transmissions are often used as lock-up clutches between different rotating parts in the gearbox, where the initial sliding velocity of the clutch interface can be quite high. Other parts of the drivetrain can have wet clutches that work with much lower sliding speeds and higher surface pressures. This is the case in Limited Slip Differentials, which normally have a rather low surface sliding speed, and seldom reach the state of lock up. For the drivetrain to work smoothly without any unnecessary noise and vibrations, the friction characteristics of the wet clutches have to be thoroughly investigated. Depending on the working conditions some clutches will work in full film, mixed and boundary lubrication, whereas others will work mainly in boundary lubrication regime. To get a better understanding of the frictional behaviour of wet clutches, several simulation models have been developed as a complement to traditional measurement methods, [32, 36, 40, 43–45]. Most investigations include simulations of clutches in automatic transmissions that start the engagement at a high difference in rotational speed and then reach a state of lock up. The high speed in these cases implies that the clutch will work in full film lubrication, the largest part of the engagement. Such an engagement process is possible to simulate with good results. There will be a torque contribution from the boundary friction at the end of the engagement. This friction is much more difficult to simulate, since it is very additive dependent. For this part of the engagement there is still a need to do frictional measurements that can be used in simulations. For clutches working mainly in boundary lubrication, during longer periods, the simulations will be very dependent on measurements. Examples of simulation models for this kind of application are temperature simulations used to predict changes in torque transfer during a long engagement with high surface pressure and a small limited slip torque as in Marklund et al [45]. For these kinds of semi empirical simulation models, we encounter a need for a more local friction measurement than what is possible to measure in a test rig that measures torque transfer from one whole friction disc [10, 36] , or larger parts of a friction disc, including grooves [30]. A measurement method to do these local measurements should measure on a quite small sample of the friction disc, to get the local effects. It should also be possible to measure the temperature inside this small sample close to the sliding interface, since it is shown in [10, 45], that the temperature will affect the friction. If the test sample has no grooves, the measured friction will not be geometry dependent. This is not the case when measuring torque transfer from a whole friction disc, where grooves and other surface patterns also can affect the torque. A measurement method based on a pin on disc test can fulfill all these demands. A special pin is designed with a holder for a small sample of the friction disc where a thermocouple is mounted to monitor the temperature during friction measurements. This method can also give a better understanding about the friction phenomena than what is possible in whole friction disc test rigs. The friction coefficient and its variation with temperature, sliding velocity and surface pressure is measured in this paper in a pin on disc test. The test is relatively fast and the normal range of operational parameters are covered within two hours. Another advantage of the proposed test is the possibility to measure the local friction effect, which is of great interest when using measurements in simulations.

B.2 Method

A measurement of boundary lubrication is needed to be able to simulate torque transfer in wet clutches working in boundary lubrication regime. This friction is very additive dependent, and is therefore a function of the additives adsorption and reaction on the surfaces. Adsorption, desorption and reactions depend critically on the operating conditions temperature, sliding velocity and contact pressure. To obtain a friction coefficient for the whole working range of temperature, velocity and pressure, many measurements are required to describe the friction. The friction in the sliding interface of a wet clutch is often measured as output torque for one whole friction disc in contact with one steel separator disc. This is a good method to measure the final output from an existing wet clutch design, but if only the output torque is measured, the friction coefficient that can be computed for the clutch is simply the mean friction coefficient. Temperature and velocity are not constant in the interface, meaning that the friction is also not constant; see [44, 45].

To get a better understanding of how the friction can be described in terms of temperature, velocity and surface pressure, a testing method that measures more local effects has been developed.

B.2.1 Pin on disc

A special holder is developed for a pin on disc test to enable these local friction measurements for the material combinations used in wet clutch systems. In a pin on disc test, a stationary pin is loaded axially in contact with a rotating disc, as in the schematic sketch shown in Fig. B.1. The friction force on the pin can be measured, thus making it easy to compute the friction coefficient. The pin on disc machine used in these tests is a Phoenix Tribology TE67.

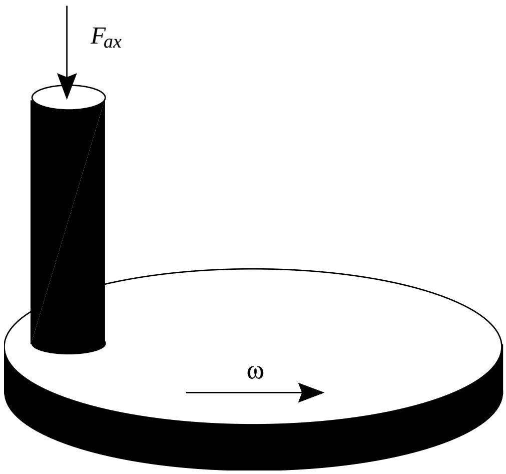

Figure B.1: Schematic sketch of a pin on disc apparatus

In these measurements, a special pin, Fig. B.2, is made which has a holder for a small specimen made of a friction disc, Fig. B.3. A thermocouple that

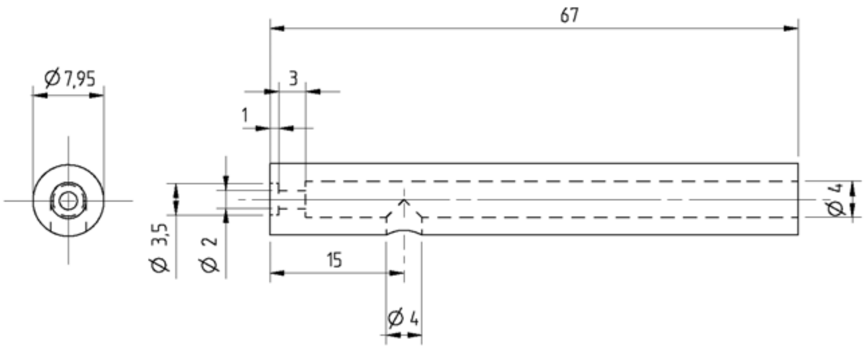

Figure B.2: Pin with holder for test specimen

measures the temperature at about 0.3 mm from the contact surface is inserted in the specimen. Since the specimen only has a diameter of 3.0 mm, a constant velocity and temperature can be assumed over the whole test specimen contact area. This makes the measured friction suitable to use in wet clutch simulations and gives a better understanding of the boundary friction. The friction material on the friction discs used in this investigation is made of sintered bronze.

The disc is designed as a holder for a piece of the steel separator disc used in the real wet clutch system. This means that the test specimen will have the same properties as the separator disc used in the clutch. The lubricant used in these experiments is a semi synthetic oil tailor-made for the Haldex Limited Slip Coupling, which is a limited slip differential manufactured by Haldex Traction AB. This application is further described in [9].

The friction measurements are in this case made to correspond with the working conditions of a wet clutch in a Limited Slip Differential, meaning that the sliding velocities will be fairly low while there will be quite high temperatures and surface pressures. The ranges for temperature, velocity and surface pressure and the resolution of the measurements are shown in Table B.1. The sampling rate during the measurements is 10Hz.

B.2.2 Test procedure

The tests start at an ambient temperature, 22°C, and the equipment is gradually heated during the measurements.

Before the test starts, the surfaces are run in with the test lubricant. The disc rotates at a speed of 100 revolutions per minute for 10 minutes with an

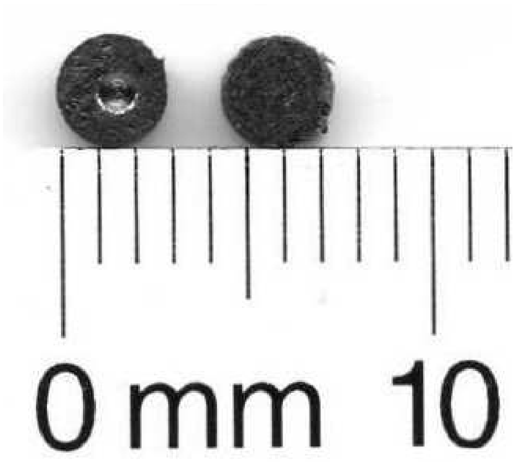

Figure B.3: Test specimens from bronze friction disc. Specimen to the left with drilled hole for thermocouple.

Table B.1: Working range and resolution.

	Working range	Resolution
Nominal Surface pressure, p [MPa]	4.0-8.0	
Temperature, T [°C]	22- 100	0.2
Rotational speed [rpm] $\Rightarrow$ Sliding speed, v [m/s]	0- 318 0- 0.5	1.0 0.0016
Friction Force, F_{fric} [N] $\Rightarrow$ Friction coefficient, μ [-]	0- 49	0.015 $< 5.3 \cdot 10^{-4}$

applied load, corresponding to a sliding speed of 0.15 m/s.

During the test, the velocity is increased from 0 to 0.5 m/s, followed by a decrease in speed to a standstill. The whole measurement takes about 30 seconds. When the test is finished, a heater is engaged to warm up the test equipment to the next temperature level and a new measurement is conducted. There is a temperature difference of 5 °C between the temperature levels. The total temperature range for which the friction is measured is 22-100 °C. The whole test series is therefore performed for 16 different measurements with different start temperatures.

B.3 Results and discussion

During each test the velocity is increased from stand still to 0.5 m/s and then decreased back to standstill. This variation in speed is not linear, and a typical velocity plot for the tests is shown in Figure B.4(a).

B.3.1 Temperature variation during test

The temperature in the test specimen increases due to frictional heating during the velocity increase. When the velocity is decreased, the temperature will decrease. This temperature behavior during the test is visualized in Fig B.4(b) for a start temperature of 25°C. It is obvious from this figure that there is no significant delay in the temperature measurement, indicating that the measured temperature is a good measure of the mean temperature in the sliding interface. The sliding interface is located about 0.3 mm from the thermocouple. The temperature measurement is also a good indicator that the temperature is very dependent on the surface heat flux, since the temperature will imme-

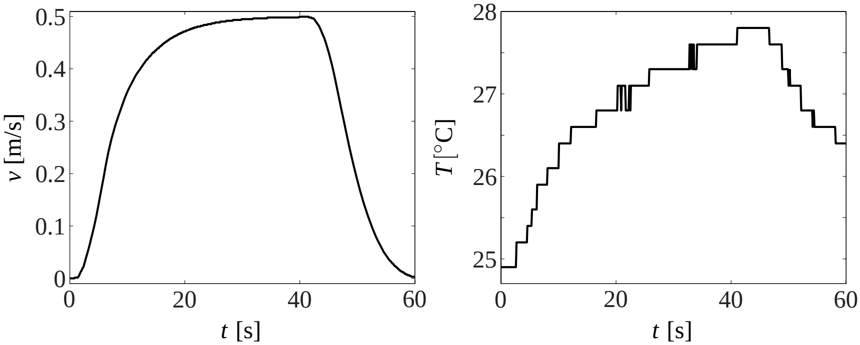

(a) Sliding speed (b) Temperature

Figure B.4: Temperature variation and sliding speed during one test cycle

diately start to decrease when the velocity is decreased; see Fig. B.4. The measured temperature in this point, 0.3 mm from the surface, will in this paper be referred to as interface temperature.

B.3.2 Friction measurements

To use the value of the friction coefficient in wet clutch simulations, or for a wet clutch control software, the most important is to describe the friction coefficient as a function of sliding speed, v, interface temperature, T, and nominal surface pressure, p. One test cycle in this pin on disc test will give this frictional behavior for one combination of friction material, lubricant and load. Results from the measurements can be visualized in differently. One way is to plot the friction coefficient as a function of sliding speed and interface temperature, as in Fig. B.5. The measurements are statistically very good with little spread between the measurements. There are basically two ways to describe the relationship between friction coefficient, sliding speed and interface temperature. A mathematical expression can be fitted to the measured friction data, or the data could be stored in a large matrix from which friction coefficients could be interpolated from nearby cases. A mix between these two methods can also be used [45]. The advantage with an approximated function is that it will not need a large storage space, and that is vital for control softwares with small memory capacities. Another advantage with this method is that the friction coefficient will be easy to compute. The disadvantage is the limited flexibility of the chosen expression that can only be applied for a

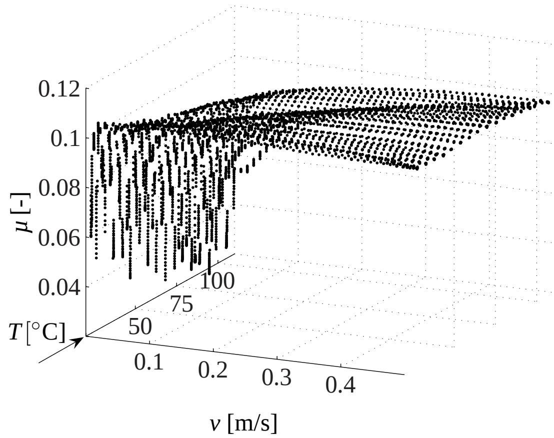

Figure B.5: Friction coefficient as function of sliding speed and interface temperature. Nominal pressure = 8.0 MPa

specific frictional behavior. For this case, the expression

$$\mu = a_1 + a_2 \cdot tanh(v \cdot a_3) + a_4 \cdot T + a_5 \cdot T^2 + a_6 \cdot T^3 + a_7 \cdot v + a_8 \cdot vT + a_9 \cdot (vT)^2 \tag{B.1}$$

gives a good approximation to the measured frictional data; see Fig. B.6. In this equation μ is the friction coefficient, v is the sliding velocity and T is the interface temperature.

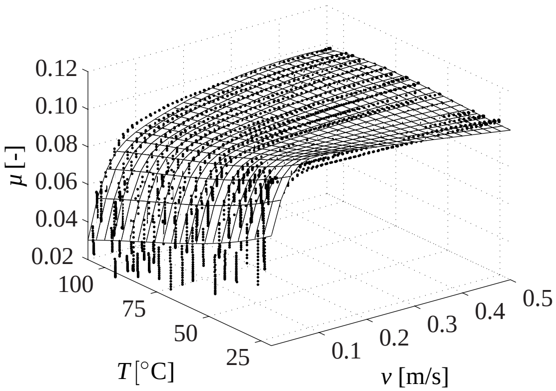

Figure B.6: Friction coefficient versus sliding speed and interface temperature. Measured data and approximative mathematical surface. Nominal pressure = 8.0 MPa. The mesh is the approximation according to Eq. B.1.

Another way to visualize frictional behavior is to use this expression and plot the friction coefficient as function of sliding speed for different interface temperatures; see Fig. B.7.

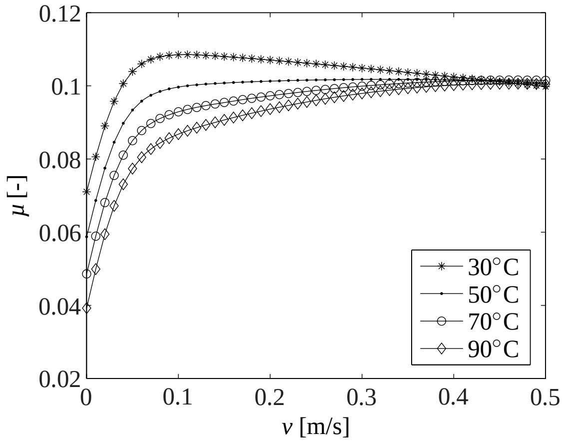

Figure B.7: Friction coefficient as function of sliding speed at different interface temperatures. Based on curve fitted mathematical surface. Nominal pressure = 8.0 MPa

B.3.3 Comparison with other test rig

Traditional friction measurements of wet clutches are performed in test rigs with one whole pair of friction discs [10, 36]. In [30], larger parts of a friction disc, including grooves, have also been tested in a pin on disc test. With this test method, where a small sample of the friction disc is tested, it is important to investigate the correlation with other performed tests. Figure B.8 shows a comparison between curve fits from the measured friction coefficient in the pin on disc and a wet clutch test rig [10] with nominal pressures of 8.0 MPa. Friction coefficients from the different measurements show the same trends in variation of friction coefficient throughout the whole range of speed and temperature. However, the friction coefficient is consistently slightly smaller in the wet clutch test rig measurements. The measured friction coefficient should not be exactly the same for the different test rigs, since grooves are not included in the pin on disc test.

The nominal pressure on the friction discs used in the Wet Clutch Test Rig is calculated for the net surfaced area in contact in the interface, i.e. the groove area subtracted from the total disc area. A smaller difference in this

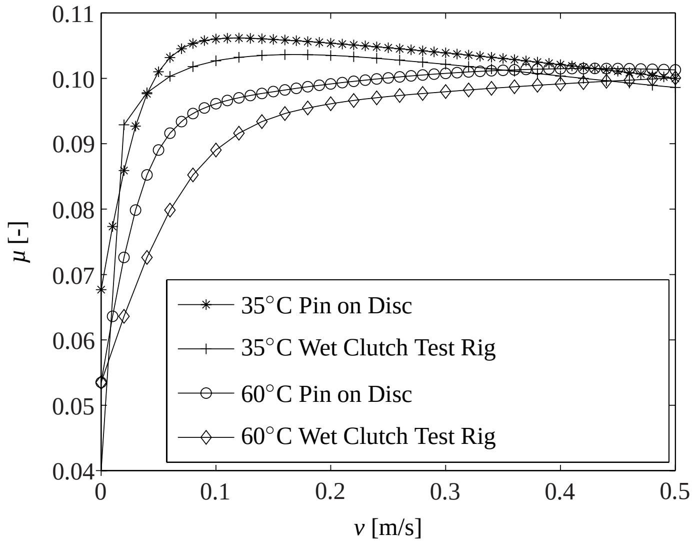

Figure B.8: Comparison between friction measurements in pin on disc and Wet Clutch Test Rig [10]. Nominal pressure = 8.0 MPa.

area from the manufacturing process of the discs, could affect the geometry of the friction material and therefore the net surface area and nominal pressure for a given axial load, which would then influence the friction coefficient's variation with pressure.

B.3.4 Load dependence

The normal load does not greatly influence on the friction coefficient in these measurements. The fact that the friction coefficient is not very load dependent has also been earlier observed in other experiments, such as Mäki [26]. Figure B.9 shows the friction coefficient for three different loads in the whole range of sliding velocity. Here, the largest difference in friction coefficient is about 5% at 30°C, Fig. B.9(a). At 50°C, Fig. B.9(b), the difference in friction coefficient at different loads is not very large; hence, at these temperatures and higher it is possible to describe friction coefficient as only a function of sliding velocity and temperature without loosing much precision. At higher temperatures, Fig. B.9(c) and B.9(d), the difference in friction coefficient for different loads is even smaller. The lowest friction coefficient is achieved for the medium pressure of the three investigated pressures. This makes the difference in friction coefficient to be dependent on the load less plausible. It is possible that the

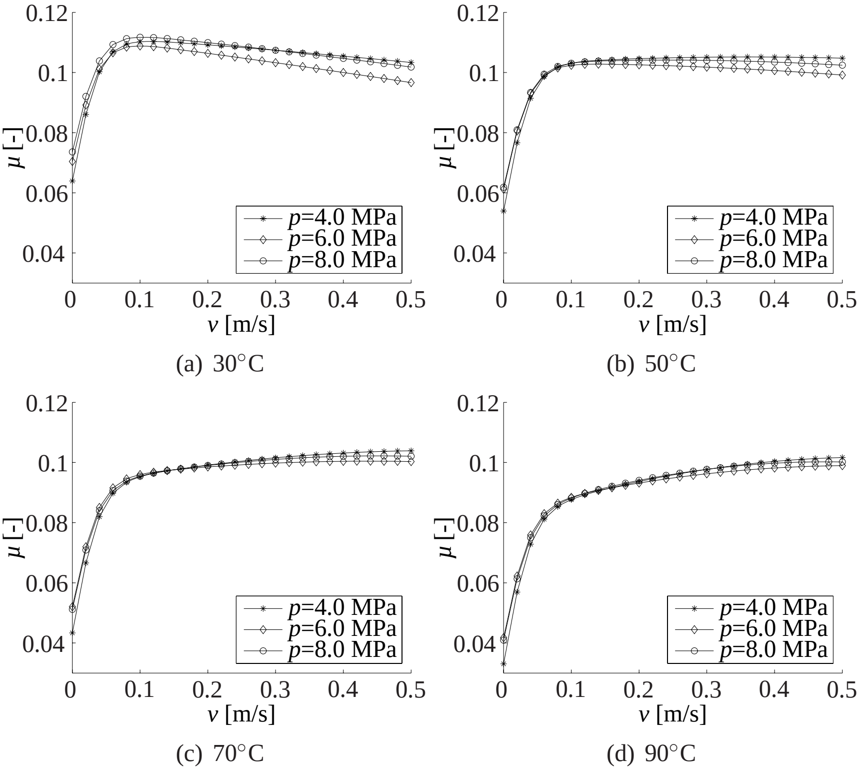

Figure B.9: The curve fitted mean friction coefficient, μ, from three measurements at each load is visualized for four different temperatures

difference in friction coefficient is instead dependent of other variables, such as surface structure and friction material composition, indicating that the friction coefficient could be described just as a function of sliding velocity and temperature for the whole temperature range. Figure B.9 also shows that for sliding velocities about 0.5 m/s, the friction coefficient, μ, will be about 0.1 for all investigated loads and temperatures.

B.3.5 Error analysis

As described in Section B.3.4 the difference in friction coefficient for different surface pressures is not large. The friction coefficient could therefore be described as a function of only interface temperature and sliding velocity without loosing much precision. As a measure of the deviation of the measured data for the maximum and minimum load, the maximum deviation from mean friction coefficient computed for maximum and minimum loads is visualized in Fig. B.10.

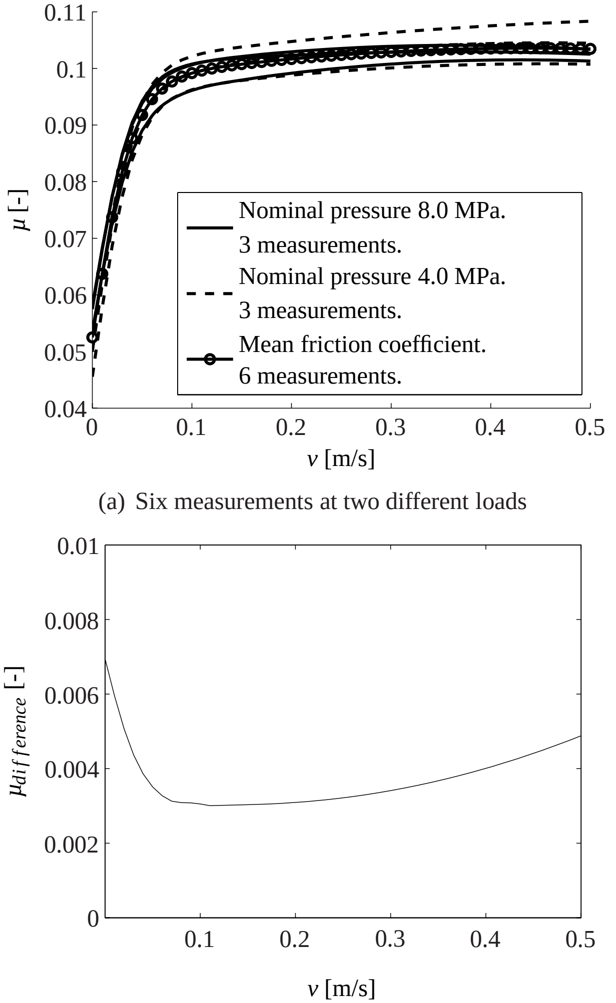

(a) Six measurements at two different loads

(b) Maximum difference of six measurements to mean friction coefficient

Figure B.10: Error analysis for six measurements with nominal pressures 4.0 and 8.0 MPa. Temperature 60 °C

Here, six subsequent measurements at two different loads are investigated. These measurements will contain over 60,000 measurement points over the measured region described in Table B.1. Figure B.10(a) shows plots from the curve fit expression (B.1) for each measurement at an interface temperature of 60°C. From these functions the mean friction coefficient for 60°C is computed. Figure B.10(b) shows the largest absolute deviation from the mean friction coefficient for each sliding velocity. This illustrates that the maximum absolute deviation in friction coefficient for these measurements in the velocity interval 0.05 - 0.4 m/s is less than 0.004.

B.4 Conclusions

A simplified experiment is developed where the boundary friction behavior of a wet clutch can be investigated in a pin on disc test. The advantages with this method are that it is inexpensive and time saving to test different combinations of friction materials and lubricants. This makes the method suitable for screening-tests where a large number of different combinations can be investigated. Another advantage is that the pin on disc test measures more local friction than what is possible with torque measurements from a test rig where whole friction discs are investigated. This local behavior is preferable when using measured friction coefficients in simulations, such as [45].

The fact that this test method is rather geometry independent can be an advantage. The hydrodynamic effects can be considered in a simulation of the clutch disc friction behavior, thus providing a possibility to study the effects of not only different materials, but also different groove geometry that otherwise could be quite expensive to investigate.

The results from the pin on disc test were compared with tests in whole friction disc test rigs. A good correlation between the different tests was achieved. Since this method does not test the complete friction disc it should be regarded as a complement of ordinary wet clutch test rigs and not a total replacement of those rigs.

The friction coefficient is not greatly affected by load at temperatures above about 50°C. Even for lower temperatures the load dependence is not substantial. At 30°C, the maximum difference in friction coefficient is about 5% between different loads, indicating an opportunity to simplify the friction coefficient function because a sufficiently accurate friction coefficent can be described as only a function of sliding velocity and interface temperature for many cases at a normal working temperature.

B.5 Acknowledgments

The authors would like to express their gratitude to colleagues at Statoil Lubricants, Haldex Traction Systems and Luleå University of Technology for their contributions to this work. Thanks also to the Swedish Foundation for Strategic Research (ProViking) and the Program Board for Automotive Research (PFF) for financial support.

Paper C

Permeability of sinter bronze friction material for wet clutches

Tribology Transactions, 2008 May; vol. 51, Issue 3, p. 303-309.

Permeability of sinter bronze friction material for wet clutches

P. Marklund and R. Larsson

Luleå University of Technology, Division of Machine Elements, Luleå, SE-971 87 Sweden

T.S. Lundström

Luleå University of Technology, Division of Fluid Mechanics, Luleå, SE-971 87 Sweden

Abstract

The characteristics of wet clutches are of great importance for the overall behavior of the drive trains of many modern vehicles. It is considered that the clutch characteristic is affected by the permeability of the friction material. The permeability is considered to influence both the time of engagement and the temperature in the clutch due to the lubricant flow in the permeable material. In this work, a permeability measurement method suitable for wet clutch friction materials is thus used to measure the permeability of a friction material made of sintered bronze. This friction material is suitable for applications such as limited slip differentials or other wet clutches which have to withstand high temperature and high torque transfer. The permeability is also investigated for friction materials with pressed groove patterns.

Wet clutch friction material permeability is often accounted for in simulations but the method used to measure the permeability is seldom described.

The permeability of the investigated friction material is shown to be so small that it hardly will affect the temperature in the material due to cooling oil flow inside the material. However, the engagement time can be influenced by the permeability. It is also shown that pressed groove patterns can seal the friction material so that it becomes almost impermeable.

C.1 Introduction

Wet clutches are often used in modern vehicles to distribute torque in transmissions and drive trains. The characteristics of these clutches are of great importance for the overall behavior of the vehicle. There are many properties of the clutch affecting the friction characteristics, such as materials, lubricants, surface roughness and permeability of the friction material. The permeability, i.e. the possibility to a fluid flow inside the friction material, is considered to decrease the time of engagement and to allow a cooling flow in the friction material. The time of engagement could be decreased due to smaller squeeze film effects on the contact areas of the friction discs and internal temperature could be decreased due to fluid flow in the material.

The permeability is one of the input parameters in many simulation models developed for wet clutches [19–24]. However, the method used to obtain the permeability for the friction material is normally not thoroughly described. The value of permeability is also widely varied between roughly $1 \cdot 10^{-15}$ and $1 \cdot 10^{-11}$ m^2 in the simulation models. The effects of the permeability are often not studied but in some work, e.g. [18, 21, 23] the permeability is varied and the influence on, for example, torque transfer during clutch engagement is investigated. However, it is not investigated how groove patterns in the friction material can influence the permeability.

Measurements of permeability range all way back to 1856 when Darcy did his experiments on sand [46]. During the latest decades much effort has been spend on methods to measure the permeability of materials having a sheet like form in connection to composites manufacturing [35, 47, 48] and making of paper [49]. For wet clutch friction materials little has been done so far. Chavdar's investigation [50] on paper based friction materials is one example of a permeability measurement made especially for wet clutch friction materials. However for thin layers of sintered friction materials there is not much work done. To get a better idea of the permeability of friction material from sintered bronze this investigation is made. It is also investigated how the permeability changes due to density of the porous friction material and groove patterns. The sintered bronze friction material investigated here is similar to the material investigated by Beavers [51] for a naturally permeable wall but the layer is much thinner. This material is used in heavy duty wet clutches which are working under limited slip conditions, i.e. limited slip during a long time with high surface pressures and torque transfer. An example of a friction disc with this friction material is shown in Fig. C.1. The grooves visible in Fig. C.1 are pressed in the friction material to make a larger cool flow possible between the friction discs even when the clutch is working under boundary lubrication condition, i.e. surfaces in contact with each other.

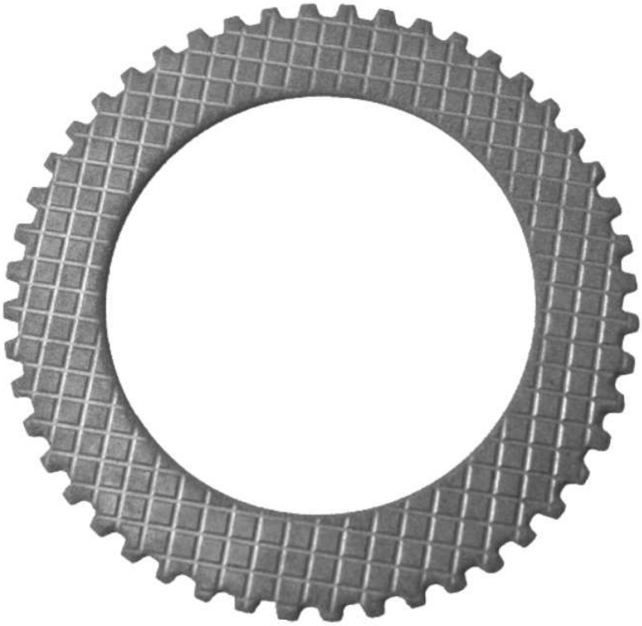

Figure C.1: Friction disc with grooves. Friction material of sintered bronze.

The permeability investigations are made in a test rig [35] originally designed to measure permeability in different textile materials such as press fabric used in paper machines. Different densities, hence porosity, of the friction material is investigated to see how this influences the permeability.

The groove pattern on the friction disc in Fig. C.1 is pressed after the sinter process of the friction material. Because of this way of manufacture the friction discs there is a possibility that the groove walls will be so dense that the fluid flow into the material will be prevented. This is why the investigation of the permeability of the friction material is extended to include also an investigation of how transversal grooves will influence the permeability.

C.2 Method

The flow through the material in one direction is measured by the use of an experimental method described by Lundström et.al. [35]. In the wet clutch application, where the friction material is used, the permeability property is supposed to cool down the friction disc as well as reduce the time of engagement. The permeability value depends on the internal structure of the material as well as the porosity. Since special test specimens have to be manufactured for the tests, it is important that the friction material used in the investigation is manufactured in the same way as the original friction discs.

C.2.1 Test rig

The test rig used is originally developed for permeability investigations of textile materials such as press fabric used in paper machines and fiber mats for different composites [35]. The rig is constructed so that different test cells can be used depending on the investigated material. Such a cell can, for instance, be designed for parallel flow measurements in plane or out of plane. In these measurements the in-plane parallel flow cell is used to measure the permeability in rectangular shaped specimens.

The test cell, see Fig. C.2, is designed as a holder for rectangular test specimens with a thickness between 1 and 5 mm and is sealed at the edges perpendicular to the flow. On top of the test specimen a closing cap is placed to prevent any flow to pass over the specimen instead of going through the permeable material. The specimen is also sealed between the cap and the test cell with a rubber layer to make sure that all flow passes through the material.

One difficulty of this method is to obtain a precise fit between the test cell and the specimen. A specimen misfit can result in leakage or suppressed flow along the sides of the sample which will influence the permeability values. Therefore the center bulk flow is separated from the edge flow so that possible leakage can be measured separately and will not influence the bulk flow measurement. The presented flow and permeability values are the values from measurements of the center bulk flow covering the middle 60% of the specimen width.

The pressure gradient through the test specimen is considered to be linear between the measured inlet pressure, p_{inlet}, and the ambient pressure, p_{amb}. The pressure transducer (WIKA type 891.13.500) is placed next to the inlet hole, see Fig. C.2, while the temperature is measured at the inlet with a thermometer (GEFRAM PT100) to be able to calculate the density and the viscosity of the fluid that is flowing through the permeable material. The mass of the fluid that is transported through the permeable test specimen is then measured with two separate balances (Precisa 3100D), one for the bulk flow and one for the edge flow both with a precision of 0.1 gram.

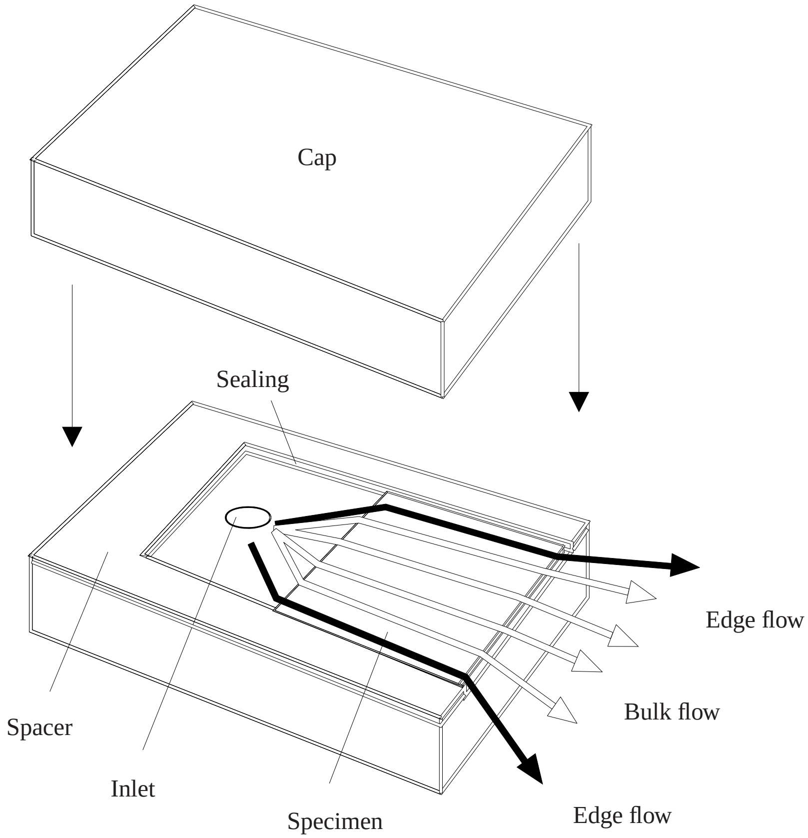

Figure C.2: Test cell for parallel flow

C.2.2 Test specimens

The test specimens are made of a rectangular steel backing plate which is covered with powder of bronze that forms the friction material layer, see Fig. C.3. The friction material is sintered to a porous structure and then the surface is flattened. This is the same manufacturing process as normally used for manufacturing friction discs with friction material of sintered bronze. However, the specimens used in this measurement only have friction material attached on one side in contrary to most of the friction discs used in wet clutches. Since the significance of the friction material density is of interest, test specimens with three different densities of friction material are investigated. The different densities give variations in porosities which are roughly estimated in Table C.1.

The dimensions of the test specimens are shown in Table C.2.

Table C.1: Estimates of porosity for friction material with different density.

Density	Porosity [%]
Normal	57
High	55
Low	61

Table C.2: Dimensions of test specimens.

	Type 1	Type 2
Size [mm]	30 x 100	45 x 100
Steel thickness [mm]	1.0	1.0
Friction material thickness [mm]	0.6	0.6

Since most of the friction discs used in wet clutches have some kind of a groove pattern it is of interest to see how the grooves are influencing the over all permeability of the friction material. Test specimens with and without pressed grooves are investigated, see Fig C.3. The groove pattern in Fig. C.3(a) consists of pressed grooves with a depth of 0.3 mm and a with of 1.5 mm, according to Fig. C.4. The spacing between the grooves is 6 mm.

(a) Groove pattern orthogonal to the flow direction

(b) Without groove pattern

Figure C.3: Examples of test specimens used for the permeability measurements.

C.2.3 Friction material analysis

A Scanning Electron Microscope (SEM) is used to investigate the surface of the friction material. The investigated specimen has a friction material with a normal density according to Table C.1. Figure C.5(a) shows a larger area of the surface and the porous structure of the friction material is clearly seen.

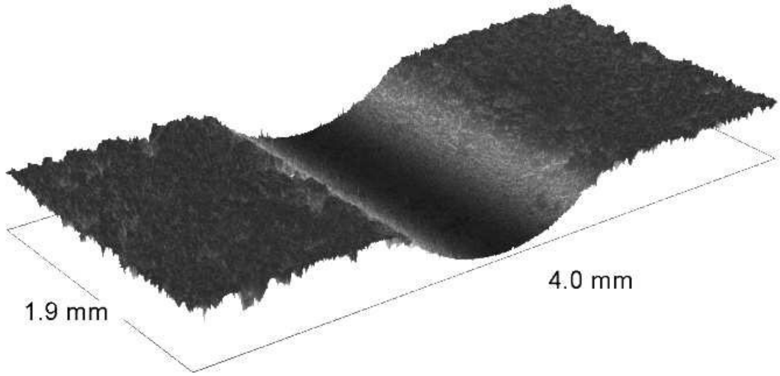

Figure C.4: Topographic picture of pressed groove.

The few contact areas are also easy to locate on the very rough surface. This structure gives large connected pores in the surface interface layer when the friction material is in contact with the quite smooth steel counter surface like the steel separator discs in the clutch.

Figure C.5(b) shows the same surface with a higher magnification. This shows the structure of the powder used in the friction material.

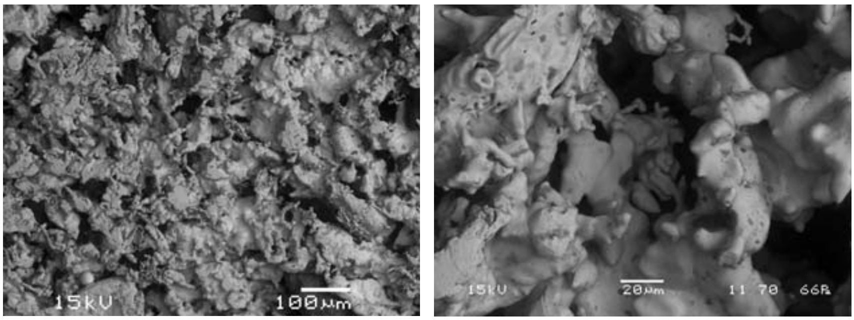

(a) Magnification 100x (b) Magnification 650x

Figure C.5: SEM pictures of friction material surface.

To see how dense the friction material is at the grooves, a cross section of one test specimen is investigated in an optical microscope, see Fig. C.6(a). In this figure it is possible to see that the material between the groove and the steel backing plate is quite dense and that there are much less pores in this area than on the sides of the groove where the material is not much compressed. As told in section C.2.2 this groove is 1.5 mm wide and 0.3 mm deep.

The groove in Fig. C.6(a) can also be compared to a similar cross section, Fig. C.6(b), of a groove from a manufactured friction disc, Fig. C.1. This

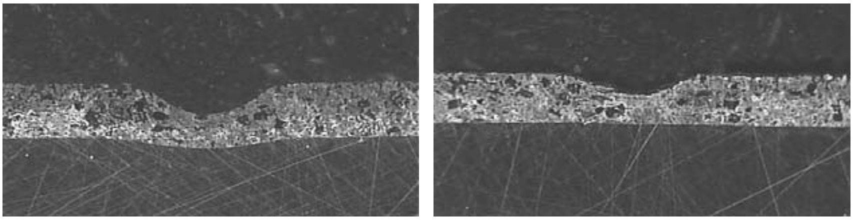

(a) Cross section of groove. Test specimen. (b) Cross section of groove. Friction disc for a wet clutch.

Figure C.6: Cross sections of test specimen and manufactured friction disc for a wet clutch analyzed in an optical microscope.

groove is slightly less deep compared to the grooves used in this investigation. However, the steel backing plate is made of steel with much higher strength than the one used for the manufacturing of the test specimens. This is why the steel backing plate in Fig. C.6(b) is virtually undeformed under the groove. The thickness of the material between the groove and the steel backing plate could therefore be regarded as quite similar to the thickness of the pressed groove material in the test specimen. It is also obvious that the material is quite dense in this friction lining too which would indicate a very low permeability for the friction material on this disc.

C.2.4 Fluid

The fluid used is water which is held in an absolute pressure of about 10^4 Pa for several hours to make sure that solved gases are separated from the water. Water is used because it is a convenient fluid to work with, it has well known properties and quite low viscosity. The low viscosity means that the flow rate for a certain pressure gradient will be larger than for a more viscous fluid, like oil, meaning a more exact measurement. The type of fluid used in the measurement does not influence the measured permeability value since permeability is a material constant and not only valid for a certain combination of material and fluid.

C.2.5 Measurements

In all tests, the measurements are made in a random order. The time of measurement is between 1 and 10 minutes for a non grooved specimen and up to 30 minutes for a grooved specimen. Each test is stopped when a steady state flow is observed. The measured mass flow will reach steady state when there is no air present in the pores of the specimen and all the pipes leading to the balances are filled with fluid. For a material with high permeability the flow will often reach the steady state faster, hence give a shorter necessary time of measurement. The permeability values showed in section C.3 are the mean permeability values during the steady state part of the measurement. The temperature in test specimen, test rig and fluid is kept at ambient condition throughout the test.

Measurements are made in a random order and the time of measurement is between 1 and 10 minutes for each test. The measured value of permeability, K, is for a steady state flow in the porous media. Two measurements are made for each test specimen in combination with each investigated counter surface.

C.2.6 Permeability model

The flow in the permeable material is governed by the one dimensional form of Darcy's law [52]

$$\frac{\dot{V}}{A_{cs}} = -\frac{\partial p}{\partial x}\frac{K}{\eta}. \tag{C.1}$$

Here $\dot{V}$ is the volumetric flow in the direction of the flow, x, A_{cs} is the cross section area of the permeable friction material, p is the pressure, η is the fluid viscosity and K is the permeability factor. If the pressure gradient is assumed to be constant through the whole specimen, the equation can be written in the form

$$K = \frac{\dot{V}\eta w_f}{A_{cs}\Delta p} \tag{C.2}$$

[35], where w_f is the length of the specimen in the flow direction and $\Delta p = p_{inlet} - p_{amb}$. The fluid viscosity, η, is easily calculated from the measured inlet temperature using a temperature-viscosity relationship. The mass flow is measured, implying that the volumetric flow can be obtained if the density of the fluid is known. The temperature-density relationship of the fluid is used in order to estimate fluid density. This gives us the final expression:

$$K = \frac{\dot{m}\eta w_f}{A_{cs}\rho(p_{inlet} - p_{amb})}, \tag{C.3}$$

where ρ is the fluid density and $\dot{m}$ is the measured mass flow.

For the fluid flow to be governed by Darcy's law the fluid should be Newtonian and incompressible and the Reynolds number should be much less than 1. For reliable input data it is also important that the viscosity of the measured fluid is fairly constant during the measurements.

If two permeable materials are placed in layers like in Fig. C.7 the total

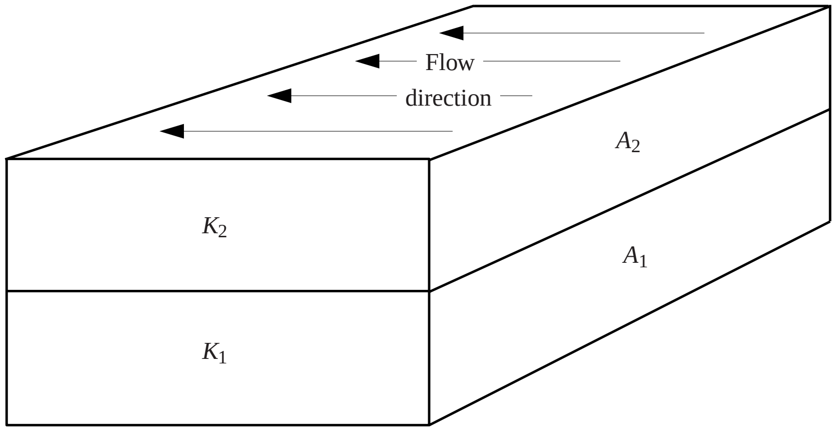

Figure C.7: Interaction between two permeable layers.

cross section area is the sum of the cross section areas of the two samples as

$$A_{tot} = A_1 + A_2. \tag{C.4}$$

Then the total permeability, K_{tot}, of both layers could be described with

$$K_{tot} \cdot A_{tot} = K_1 \cdot A_1 + K_2 \cdot A_2. \tag{C.5}$$

If the permeability of layer 2, K_2, is of interest and K_{tot} and K_1 is measured, K_2 can easily be solved as

$$K_2 = \frac{K_{tot} \cdot A_{tot} - K_1 \cdot A_1}{A_2}. \tag{C.6}$$

C.3 Results and discussion

The results are divided into two parts:

The first part, in section C.3.1, is an investigation of the permeability of the bulk material and in surface top layer. To see how large the flow can be in the bulk material, first the surface of the test specimens are sealed so that no fluid can flow on top of the specimen. This is then compared to measurements where the seal is replaced with a steel counter surface. This measurement corresponds well to the case in a real wet clutch application. Many pores are open and connected with each other in the interface between the friction material and steel separator disc and a great deal of the liquid can flow through this surface porosity. The difference between these two cases show the distribution between bulk and surface flows.

The second part, in section C.3.2, is focused on the influence from the groove patterns on the bulk permeability of the friction material.

C.3.1 Bulk flow versus surface flow for friction material without grooves

The permeability value, K, is investigated for test specimens with different density and porosity according to Table C.1. All specimens are tested with a sealed top surface and a steel counter surface to be able to measure the permeability of the bulk material as well as the permeability of the surface layer.

Figure C.8(a) shows the measurement made with a sealed surface. The value of K is obviously dependent of the density of the friction material since K is varying between roughly $2.5 \cdot 10^{-13}$ m^2 for a high density specimen and $10 \cdot 10^{-13}$ m^2 for a low density one. The permeability of the friction material with normal density is about $5 \cdot 10^{-13}$ m^2, see Fig. C.8(a). From Fig. C.8(a) it is also obvious that the variation between different measurements is fairly small.

This bulk permeability of the friction material is often used to describe the permeability properties of a friction material for wet clutch friction discs. However, in a real application the friction material is normally in contact with the relatively smooth surface of the steel separator disc. Because of the rough surface of the friction material there will be a percolating flow in the interface layer between the friction material and steel separator disc. Hence the total permeability of interest in such a wet clutch application is the total permeability computed on the total bulk flow and surface flow. This total permeability is shown in Fig. C.8(b). The total permeability in Fig. C.8(b) is between $30 - 75\%$ higher than the bulk permeability in Fig C.8(a). This indicates the importance of measuring the permeability of a complete system insted of just the bulk properties, if the permeability is going to be used to estimate the total porous flow in an application such as a clutch or a porous bearing.

The permeability in the surface layer can be computed with Eq. (C.6) if

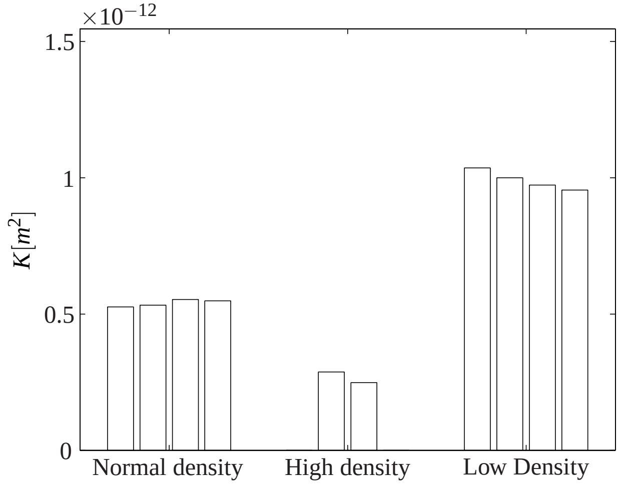

(a) Sealed

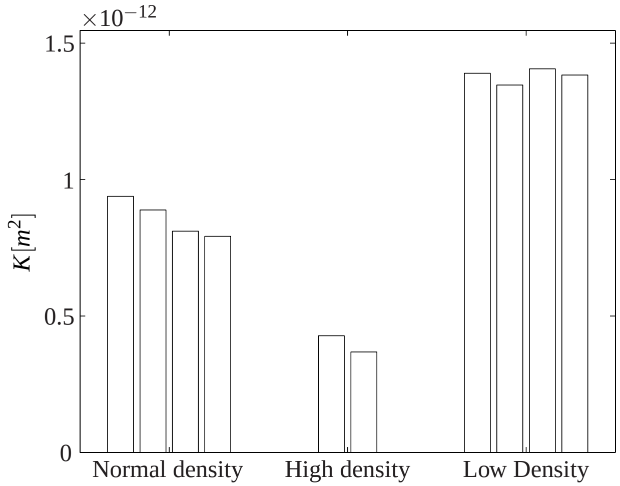

(b) Steel counter surface

Figure C.8: Permeability for different density of friction material. Values for sealed test specimen and test specimen with a steel plate counter surface.

the thickness of the permeable interface layer is known. If 50% of the height from the Abbot-Firestone bearing ratio curve is regarded as the thickness of the permeable surface layer the permeable surface thickness is roughly 60 μm for the sintered friction material in this investigation. This gives the surface permeability shown in Fig. C.9. This could be used as a permeability value for the surface if it is of interest to separate the bulk flow from the interface flow and that is a more correct way of treating the bulk and surface flow. However in many simulations when the flow in the porous media is of interest, e.g. cooling oil flow in temperature simulations for wet clutches, the combined permeability in Fig. C.8(b) can give a easy and enough accurate description of the flow.

The permeability measured in this investigation can be compared to the permeability used in simulations earlier. One common value of the permeability [19, 21] in a friction material for wet clutches is $1 \cdot 10^{-13}$ m^2. This value is smaller than the results showed in Fig. C.8. However, the materials in [19, 21] are paper based and the permeability could therefore be different compared to the measured permeability in Fig. C.8.

C.3.2 Friction material with and without grooves

The results from section C.3.1 show the permeability in the bulk material as well as in the surface layer. To get an idea of how the bulk permeability alters when the friction lining is covered with a pressed groove pattern, like in Fig. C.1, the permeability is investigated for test specimens with a pressed groove pattern according to the description in section C.2.2. The groove pattern is built up by grooves that are perpendicular to the flow direction, Fig.

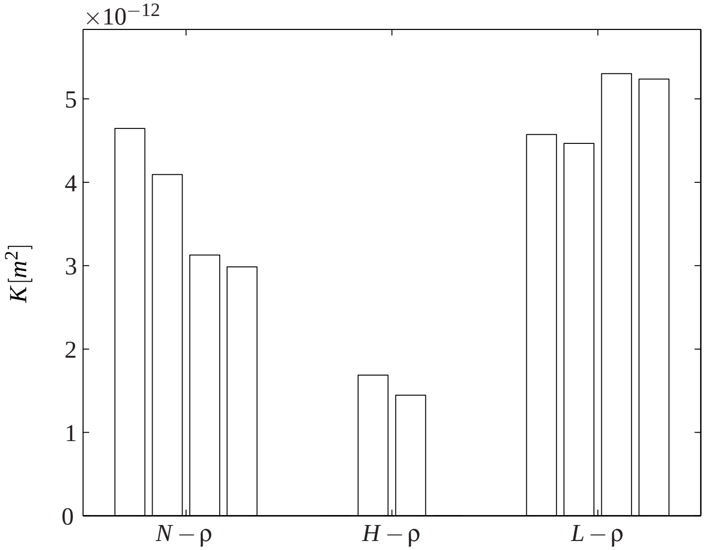

Figure C.9: Permeability of porous interface layer.

C.3(a). The bulk permeability is measured before and after the groove pattern is pressed which gives an indication of how a groove pattern can change the overall permeability of a friction lining on a friction disc. Test specimens with three different densities are used and results from the measurements are shown in Fig. C.10 where the three test specimens are marked in Fig. C.10 as 1,2 and 3. The permeability for grooved test specimens are the black bars.

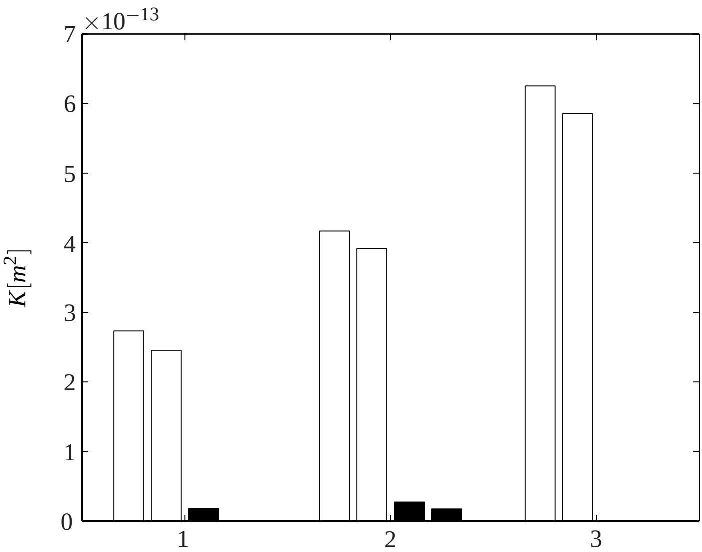

Figure C.10: Permeability for different densities before and after groove pattern is pressed into the friction material. Test specimens with groove patterns are marked with black.

The permeability, K, is greatly influenced by the pressed groove patterns and K is reduced by an order of magnitude in all measurements. In one of the measurements, test specimen 3, the specimen became totally impermeable after the groove pattern was pressed. These results indicates that pressed groove pattern in sintered wet clutch friction materials can make the friction material impermeable even if the original sintered structure is permeable.

C.4 Conclusions

The test rig used in this investigation is suitable to measure permeability in wet clutch friction materials. Normal thickness and density of the friction material can be used in the measurements. This is important to obtain a correct permeability value that is possible to use in simulations and comparisons with other materials.

Different types of friction materials can easily be investigated since the geometry of the measured test specimens is suitable to measure the permeability of thin layers of wet clutch friction materials.

The measured permeability of a sintered bronze friction material differs somewhat from permeability values of paper based materials in other publications.

For a sintered friction material the permeability is much influenced by the density of the friction lining.

Since the friction material most often is in contact with a relatively smooth separator disc in the wet clutch, it is important to measure the permeability under similar conditions. The permeability in the surface interface is of the same order of magnitude as the permeability in the bulk friction material.

When groove patterns are pressed into a sintered friction material the permeability is much decreased. This means that the total permeability could be quite low even if the measured bulk permeability for the material in the friction lining without groove pattern is relatively large.

When comparing permeabilities for different types of friction discs, e.g. different materials, densities, surface roughness and groove patterns, it is of great importance to investigate the permeability for the specific friction material that is of interest. All mentioned parameters influence the porous flow, so it is hard to predict the permeability from other measurements if not the specific combination of parameters is investigated before.

From this investigation it is also concluded that the permeability of the friction material is so small that the possible cooling oil flow in the permeable material, with the pressures present in a wet clutch, probably will be insignificant.

C.5 Acknowledgments

The authors would like to thank the colleagues at Haldex Traction Systems, Statoil Lubricants and Luleå University of Technology for their contributions to this work and Prof Staffan Toll at Chalmers University of Technology for facilitate the usage of the permeability test rig . The SEM investigation is made together with Mr Jens Hardell and his help is very appreciated. Thanks also to the Program Board for Automotive Research (PFF) and the Swedish Foundation for Strategic Research (ProViking) for financial support.

Paper D

The influence on boundary friction of the permeability of sintered bronze

Tribology Letters, 2008 July; vol. 31, no. 1, p. 1-8.

The influence on boundary friction of the permeability of sintered bronze

P. Marklund, K. Berglund and R. Larsson

Luleå University of Technology, Division of Machine Elements,
Luleå, SE-971 87 Sweden

Abstract

Components made of sintered bronze are often used in tribological systems. Examples of applications are self lubricated bearings, wet clutches and brakes and synchromesh components for manual gearboxes. The bronze material in these applications is often porous and permeable. However, the required level of permeability *i.e.* the ability for a fluid to flow inside the material varies widely for different applications. This implies the need to investigate if the permeability can influence the properties of a tribological system. Various studies have been performed in order to investigate the permeability of different materials but a possible relationship between permeability and boundary lubrication performance has not yet been thoroughly investigated. In this paper this relationship has been investigated in a pin on disc apparatus for test specimens with a permeability that is well-defined. Materials with three different permeabilities were investigated together with non-permeable test specimens. The results indicate that permeability has a small influence on the friction coefficient when the tribological system is operating with good lubrication of the contact. The function of the tribological system when working under starved conditions is also investigated and a very clear relationship between permeability and the ability to cope up with starved running conditions is shown. This is explained in terms of the varying ability of the materials' to store lubricant in pores. Non-porous test specimens were also tested as a comparison with the permeable test specimens in the investigation with starved running conditions. The results show that a material with high permeability works much better under starved running conditions than that with low permeability.

D.1 Introduction

Materials with a porous permeable structure made of sintered bronze are frequently used in lubricated tribological systems such as wet clutches, wet brakes, self lubricated bearings, and synchromesh components in manual gearboxes. Well defined and stable friction characteristics and the ability to work for shorter periods of time under starved conditions are examples of desired features in these applications. Applications where sintered bronze materials are used may work under various lubrication conditions, fully flooded or starved. Starved conditions could for instance occur in a wet clutch which is working with a shortage of lubricant due to a leaning vehicle, or a self lubricated bearing where the small amount of lubricant supplied when manufactured has to last during its entire lifetime. The porous permeable structure of the bronze material is thought to work as a reservoir for the lubricant. It is, therefore, of interest to investigate how permeability influences the boundary lubrication friction of a system where a sintered bronze material impregnated with lubricant is sliding against a smooth and dry steel surface.

Earlier permeability investigations of sintered bronze materials [53] have shown that the permeability is too low to allow a significant flow through the material. Permeability can not, therefore, influence the temperature of the material much by the action of the cooling flow through the pores. These earlier investigations also showed that pressed groove patterns on friction discs used in wet clutches and brakes can further reduce the permeability in the groove walls to such an extent that the groove walls can be almost completely non-permeable.

To the authors' knowledge there are no earlier investigations on the influence of bronze material permeability on boundary lubrication friction. Permeability itself, however, is often taken into account in simulation models of wet clutches [19–24] where it is a factor influencing engagement time, but the prospective dependency between permeability and boundary lubrication friction is not considered. This is also not a factor in investigations on permeability of wet clutch friction materials such as [50, 53].

Permeability is also an important factor in simulation models for porous bearings [54–56] and the frictional behavior has been experimentally validated for some types of bearings [56]. These publications point out the importance of pores in the material in order to obtain proper bearing function, but the investigations focus on how the bearings can maintain full film lubrication even if no extra lubricant is added. The influence of permeability on frictional behavior when working under boundary lubrication conditions therefore is not investigated to any degree.

In this investigation, test specimens used in the permeability study [53] have been used in pin on disc friction tests according to a method developed by the authors [57]. This enables investigations of frictional behavior, *i.e.* how friction varies with contact temperature, contact pressure and sliding speed, for materials with different permeability.

D.2 Method

Tests are carried out using a pin on disc set-up according to a technique developed for wet clutch friction materials [57], where a small test specimen as described below in section D.2.1 is mounted in the stationary pin and the rotating disc is made from the steel separator disc material used in a wet clutch. The pin on disc machine used in this investigation is a Phoenix Tribology TE67. Test specimens made for the pin on disc tests are cut out from the test specimens used in the permeability measurements [53] with spark erosion. The specimen is mounted in a holder in the stationary pin with the wet clutch friction material facing the rotating disc. Temperature is measured with a thermo couple mounted inside the friction material in a hole from the back of the specimen at about 0.3 mm from the sliding interface. The counter surface is a disk manufactured from the same carbon steel material and with the same hardening processes as the separator discs used in a wet clutch. More information about the measurement technique is found in [57] where the test method is described in detail. Another investigation with some similarities to this test method is presented by Ost et al. [30] but in that investigation the test specimens are much larger and made from a wet clutch friction disc with groove patterns.

D.2.1 Test specimens

The friction material used in the test specimens is a material made of sintered bronze which is shown in Fig. D.1 where the permeable structure of the material is shown. Two different kinds of test specimens are used in this investigation. They are shown in Fig. D.2. The test specimen on the right hand side in Fig. D.2 is a test specimen with porous and permeable edges shaped by the spark erosion manufacture of the specimens. Spark erosion is a preferable method because of the small zone affected by heat, whereby the structure and other properties of the materials of the samples do not change. The diameter of the cylindrical sample is 3.0 mm.

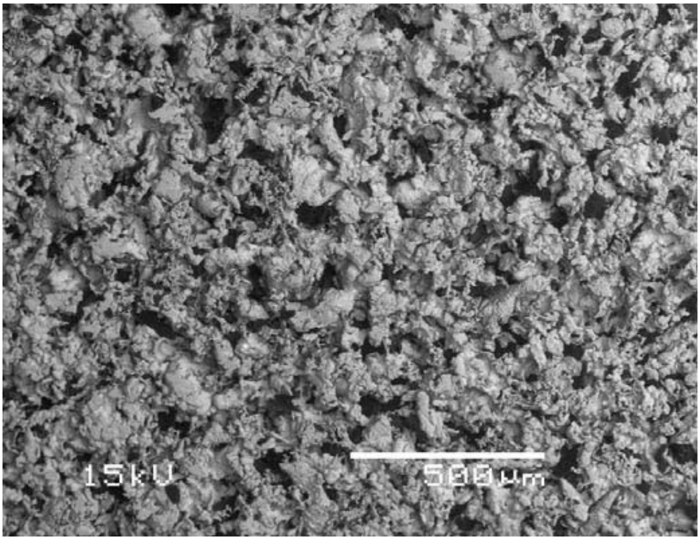

Figure D.1: SEM picture of permeable bronze material used in test specimens.

Since the permeability measurements in [53] showed that a pressed groove pattern can decrease the permeability of the friction material to a non-permeable state, the pin on disc tests were extended to include measurements on test specimens with a pressed edge around the test specimen to seal off the edge. This type of test specimens is shown on the left hand side in Fig. D.2. The test specimens with "‘sealed edges"’ also have a contact area against the rotating disc of 3.0 mm, which is the same as for the test specimens with "‘porous edges"’, but the side of the test specimens which is mounted in the pin is 5.0 mm in diameter. Test specimens with three different permeabilities according to [53] and non-permeable test specimens are used in the investigations, see Table D.1.

Table D.1: Permeability of test specimens

Term	Permeability (m^2)
High	$1.0 \cdot 10^{-12}$
Normal	$0.55 \cdot 10^{-12}$
Low	$0.25 \cdot 10^{-12}$
Non-permeable	-

Figure D.2: Test specimens used in pin on disc tests. Left hand side: sealed edges. Right hand side: porous edges. The contact area of both test specimens is circular with a diameter of 3.0 mm.

D.2.2 Lubrication and test procedures

Frictional behavior is normally investigated for a flooded state, as in [57], but here tests are also carried out under starved conditions. The lubricant used in the investigation is a commercial semi-synthetic lubricant developed for use in Limited Slip differentials with friction discs made of sintered bronze. To fill up the pores in the test specimen with lubricant or "‘impregnate"’ the test specimens with lubricant before the starved tests, the specimens are put into the lubricant and the surrounding pressure is decreased to an absolute pressure of about 10^4 Pa with a vacuum pump. This makes the air inside the pores exit the material. The lubricant fills the pores of the friction material when the surrounding pressure is restored to normal atmospheric pressure.

The total investigation consisted of a total of five different types of tests. All the tests were carried out in the pin on disc apparatus where the small test specimens, see Fig. D.2, were mounted in the stationary pin. Four different permeabilities according to Table D.1 were used for the tests and both test specimens with porous and sealed edges were investigated for all four permeabilities. The nominal surface pressure is 8.0 MPa in all the tests.

The five tests were:

1. **Tests with good lubrication**
   Friction was measured with the rotating disc and the test specimen mounted in the pin submerged in the lubricant. Working conditions in these tests comprised sliding speeds of 0-0.5 m/s and temperatures of 20-100°C.

The sliding speed was increased from 0 to 0.5 m/s in 60 s and then decreased to standstill in 50 s. This was repeated for every 5°C step in start temperature from 20°C up to 100°C. This start temperature was generated with an external heater of the test rig.
This test investigated the normal frictional behavior when working under normal lubrication.

2. **Tests with poor lubrication**
   The same test specimens were used in all four tests, 2a- 2d. The first three tests, *i.e.* 2a- 2c, were made to show the frictional behavior before, during and after running a long time under starved conditions. Test 2d showed if the tribological system could work properly after extensive wear if the old lubricant was changed to new lubricant.

   (a) **Frictional behavior before severe wear.**
   The frictional behavior was investigated with a similar variation in sliding speed as in the lubricated test, 1. Measurements were made at a temperature of $\sim$30°C for test specimens impregnated with lubricant working under starved conditions *i.e.* no lubricant is present except the one in the pores of the material.
   This test investigates whether the tribological system works according to the behavior observed in test 1 where there is a good lubrication even though it works a for a short period of time under starved conditions.

   (b) **Long wear sequence**
   Friction was measured under starved conditions with test specimens impregnated with lubricant. The test duration was 3 hours which would lead to severe wear of the mating surfaces. The sliding speed was constant at 0.2 m/s and there was no external heat generation of the test rig so all heat generated was due to friction inside the sliding contact.
   This test investigates endurance of the tribological system when working for a long periods of time under starved conditions. The test is designed to show how the system is influenced by the permeability, or the ability to supply lubricant to the contact from the pores in the material. Both the changes in friction coefficient and the wear of the surfaces are of interest to see the damage to the tribological system, but the main interest is in the change in frictional behavior as an indication of the state of the contact.

(c) **Frictional behavior after severe wear.**
This was basically the same investigation as test 2a, but carried out after test sequence 2b where the test specimens were worn, the permeable surfaces were clogged by wear particles and the lubricant and its additives were consumed. During the wear sequence in test 2b, the lubricant was totally consumed: there was no lubricant left in the pores and there was a dry contact between the test specimen and the disc.
This test investigated the frictional behavior for a worn system working under starved conditions.

(d) **Frictional behavior after severe wear when lubricated with fresh lubricant**
The worn test specimens were covered with fresh lubricant and the frictional behavior was investigated for a variation in sliding speed between 0-0.5 m/s at temperature $\sim$30°C.
This test investigated the frictional behavior for a worn system working under normal lubricated conditions and the ability of the lubricant to restore the function of the worn tribological system.

D.3 Results and discussion

The results of the various tests are presented in sections corresponding to section D.2.2.

D.3.1 Tests with good lubrication; test 1.

In test 1 the normal frictional behavior for the tribological system was investigated using the method described in [57]. The results from test 1 for test specimens with porous and sealed edges are shown in Fig. D.3. With good lubrication of the contact there is no great difference in behavior between the test specimens with porous edges, Fig. D.3(a), and sealed edges, Fig. D.3(b). These figures show results for test specimens with three different permeabilities according to Table D.1.

The measurements on test specimens with sealed edges, Fig. D.3(b), do not show any influence on friction coefficient from the permeability *i.e.* it is not possible to see that a different permeability will give a different friction coefficient. However, for test specimens with porous edges there is a small difference in friction between test specimens with different permeability as shown in Fig. D.4. This shows that the difference in frictional behavior with respect

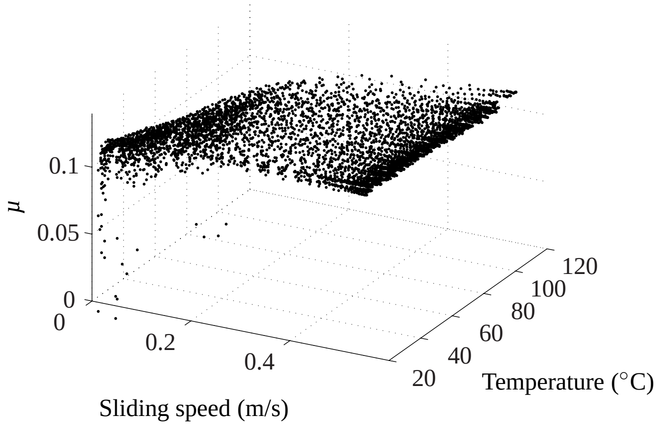

(a) Porous edges.

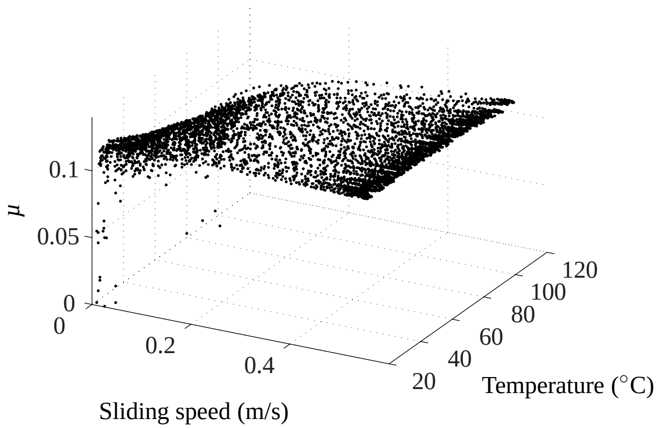

(b) Sealed edges.

Figure D.3: Comparison of friction behavior between test specimens with different permeability.

to different permeability of the materials can be large enough to influence the behavior of the tribological system when working with sufficient lubrication. A lower permeability of the test specimens gives a higher friction coefficient. Due to the high sampling rate in the measurements there are a lot of measured point from which the mean friction coefficients in Fig. D.4 are calculated. The results are calculated from measurements of several test specimens of each permeability. The maximum standard deviation for the visualized values in Fig. D.4 is 3.1%.

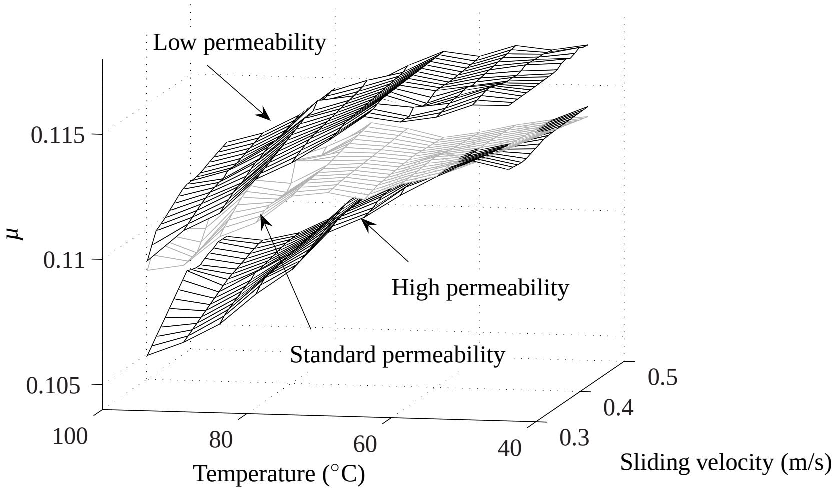

Figure D.4: Frictional behavior of materials with different permeability for test specimens with porous edges. Each surface represents mean values calculated from two different measurements from test specimens with the same permeability.

D.3.2 Tests with poor lubrication; test 2a-2d.

D.3.2.1 Frictional behavior before severe wear; test 2a.

Figure D.5 shows the behavior of permeable and non-permeable test specimens when sliding under starved conditions before the surfaces are severely worn. The pores in the permeable test specimens work as a lubricant reservoir and the small amount of lubricant in the pores is sufficient to lubricate the contact. There is no significant difference in the friction coefficient between the different permeability levels, but the non-permeable test specimens show a completely different frictional behavior compared to the permeable specimens. The friction coefficient of the non-permeable test specimen is generally much higher and the derivative of the friction coefficient for lower sliding speeds is negative. This can lead to stick slip in the tribological system. The non-permeable test specimens also show an interesting frictional behavior at higher sliding speeds when the friction is increasing. This is not the case for the permeable test specimens.

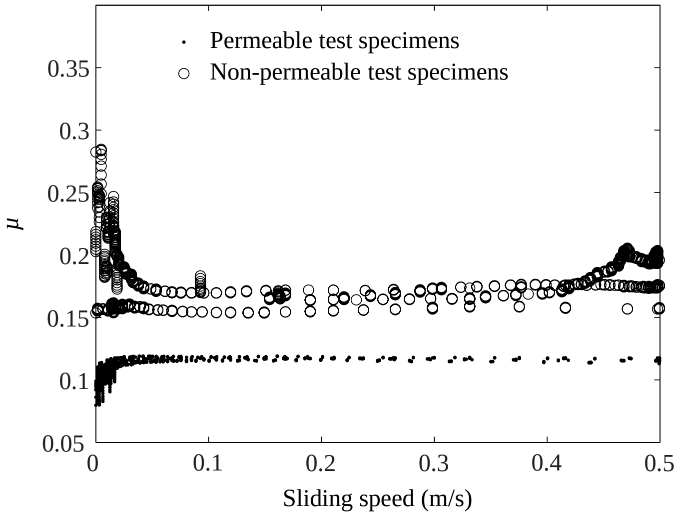

Figure D.5: Friction behavior before test 2b for starved sliding conditions for test specimens with porous edges impregnated with lubrication. Three different permeabilities and non-permeable test specimens according to Table D.1. Temperature $\sim 30^{\circ}$C.

D.3.2.2 Long wear sequence; test 2b.

During test 2b where the test specimens are running under starved conditions during 3 hours it is obvious that the permeability of the specimen and the type of edge influence the friction coefficient, Fig. D.6 and D.7 respectively. The most obvious difference in behavior occurs during the first ten minutes of the test and this period is shown in Fig. D.6 and D.7.These two figures show that pores, acting as reservoirs, influence the ability for a material of sintered bronze to work under starved running conditions.

A material with many pores can supply new lubricant to the contact from the pores. This gives a tribological contact which can be maintained for a quite long time with an almost constant friction coefficient although there is a shortage of lubricant. The friction coefficient increases when the lubricant is consumed from the pores and no new lubricant can be supplied to the contact. With all the lubricant in the pores consumed the friction coefficient is increased to a value between 0.15 and 0.2.

Figure D.6 shows that higher permeability gives better ability to maintain a constant friction coefficient when working under starved conditions. The results for the non-permeable test specimens also indicate that all lubricant in the

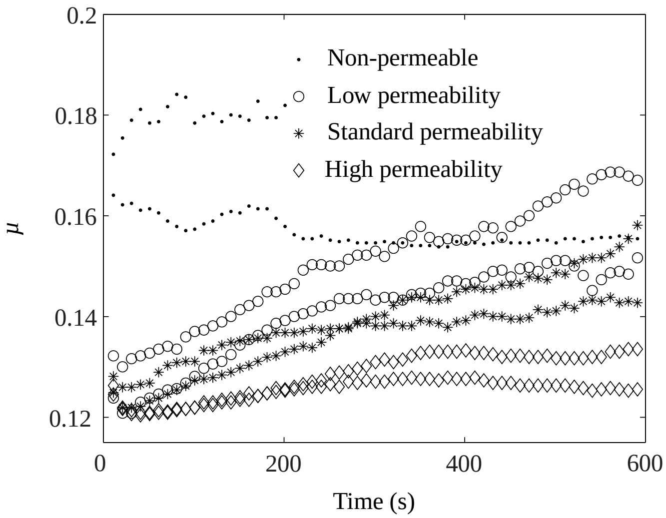

Figure D.6: Comparison of the frictional behavior under starved conditions for test specimens with permeabilities according to Table D.1 for the first ten minutes of test 2b. All test specimens have porous edges.

contact was consumed in the short test made before the longer wear sequence, see Fig. D.5. That explains the fact that the non-permeable test specimens have a friction coefficient over 0.15 from the beginning of this starved test.

Figure D.7 shows the difference between test specimens with sealed or porous edges. Except for one measurement all test specimens with sealed edges show a great ability to maintain a constant friction coefficient when running under starved conditions compared to the test specimens with porous edges. With sealed edges the ability to retain the lubricant in the permeable material increases which further improves performance. This can be explained as shown in Fig. D.8 where the possible ways for lubricant to exit the pores of the permeable material are shown. Figure D.8(a) shows a test specimen with porous edges. Porous edges make it possible for the lubricant to exit the material through the side walls. When the lubricant exits the material through the pores of the top surface, which is in sliding contact with the disc, it lubricates the contact, but when it exit the material through the side walls the lubricant is "‘lost"’ since it does not lubricate the contact. With sealed edges, as in Fig. D.8(b), the lubricant can not flow out of the material through the side walls and will last longer in the sliding contact. This can explain the behavior shown in Fig. D.7 where most of the test specimens with sealed edges work for a longer

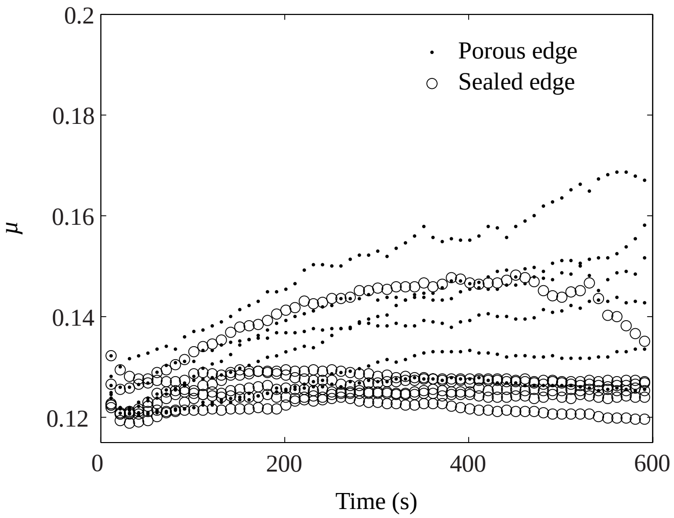

Figure D.7: Comparison of the frictional behavior under starved conditions for test specimens with porous and sealed edges for the first ten minutes of test 2b. Three different permeabilities (high, standard and low) according to Table D.1. Measurements on test specimens with porous edges are the same as in Fig D.6.

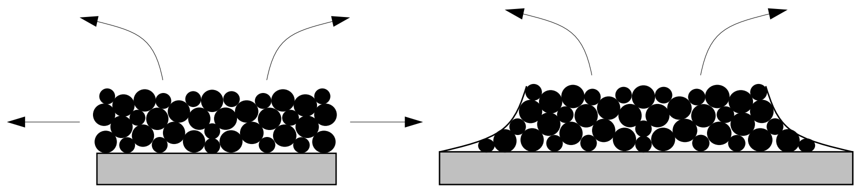

(a) Porous edges. (b) Sealed edges.

Figure D.8: Schematic sketches of test specimens with porous and sealed edges. The arrows show possible ways for the lubricant to flow out of the pores of the test specimens.

time under starved conditions.

During the test with poor lubrication, test 2b, the wear on the test specimens is extensive. Roughness measurements for different test durations is shown in Fig. D.9. Figures D.9(a) to D.9(c) show a permeable test specimen before test 2b and after a test duration of 15 and 180 min and the transition between a rough to a much smoother surface is shown. A roughness measurement from a non-permeable test specimen before the test sequence is shown in Fig. D.9(d) as a comparison to the permeable test specimens. The height of the surface roughness, Sz, is about the same for the non-permeable test specimen before the starved test as for the permeable test specimen after a test duration of 45 minutes. The pores on the surface are also not large enough to work as reservoir for the lubricant. The lack of reservoirs for the lubricant in worn permeable test specimens, Fig. D.9(c), and non-permeable test specimens, Fig. D.9(d), give an unfavorable frictional performance when running under starved conditions.

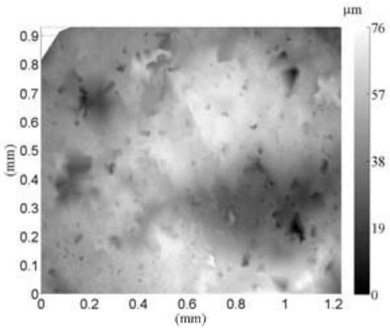

(a) High permeability. Before long wear sequence, test 2b. Sa= 10.6 μm, Sz= 67.5 μm.

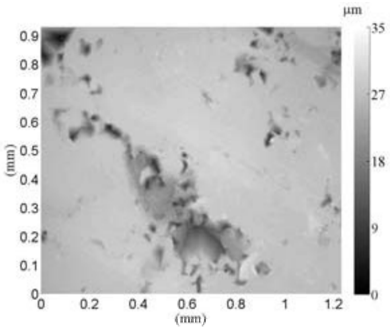

(b) High permeability. 15 min. Sa=1.22μm, Sz= 28.2 μm.

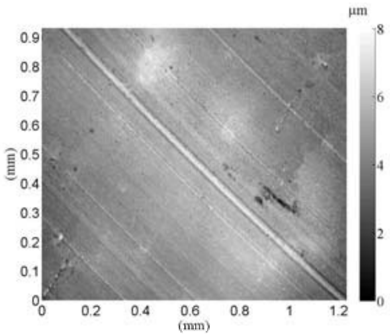

(c) High permeability. 180 min. Sa=728nm, Sz= 8.23 μm.

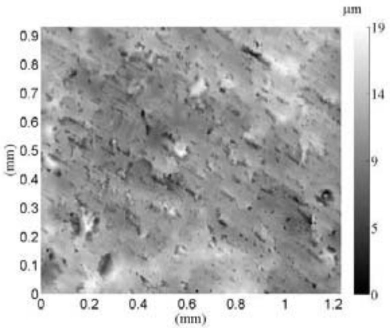

(d) Non-permeable. Before long wear sequence, test 2b. Sa= 1.57 μm, Sz= 18.3 μm.

Figure D.9: Surface roughness of a test specimen with high permeability measured at different test durations, Fig. D.9(a)- D.9(c), compared with a non-permeable test specimen before test, Fig. D.9(d). Roughness height is indicated at the right of each measured surface.

D.3.2.3 Frictional behavior after severe wear; test 2c

There is not a great difference in the frictional behavior of permeable and non-permeable test specimens after the long wear sequence when working under starved running conditions. All test specimens have a very low permeability after test 2b because they are worn out and the pores on the surface of the specimens are clogged with wear particles. The difference between permeable and non-permeable test specimens in Fig. D.10 is much smaller compared to the measurements before the long wear sequence 2b shown in Fig. D.5. Another

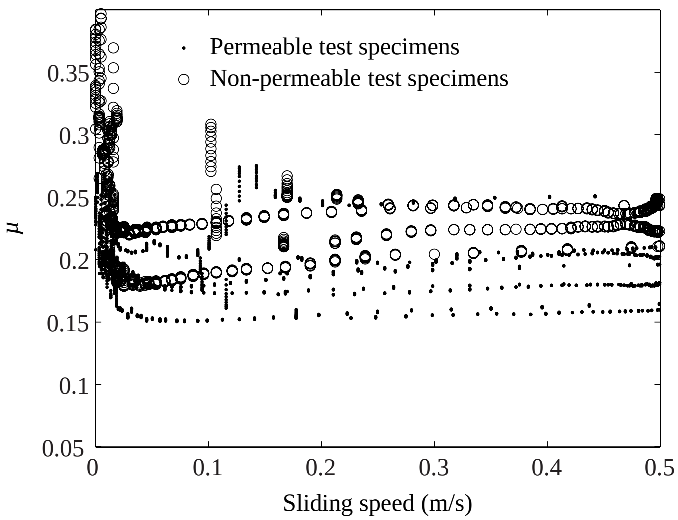

Figure D.10: Friction behavior for dry sliding with lubrication impregnated test specimens after test 2b. Two different permeabilities and non-permeable test specimens. Temperature $\sim 30^{\circ}$C.

interesting aspect of Fig. D.10 is that the overall frictional behavior for the permeable test specimens is completely changed compared to the measurements shown in Fig. D.5 because there is no lubricant left in the contact. The frictional behavior for the low sliding speeds shown in Fig. D.10 can lead to serious stick slip and shudder problems in applications such as wet clutches and brakes and can not be tolerated for such applications. This behavior indicates that the tribological system has run out of friction modifying additives in the sliding contact.

D.3.2.4 Frictional behavior after severe wear when lubricated with fresh lubricant; test 2d

The ability for a tribological system to continue to work properly after being worn out when running for a long period of time under tough starved conditions is investigated by submerging the worn test specimens into fresh lubricant. The results from these measurements are shown in Fig. D.11. This shows if the additives in the lubricant can recreate the frictional behavior for a normal lubricated system such as is shown in Fig. D.3. The difference between per-

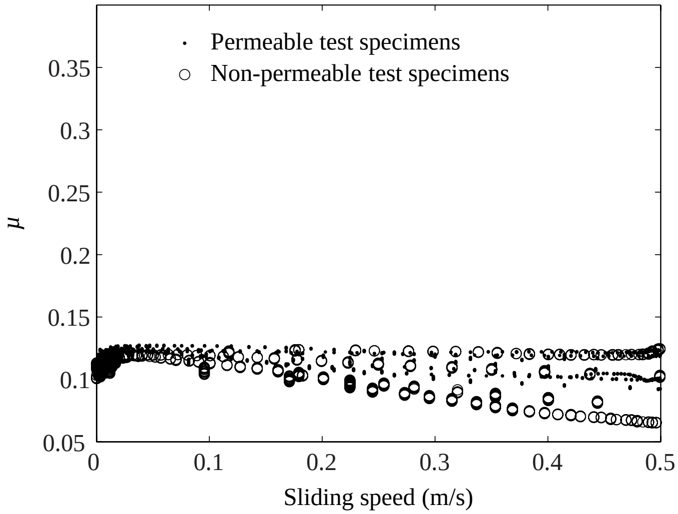

Figure D.11: Friction behavior for normal lubrication conditions after long wear sequence at $\sim 30^{\circ}$C. The test specimens are severe worn and re-flooded with fresh lubricant. Two different permeabilities and non-permeable test specimens.

meable and non-permeable test specimens is marginal. However, the friction of non-permeable test specimens show a slightly larger tendency to decrease with increasing sliding speed than for the permeable test specimens, which could induce stick-slip in the tribological system. When comparing Fig. D.11 with Fig. D.10 the difference in friction is evident. This indicates that the lubricant, which is tailor made to work as a lubricant for a sintered bronze friction material, works well with the material combination used in this investigation.

All investigation of the starved tribological system implies that one reason for using a permeable friction material is that the porosities can work as reservoirs for the lubricant and additives hence give the system better properties when working under starved conditions and increase life time. The starved tests show that a permeable material can make the system more robust and durable and less sensitive when running with a shortage of lubricant.

D.4 Conclusions

This investigation was carried out to test how the permeability of a material made of sintered bronze can influence the frictional behavior for a tribological system working in boundary lubrication under fully flooded and under starved lubrication conditions. The fully flooded tests were designed for investigating boundary lubrication behavior where the nominal surface pressure is quite high while the sliding speed is fairly low. The sintered bronze material used in the investigation is normally used in applications such as wet clutches or brakes, self lubricated bearings and synchromesh components for manual gearboxes.

The conclusions are:

- The permeability of the sintered bronze material does not have any great influence on the friction coefficient when the system is fully flooded with lubricant. However, lower permeability of the material may imply a friction coefficient that is up to 10% higher in a sliding contact compared to a material with lower permeability for some working conditions.

- The frictional behavior when running under starved conditions is much influenced by the permeability of the material. Higher permeability gives much better frictional behavior than a material with lower permeability. This indicates that the pores in the permeable material can work as reservoirs for the lubricant and can supply the contact with lubricant. This gives a contact which can withstand longer times of sliding under starved conditions than a non-permeable material before the surface is damaged and the frictional behavior is changed.

- A sealed edge around a smaller contact area is desirable in order to get the system to work for a longer time under starved conditions. This improves the reservoir properties by preventing the lubricant from flowing out of the material away from the contact.

- In the investigated tribological system, severe worn and smooth surfaces and low permeability still worked quite well when the contact was supplied with fresh lubricant. This shows that tribological systems with materials of sintered bronze and a smooth steel counter surface are very robust systems which can withstand tough running conditions if used together with a suitable lubricant.

D.5 Acknowledgments

The authors would like to thank the colleagues at Haldex Traction Systems, Statoil Lubricants and Luleå University of Technology for their contributions. The authors also thank the Program Board for Automotive Research (PFF) and the Swedish Foundation for Strategic Research (ProViking) for financial support.

Paper E

Modeling and simulation of thermal effects in wet clutches operating under boundary lubrication conditions

To be submitted for publication in journal.

Modeling and simulation of thermal effects in wet clutches operating under boundary lubrication conditions.

P. Marklund, F. Sahlin and R. Larsson

Luleå University of Technology, Division of Machine Elements,
Luleå, SE-971 87 Sweden

Abstract

Wet clutches are frequently used in the drive trains of many modern vehicles. The behavior of the clutches influences the behavior of the whole drive train and therefore of the whole vehicle. The design of the clutch is very important because it operates in cooperation with the other parts of the drive train. The clutch also often has to work in the lubricant present in the transmission. To optimize the clutch for an application, properties such as disc geometry, materials, friction disc surface and engagement axial force can be varied when designing the clutch. Today, the design process involves much testing which is expensive and time consuming. There are no good hand-book solutions or engineering tools available, hence the designer has to be very experienced and often use trial and error methods in order to end up with a working clutch for an application.

A design tool for wet clutches is presented in this paper. A simulation model is developed which in combination with a simple measurement technique for measuring the boundary lubrication friction coefficient is used to estimate temperature and torque transfer for a wet clutch working under limited slip conditions. This approach can be used to investigate torque behavior for wet clutches which have not been built yet and is, therefore, suitable to use when optimizing the performance of a new clutches. The model includes fluid dynamics, contact mechanics and temperature computations in the fluid film between the friction disc and the separator disc. Temperature computations in

the clutch discs are also included in the model. The fluid dynamics calculations use homogenized flow factors to enable simulations of flow on a coarser grid and still include all surface roughness effects. The temperature distribution in the film in the sliding interface is approximated as a polynomial of the second order. The heat transfer in the grooves of the friction discs is solved by means of an equilibrium equation which includes radial cooling flow effects due to centrifugal flows. The temperature in the friction disc and separator disc is obtained from the solution of the full 3D energy equation in polar cylindrical coordinates.

The model is validated by measurements made in a test rig and good agreement between measurements and simulations is obtained, both with regard to temperature and transfered torque.

The use of this model can reduce the time needed to develop a limited slip wet clutch application since the systematic way of finding the optimal clutch design will be more efficient than the often used Edisonian trial and error approach.

E.1 Introduction

Wet clutches are frequently used in modern vehicles to distribute torque in transmissions and drive trains. The behavior and characteristics of the clutch are therefore important design parameters when further developing and optimizing the transmissions of the vehicles. Their performance influences the performance of the vehicle, fuel consumption, safety, and the comfort of the driver.

The most common type of wet clutch, used in the drive trains of vehicles, operates during a quite short time of engagement, around one second or less. This is normally the case in automatic transmissions (ATs) where the clutch is used to change gear ratio in the transmission. During this short engagement the energy input is large and much heat is generated.

Another common type of wet clutch is the limited slip (LS) clutch which transfers high torque in applications working with a small difference in rotational speed for a long time. Such applications are limited slip differentials which are used to enhance both handling and traction of the vehicle. They can limit the slip between right and left wheel on one axle or between the front and rear axle of the vehicle. The operating conditions of these clutches are much different compared to those of clutches in ATs.

The behavior of the clutch is primarily governed by its tribological performance so to describe the performance of the drive train it is important to investigate the behavior of the wet clutches. These tribology investigations often involve much testing and less modeling. This costs a great deal and takes much time since complicated tests are required. It can also be difficult to design a test to imitate the real application because of the variations of the engagements in the applications. The measurements for certain working conditions are often difficult to use to describe other working conditions than the ones measured since *e.g.* temperature and hydrodynamic forces are not the same.

A test rig often used to imitate the working principles of an engaging clutch is the SAE II test rig, described in [30]. In the SAE II test rig a flywheel is accelerated to a fairly high rotational speed and then a wet clutch is used to brake the flywheel to stand still. Other similar test rigs with a flywheel retardation are also used in laboratory tests. For LS differentials other types of test rigs are usually suitable, such as the test rig described by Mäki et al. [10]. In the LS wet clutch test rig the rotational speed and axial force are varied independently of each other and the transfered torque can be investigated for a variety of axial loads and rotational speeds during a longer time of engagement.

Modeling and simulations are required as a complement to laboratory measurements to lower the cost and optimize the performance in a short time. The most common simulation model for wet clutches involves a wet clutch working under AT conditions, and good agreement with experimental data can be achieved [19–24]. During a clutch engagement the transmitted torque is a combination of viscous shear forces between the discs and boundary lubrication friction forces. In the numerical simulation models the temperature is normally only accounted for by adjusting the viscosity and density of the fluid in the sliding interface. Since the engagement in an AT clutch is short and the viscous torque is much smaller than the contact torque, there is not always a need for thermal calculations if only the transmitted torque is of interest in the simulations. The difference between the results from isothermal simulations and thermal simulations is not always large, but in cases with a large temperature variation in the clutch, such as Limited Slip clutches, a adequate temperature model is required to obtain satisfactory simulation results. The thermal simulations can also give important information about the temperatures in the surface contact which can be an important parameter to study so that thermal degradation of the clutch system can be reduced. Hot spotting [44] is also important and can be investigated with thermal simulations of the clutch system.

One property of the friction material is its permeability, which is often used as an input parameter in many simulation models developed for AT wet clutches [19–24]. The effects of the permeability are often not studied in detail, but in some work, *e.g.* [21, 23] the permeability is varied and the influence on torque transfer during clutch engagement is investigated. The importance of the permeability on the time of engagement is explained by the fact that a clutch with a permeable material will operate a shorter time in full film lubrication, hence it will operate a longer part of the engagement in boundary lubrication and transfer higher torque which shortens the time of engagement. The permeability also influences the boundary lubrication friction behavior which is shown by Marklund et al. in [58].

The engagement time is also influenced by the surface roughness of the friction materials. The surface roughness influences the flow in the sliding interface, and thus influences the time of engagement. Surface roughness is normally accounted for by solving Reynolds equation including Patir and Cheng flow factor compensation [39].

Since most of the developed simulation models deal with an AT type of wet clutch other types of simulations models are needed to study the behavior of limited slip wet clutches. The full clutch engagement which comprises both full film lubrication, mixed lubrication and boundary lubrication in the sliding interface, is often not of interest since the LS clutch works more or less fully engaged with limited slip in boundary lubrication while in use. Of interest in these applications is that the temperature in the sliding interface plays an crucial role in the transfered torque even though the system mainly works in boundary lubrication. This is shown as the viscosity has no great effect on the torque transfer [59]. This implies that the boundary lubrication friction coefficient has to be temperature dependent in a simulation model of a LS clutch, which is not always the case in the AT clutch engagement simulation models described above.

Marklund et al. [45] introduced a way of modeling LS clutches where the temperature is simulated during a limited slip sequence and the torque is modeled by a measured sliding velocity and temperature dependent friction coefficient. Here the temperature model was axisymmetric and the cooling effect from the lubricant was an empirical model developed from the test rig described in [10]. In the paper by Marklund et al. [45], much empirical data were needed in order to simulate the temperature in the clutch and surface roughness was not taken into account.

In this paper a simulation model is developed which is an improvement of the model in [45]. Here the model is extended into a 3D model where the full energy equation is solved in the clutch discs. In the fluid film the energy equation in the sliding interface is solved with a second order polynomial approximation of the temperature distribution across the film. The film temperature calculations include conduction, convection, shear heating and compression. A simplified convective model is used in the grooves to include the cooling due to the centrifugal effects. This 3D temperature model gives a better estimate of the temperature in the sliding interface than what was possible with the 2D model in [45]. A better torque transfer accuracy is thus attainable with the 3D model. No empirical input data are needed in the model except from the temperature and velocity dependent boundary lubrication friction coefficient which is measured in a pin on disc apparatus with the method described by Marklund et al. in [57].

The hydrodynamic pressure in the fluid film between the discs is computed with Reynolds equation including homogenized flow factors as described in [60]. The contact pressure is computed with an FFT-method with a force balance together with the applied axial force and the hydrodynamic pressure.

The proposed model facilitate investigation of the influence of groove patterns, surface roughness, material properties and fluid properties on temperature and torque in a LS wet clutch. The model is thus a good complement to expensive and time consuming laboratory measurement.

E.2 Method

The main objectives with the simulation model are to predict the temperature in the clutch as well as the torque transfer from the clutch. Marklund et al. [45] showed that it is of interest to use a boundary lubrication friction coefficient which is dependent on both sliding velocity and temperature to achieve simulated results which better correspond to the behavior of a real clutch application. In this work the temperature is solved in 3D in the friction disc and axisymmetrical in the separator disc to achieve a precise temperature estimation for the sliding interface between the friction lining and separator disc. This is required for a precise torque transfer calculation.

An overview of the modeling methodology is given by the following:

- The surface roughness for the friction lining is measured with a suitable method. In this work an optical profiler (WYCO NT1100) is used to measure surface roughness. The surface of the separator disc can be considered smooth in comparison with the friction lining surface.

- The velocity and temperature dependent boundary lubrication friction coefficient is measured for a small sample of the friction lining in a pin on disc apparatus according to the method described by Marklund et al. in [57].

- The flow factors for the measured surface roughness of the friction lining are computed according to the methods described in detail by Sahlin et al. in [38].

- The flow factors are used to solve the homogenized Reynolds equation on the nominal contact areas of the friction disc. These calculations give pressure distributions on the nominal contact areas, mean film thickness and transfered hydrodynamic torque.

- The contact force is computed with a force balance equation with the axial force and the computed hydrodynamic force in the region of the nominal contact areas. The contact force is used together with the measured boundary lubrication friction coefficient to compute the boundary lubrication torque.

- The energy equation is solved in the clutch discs and fluid giving the temperature distribution in the clutch.

- Friction coefficients, viscosities and densities are computed explicitly for the following time step in all computational nodes in the friction interface from the simulated temperatures in the interface. The explicit scheme is shown to be accurate enough and reduces the time needed to solve the system since no iterative scheme is needed.

E.2.1 Temperature in solids and fluid

The geometry of the domain in which the temperature is computed is shown in Fig. E.1 where the solids and the separating fluid film, *h*, is shown. This

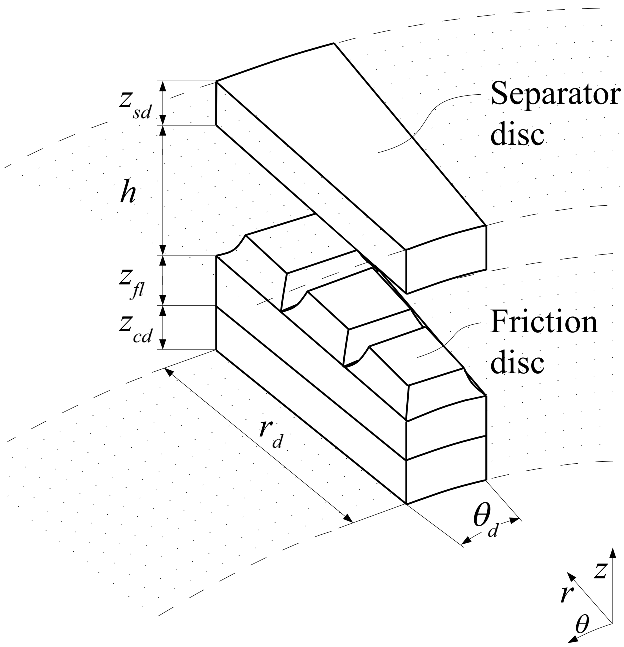

Figure E.1: Computational domain used in temperature model, 1/64th of one complete friction disc and separator disc.

domain is 1/64th of one complete friction disc and separator disc in angular direction, marked with θ_d in the figure. The groove pattern is an approximation in polar cylindrical coordinates of the real groove pattern shown in Fig. E.2. The total nominal contact area of the groove pattern used in the simulation model is the same as the nominal contact area of the real friction disc. The sizes of the quadratic contact areas shown in Fig. E.2 are also very close to the dimensions of the contact areas in the simulation model, see Fig E.3, and the

Figure E.2: Photo of the friction lining on the friction discs.

dimensions of the grooves are similar in both cases. The reason for calculating in 3D instead of 2D as in [21, 34, 40, 45]is to gain a better and more detailed understanding of how the temperature in the clutch discs is increased during engagement. In models where the boundary lubrication friction coefficient is temperature dependent, such as [34,45], the temperature in the sliding interface governs the friction coefficient. For an axisymmetric 2D temperature model as in [34, 45] the computed interface temperature is an average temperature consisting of both groove and contact area temperatures. Since the temperature in the sliding interface, *i.e.* the temperature on top of the contact areas, can be much higher than the temperature in the grooves, a 3D temperature model can give a better and more detailed prediction of the boundary lubrication friction coefficient.

The temperature in the friction disc is solved in 3D and is governed by the heat equation in polar cylindrical coordinates;

$$\rho c_p \frac{\partial T}{\partial t} = k\left(\frac{\partial^2 T}{\partial r^2} + \frac{1}{r}\frac{\partial T}{\partial r} + \frac{1}{r^2}\frac{\partial^2 T}{\partial \theta^2} + \frac{\partial^2 T}{\partial z^2}\right). \tag{E.1}$$

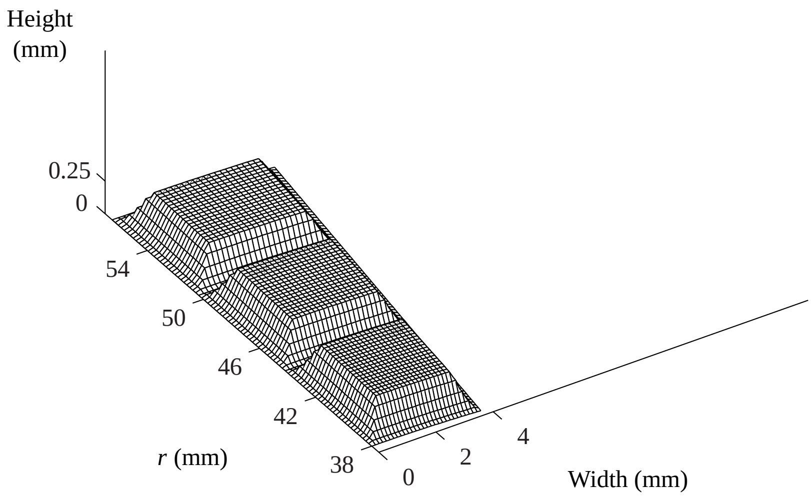

Figure E.3: Surface geometry on simulated domain.

The temperature in the separator disc is solved axisymmetrically since the separator disc has no geometric variations in the angular direction and the small temperature variations in the angular direction are considered negligible. This can be compared with models of tilting pad thrust bearings where the runner often is modeled in 2D as in [37].

E.2.1.1 Boundary conditions

The external boundary conditions for Eq. (E.1), *i.e.* the boundaries on the outer edges of the computed domain shown in Fig. E.1, are:

- θ-direction: Periodic boundary conditions
- r-direction: Neumann boundary conditions of the type

$$\frac{\partial T}{\partial r} = \alpha_r \cdot (T - T_{amb}), \tag{E.2}$$

where α_r is the heat transfer coefficient across the radial boundaries, corresponding to a combined effect of both spline, *i.e.* steel-steel contact, and lubricant at the inner and the outer radius.

- z-direction: Neumann boundary conditions of the type

$$\frac{\partial T}{\partial z} = \alpha_z \cdot (T - T_{amb}), \tag{E.3}$$

where α_z is the heat transfer coefficient over the axial boundaries. The value of α_z is quite high since the axial boundaries are in contact with a piston and a holder made of steel. In many real applications it is possible to calculate the temperature on half the thickness of separator disc and core disc and consider the boundaries as insulated, $\partial T/\partial z = 0$ *i.e.* $\alpha_z = 0$ in Eq. (E.3) above. This is explained by the fact that discs normally are stacked in clutch packs where the two types of disc are mounted in pairs. This implies more sliding interfaces, hence higher transfered torque. In such a configuration the same amount of heat is generated on both sides of the discs, implying negligible heat transfer over the axial center line of the disc, hence the boundary can be considered insulated. However, in this work the simulation is compared with one pair of discs mounted in a limited slip wet clutch test rig where the boundaries can not be considered as insulated and temperature distribution in the full thickness of the discs has to be described in the model.

The internal boundary conditions, *i.e.* the boundaries between solid materials and fluid inside the computed domain shown in Fig. E.1, are:

- In the boundary between friction lining (*fl*) and core disc (*cd*)

$$T_{fl} = T_{cd}; \quad k_{fl}\frac{\partial T_{fl}}{\partial z} = k_{cd}\frac{\partial T_{cd}}{\partial z}. \tag{E.4}$$

- The calculations describing the fluid film between friction lining and separator disc is presented in the separate section E.2.2.

E.2.2 Interface calculations

First the fluid film velocity-fields in $r-$ and $\theta-$ direction including centrifugal and inertia effects can be derived from the two equations

$$\eta\frac{\partial^2 v}{\partial z^2} = \frac{1}{r}\frac{\partial p}{\partial \theta} \tag{E.5}$$

and

$$\eta\frac{\partial^2 u}{\partial z^2} = \frac{\partial p}{\partial r} - \frac{\rho v^2}{r} \tag{E.6}$$

with the boundary conditions

$$v = r\omega_1,\ u = 0 \text{ at } z = 0$$
$$v = r\omega_2,\ u = 0 \text{ at } z = h.$$

These equations are valid for a thin film approximation and Newtonian and isoviscous or mean tempered fluids.

Integrating Eq (E.5) and using boundary conditions yields

$$\frac{\partial v}{\partial z} = \frac{1}{\eta r}\frac{\partial p}{\partial \theta}\left(z - \frac{h}{2}\right) + \frac{r}{h}\left(\omega_2 - \omega_1\right) \tag{E.7}$$

and

$$v = \frac{z(z-h)}{2\eta r}\frac{\partial p}{\partial \theta} + \frac{r}{h}\left(\omega_1(h-z) + \omega_2 z\right). \tag{E.8}$$

The mean value of the velocity in θ-direction, $\overline{v}$, is used as velocity v when integrating Eq. (E.6) to

$$\frac{\partial u}{\partial z} = \frac{(z-h/2)}{\eta}\left(\frac{\partial p}{\partial r} - \frac{\rho \overline{v}^2}{r}\right) \tag{E.9}$$

and

$$u = \frac{\left(z^2 - zh\right)}{2\eta}\left(\frac{\partial p}{\partial r} - \frac{\rho \overline{v}^2}{r}\right). \tag{E.10}$$

This approximation of using $\overline{v}$ is explained by the fact that the pressure gradient is solved with a thin film approximation and that the difference in rotational speed between the two discs, ω_1 and ω_2, normally is much smaller than the mean rotational-speed of the two discs. The average velocity $\overline{v}$ can be calculated from Eq (E.8) as

$$\overline{v} = \frac{1}{h}\int_0^h v dz = \frac{r}{2}\left(\omega_2 + \omega_1\right) - \frac{h^2}{12 r\eta}\frac{\partial p}{\partial \theta} \tag{E.11}$$

In a similar way $\overline{u}$ can be derived as

$$\overline{u} = \frac{1}{h}\int_0^h u dz = \frac{h^2}{12\eta}\left(\frac{\rho \overline{v}^2}{r} - \frac{\partial p}{\partial r}\right). \tag{E.12}$$

The energy equation in polar cylindrical coordinates in the fluid film [37] is needed to calculate the temperature in film and surrounding solids. The equation assumes steady flow and constant specific heat c_p and thermal conductivity k. The equation is written as

$$\begin{aligned} &\rho c_p u\frac{\partial T}{\partial r}+\frac{\rho c_p}{r}v\frac{\partial T}{\partial \theta}+\rho c_p w\frac{\partial T}{\partial z} \\ &= k\left(\frac{\partial^2 T}{\partial r^2}+\frac{1}{r}\frac{\partial T}{\partial r}+\frac{1}{r^2}\frac{\partial^2 T}{\partial \theta^2}+\frac{\partial^2 T}{\partial z^2}\right) \\ &+\eta\left(\left(\frac{\partial u}{\partial z}\right)^2+\left(\frac{\partial v}{\partial z}\right)^2\right)+\varepsilon T\left(u\frac{\partial p}{\partial r}+\frac{v}{r}\frac{\partial p}{\partial \theta}\right). \end{aligned} \tag{E.13}$$

Equation (E.13) can be simplified by neglecting smaller terms such as convection across the fluid film and heat conduction in $r-$ and $\theta-$ direction, which gives the total fluid film energy equation

$$\rho c_p u\frac{\partial T}{\partial r}+\frac{\rho c_p}{r}v\frac{\partial T}{\partial \theta}=k\left(\frac{\partial^2 T}{\partial z^2}\right)+\eta\left(\left(\frac{\partial u}{\partial z}\right)^2+\left(\frac{\partial v}{\partial z}\right)^2\right)+\varepsilon T\left(u\frac{\partial p}{\partial r}+\frac{v}{r}\frac{\partial p}{\partial \theta}\right). \tag{E.14}$$

The two last terms are dissipative terms or heat sources. The most important heat source, the heat generation due to boundary lubrication friction forces is not described in Eq. (E.14), but instead implemented as a boundary condition for the solids in the sliding interface: boundary lubrication heat generation only occurs when the surfaces are in contact, only separated by a thin additive film. Hence, the boundary lubrication heat generation should not be applied in the middle of the lubricant film, *i.e.* in Eq. (E.14). Since the total energy has to be divided between the two solids a distribution dependent on the heat transfer coefficients of the different materials is used according to

$$T_{fluid}=T_{fl};\quad k_{fluid}\frac{\partial T_{fluid}}{\partial z}-\frac{k_{fl}}{(k_{sd}+k_{fl})}\mu pr|\omega_2-\omega_1|=k_{fl}\frac{\partial T_{fl}}{\partial z}, \tag{E.15}$$

and

$$T_{fluid}=T_{sd};\quad k_{fluid}\frac{\partial T_{fluid}}{\partial z}+\frac{k_{sd}}{(k_{sd}+k_{fl})}\mu pr|\omega_2-\omega_1|=k_{sd}\frac{\partial T_{sd}}{\partial z}. \tag{E.16}$$

This approximation implies that more of the generated heat is conducted into the material with the higher conductivity.

The calculations in the film are computed between the friction disc and separator disc, see h in Fig. E.1, and this region is shown in more detail with dimensions in Fig. E.3. The computations are divided into calculations over the contact area, section E.2.2.1, and in the grooves, section E.2.2.2 . The calculations over the contact area are used on the rectangular shaped contact areas visible in Fig. E.3 and between them the grooves are located special groove computations are used.

E.2.2.1 Energy calculations in the contact region

The temperature distribution in the fluid film between the two discs is considered to be a polynomial of the second order,

$$T(r,\theta,z) = (3T_{fl} + 3T_{sd} - 6T_m)\left(\frac{z}{h}\right)^2 + (6T_m - 4T_{fl} - 2T_{sd})\left(\frac{z}{h}\right) + T_{fl}, \quad \text{(E.17)}$$

according to [61], where T_m is the mean temperature in the fluid film. The derivative

$$\frac{dT}{dz} = (3T_{fl} + 3T_{sd} - 6T_m)\left(\frac{2z}{h^2}\right) + \frac{6T_m - 4T_{fl} - 2T_{sd}}{h} \quad \text{(E.18)}$$

which can be used in Equation (E.15) and (E.16) evaluated at $z = 0$ and $z = h$ respectively;

$$\left.\frac{dT}{dz}\right|_{z=0} = \frac{6}{h}T_m - \frac{4}{h}T_{fl} - \frac{2}{h}T_{sd} \quad \text{(E.19)}$$

$$\left.\frac{dT}{dz}\right|_{z=h} = -\frac{6}{h}T_m + \frac{2}{h}T_{fl} + \frac{4}{h}T_{sd}. \quad \text{(E.20)}$$

The second derivative to Eq (E.17) is

$$\frac{d^2T}{dz^2} = \frac{6T_{fl} + 6T_{sd} - 12T_m}{h^2}, \quad \text{(E.21)}$$

The energy equation, (E.14), is solved by calculating mean values of the different terms across the fluid film, *i.e.* the conductive, convective, compressible and shear heat terms.

The mean convective term is described by

$$\begin{aligned}
\overline{\left(\rho c_p u\frac{\partial T}{\partial r}+\frac{\rho c_p}{r}v\frac{\partial T}{\partial \theta}\right)} &= \frac{1}{h}\int_0^h\left(\rho c_p u\frac{\partial T}{\partial r}+\frac{\rho c_p}{r}v\frac{\partial T}{\partial \theta}\right)dz = \\
&\frac{1}{120}\frac{\rho c_p}{\eta}h^2\frac{\partial p}{\partial r}\left(\frac{\partial T_{fl}}{\partial r}+\frac{\partial T_{sd}}{\partial r}-12\frac{\partial T_m}{\partial r}\right)\\
&+\frac{1}{120}\frac{\rho c_p}{\eta}\frac{h^2}{r^2}\frac{\partial p}{\partial \theta}\left(\frac{\partial T_{fl}}{\partial \theta}+\frac{\partial T_{sd}}{\partial \theta}-12\frac{\partial T_m}{\partial \theta}\right)\\
&+\frac{1}{120}\frac{\rho^2\overline{v}^2h^2c_p}{r\eta}\left(12\frac{\partial T_m}{\partial r}-\frac{\partial T_{fl}}{\partial r}-\frac{\partial T_{sd}}{\partial r}\right)\\
+\frac{1}{12}\rho c_p\left(6\frac{\partial T_m}{\partial \theta}(\omega_1+\omega_2)+\frac{\partial T_{fl}}{\partial \theta}(\omega_1-\omega_2)-\frac{\partial T_{sd}}{\partial \theta}(\omega_1-\omega_2)\right)&,
\end{aligned} \tag{E.22}$$

the mean conductive term is

$$\overline{k\left(\frac{\partial^2 T}{\partial z^2}\right)}=\frac{1}{h}\int_0^h k\left(\frac{\partial^2 T}{\partial z^2}\right)dz=\frac{k}{h^2}\left(6T_{fl}+6T_{sd}-12T_m\right), \tag{E.23}$$

the mean shear heating term is

$$\begin{aligned}
\overline{\eta\left(\left(\frac{\partial u}{\partial z}\right)^2+\left(\frac{\partial v}{\partial z}\right)^2\right)}=\frac{1}{h}\int_0^h\eta\left(\left(\frac{\partial u}{\partial z}\right)^2+\left(\frac{\partial v}{\partial z}\right)^2\right)dz= \\
\frac{1}{12}\frac{h^2}{\eta}\left(\left(\frac{\partial p}{\partial r}\right)^2+\frac{1}{r^2}\left(\frac{\partial p}{\partial \theta}\right)^2\right)+\frac{1}{12}\frac{h^2}{\eta}\left(\frac{\rho^2\overline{v}^4}{r^2}+\frac{2\rho\overline{v}^2}{r}\frac{\partial p}{\partial r}\right)+\frac{r^2\eta}{h^2}(\omega_1-\omega_2)^2
\end{aligned} \tag{E.24}$$

and the mean compression term is

$$\begin{aligned}
\overline{\left(\varepsilon T\left(u\frac{\partial p}{\partial r}+\frac{v}{r}\frac{\partial p}{\partial \theta}\right)\right)} &= \frac{1}{h}\int_0^h\left(\varepsilon T\left(u\frac{\partial p}{\partial r}+\frac{v}{r}\frac{\partial p}{\partial \theta}\right)\right)dz = \\
&\frac{1}{120}\frac{\varepsilon h^2}{\eta}(T_{fl}+T_{sd}-12T_m)\left(\left(\frac{\partial p}{\partial r}\right)^2+\frac{1}{r^2}\left(\frac{\partial p}{\partial \theta}\right)^2\right)\\
&+\frac{1}{120}\frac{\varepsilon h^2\rho\overline{v}^2}{\eta}\frac{1}{r}\frac{\partial p}{\partial r}(12T_m-T_{fl}-T_{sd})\\
+\frac{1}{12}\varepsilon\frac{\partial p}{\partial \theta}\left(6T_m(\omega_1+\omega_2)+T_{fl}(\omega_1-\omega_2)-T_{sd}(\omega_1-\omega_2)\right)&.
\end{aligned} \tag{E.25}$$

Multiplying all terms with h^2/k provides the total expression for the film temperature

$$
\begin{aligned}
&6T_{fl}+6T_{sd}-12T_m \\
&+\frac{1}{120}\frac{\rho c_p}{k\eta}h^4\frac{\partial p}{\partial r}\left(12\frac{\partial T_m}{\partial r}-\frac{\partial T_{fl}}{\partial r}-\frac{\partial T_{sd}}{\partial r}\right) \\
&+\frac{1}{120}\frac{\rho c_p}{k\eta}\frac{h^4}{r^2}\frac{\partial p}{\partial \theta}\left(12\frac{\partial T_m}{\partial \theta}-\frac{\partial T_{fl}}{\partial \theta}-\frac{\partial T_{sd}}{\partial \theta}\right) \\
&+\frac{1}{120}\frac{\rho^2\bar{v}^2h^4c_p}{kr\eta}\left(\frac{\partial T_{fl}}{\partial r}+\frac{\partial T_{sd}}{\partial r}-12\frac{\partial T_m}{\partial r}\right) \\
&-\frac{1}{12}\frac{h^2\rho c_p}{k}\left(6\frac{\partial T_m}{\partial \theta}(\omega_1+\omega_2)+\frac{\partial T_{fl}}{\partial \theta}(\omega_1-\omega_2)-\frac{\partial T_{sd}}{\partial \theta}(\omega_1-\omega_2)\right) \\
&+\frac{1}{12}\frac{h^4}{k\eta}\left(\left(\frac{\partial p}{\partial r}\right)^2+\frac{1}{r^2}\left(\frac{\partial p}{\partial \theta}\right)^2\right)+\frac{1}{12}\frac{h^4}{k\eta}\left(\frac{\rho^2\bar{v}^4}{r^2}+\frac{2\rho\bar{v}^2}{r}\frac{\partial p}{\partial r}\right)+\frac{r^2\eta}{k}(\omega_1-\omega_2)^2 \\
&+\frac{1}{120}\frac{\varepsilon h^4}{k\eta}(T_{fl}+T_{sd}-12T_m)\left(\left(\frac{\partial p}{\partial r}\right)^2+\frac{1}{r^2}\left(\frac{\partial p}{\partial \theta}\right)^2\right) \\
&+\frac{1}{120}\frac{\varepsilon h^4\rho\bar{v}^2}{k\eta}\frac{1}{r}\frac{\partial p}{\partial r}(12T_m-T_{fl}-T_{sd}) \\
&+\frac{1}{12}\frac{h^2\varepsilon}{k}\frac{\partial p}{\partial \theta}\left(6T_m(\omega_1+\omega_2)+T_{fl}(\omega_1-\omega_2)-T_{sd}(\omega_1-\omega_2)\right)=0,
\end{aligned}
\tag{E.26}
$$

which is used to solve the mean film temperature, T_m. The equation is solved with an upwind discretization scheme in r and θ direction to minimize the numerical instability.

The mixed lubrication simulation model from paper E in [38] is used in this paper to simulate the operation of the lubricated interface between the friction disc and the separator disc in the wet clutch. The model is based on computing flow factors that considers the effects of the specific surface roughness in all lubrication regimes from completely separated surfaces to mixed and boundary lubrication. Measured 3D surface topography of the clutch is used as input to the model, which merges an FFT-based contact mechanics model (DC-FFT) to calculate the elasto-plastic displacement of rough surfaces with a fluid flow model based on the homogenized Reynolds equation. A more detailed description of the model is given in paper E from [38]. However, for the readers convenience, the elastic surface displacement and the fluid flow model are here biefly described.

The elastic displacement, δ_e, of an elastic halfspace may be written as the linear convolution between a kernel, G, and the contact pressure, p_c, according to the Bousinesq-Cerrutti assumption:

$$\delta_e = G * p_c, \tag{E.27}$$

where '*' is the convolution operator and

$$G(x-s) = \frac{2}{\pi E'} \frac{1}{\sqrt{(x_1-s_1)^2 + (x_2-s_2)^2}}, \tag{E.28}$$

where x is the cartesian spatial coordinate and E' is the composite Young's modulus for the two materials in contact expressed as

$$\frac{1}{E'} = \frac{1-\nu_1}{E_1} + \frac{1-\nu_2}{E_2}, \tag{E.29}$$

with E being Young's modulus of elasticity and ν being the Poisson ratio for each surface. The pressure at one point will affect the surface deflection at all other points. That leads to a problem that is demanding to compute especially when rough surfaces are to be treated. However, the cyclic convolution may be evaluated as simple point-wise multiplication in the Fourier space by utilizing the convolution theorem, here through the use of descrete convolution FFT (DC-FFT). This procedure drastically increases the computing efficiency and the system also has the advantage of being periodic, wich is a demand also of the fluid flow model.

A deformed rough aperture will have a contact area that is less than the total nominal area, *i.e.* unless completely deformed demonstrating 100% contact area, the aperture consists of patches with and without contact. Thus, the following auxilliary system may be posed:

$$h > 0, \quad p_c = 0, \quad \text{Out of contact}, \tag{E.30a}$$

$$h = 0, \quad p_c > 0, \quad \text{In contact}, \tag{E.30b}$$

$$0 \leq p_c \leq p_p, \quad \text{Everywhere}, \tag{E.30c}$$

Where h is the film thickness of the deformed surface and p_c is the contact pressure. The pressure where plastic flow occures is defined as p_p, i.e. the plasticity pressure of the softer material in contact.

The fluid flow model is based on the Reynolds equation, homogenized with respect to the surface roughness. The homogenized Reynolds equation is written on the form

$$\nabla \cdot (C(\theta, r)) - \nabla \cdot (B(\theta, r) \nabla p) = 0, \tag{E.31}$$

with the homogenized pressure p as output. The homogenized coefficients B and C are

$$B = \begin{pmatrix} B_{11} & B_{12} \\ B_{21} & B_{22} \end{pmatrix}, \tag{E.32a}$$

$$B_{11} = \iint\limits_Y \frac{h^3}{r}\left(1 + \frac{\partial \chi_1}{\partial y_1}\right) dy, \tag{E.32b}$$

$$B_{12} = \iint\limits_Y \frac{h^3}{r}\frac{\partial \chi_2}{\partial y_1} dy, \tag{E.32c}$$

$$B_{21} = \iint\limits_Y h^3 r \frac{\partial \chi_1}{\partial y_2} dy, \tag{E.32d}$$

$$B_{22} = \iint\limits_Y h^3 r \left(1 + \frac{\partial \chi_2}{\partial y_2}\right) dy, \tag{E.32e}$$

and

$$C = \begin{pmatrix} C_1 \\ C_2 \end{pmatrix}, \tag{E.33a}$$

$$C_1 = \iint\limits_Y \left(\lambda h r - \frac{h^3}{r}\frac{\partial \chi_3}{\partial y_1}\right) dy, \tag{E.33b}$$

$$C_2 = \iint\limits_Y -h^3 r \frac{\partial \chi_3}{\partial y_2} dy. \tag{E.33c}$$

where the local coordinate $y \in Y = [0,1]^2$. χ_1, χ_2 and χ_3, are solutions to the periodic local problems, defined on Y, given below

$$\nabla_y \cdot \left(h^3 \nabla_y \chi_1\right) = \frac{1}{r}\frac{\partial h}{\partial y_1}, \tag{E.34a}$$

$$\nabla_y \cdot \left(h^3 \nabla_y \chi_2\right) = -r\frac{\partial h}{\partial y_2}, \tag{E.34b}$$

$$\nabla_y \cdot \left(h^3 \nabla_y \chi_3\right) = \lambda r \frac{\partial h}{\partial y_1}. \tag{E.34c}$$

In the simulation procedure, the coefficents B and C are computed as flow factors for the particular surface topography sample covering all lubrication regimes from full film to mixed and boundary lubrication.

With the flow factor method, a measured topography sample from only a small part of the clutch disc surface is needed to be considered. That strongly improves the computational efficiency compared to direct simulation where the topography for the whole clutch must be included in one computation. Once flow factors are computed for the surface topography sample, the operation of the clutch may be efficiently calculated on a coarse grid by simply including the pre-computed flow factors.

In order to calculate the friction torque the following additional coefficients need to be evaluated as flow factors:

$$D = \left(\iint_Y h\left(1 + \frac{\partial\chi_1}{\partial y_1}\right) dy, \quad \iint_Y h\left(\frac{\partial\chi_2}{\partial y_1}\right) dy \right),$$

$$d = \iint_Y \frac{1}{h} dy, \quad e = \iint_Y h\frac{\partial\chi_3}{\partial y1} dy.$$

Then the friction torque may be computed through the following integral:

$$Tq_{hyd} = \int_\theta \int_r \left(\eta\omega rd + \frac{1}{2r}\left(e + D\cdot\nabla p_0\right)\right) r^2\, dr\, d\theta. \tag{E.35}$$

The boundary lubrication torque is integrated over the interface between the clutch discs where the friction coefficient is varying due to sliding velocity and temperature in various locations of the sliding interface according to

$$Tq_{bl} = p_c \int_\theta \int_r \mu r^2 dr d\theta \tag{E.36}$$

The total torque transferred by the clutch is the sum

$$Tq = Tq_{hyd} + Tq_{bl}. \tag{E.37}$$

E.2.2.2 Energy calculations in the grooves

The mean temperature in the grooves is computed with a power equilibrium in every computational node. The power equilibrium takes into account power flow in radial and axial direction and the absorbed power in the fluid volume. The power equilibrium in θ-direction is not used in the calculations since the flow in angular direction in the grooves normally has a circular motion and is stirring the lubricant rather than transporting it angularly. More details about the lubricant flow in grooves is described in [62, 63]. It should be noted that the total angular velocity of the clutch pack in many applications can be substantially higher than the difference in rotational speed between the different discs, implying that the fluid flow in the radial direction can be much larger than the fluid flow in the angular direction, which further motivates that the angular flow not is accounted for in the grooves.

The power equilibrium function in the grooves is described by

$$\left(\frac{Tq_r c_p}{2}\right)_{i-1} - \left(\frac{Tq_r c_p}{2}\right)_{i+1} + \left(k\frac{\partial T}{\partial z}A\right)_{l-1} - \left(k\frac{\partial T}{\partial z}A\right)_{l-1} = \rho c_p V\frac{\partial T}{\partial t} \tag{E.38}$$

for each computational volume in the groove with the subscripts i and l in r and z-direction, respectively. The radial mass flow q_r is described with the cross section area, A_{cs}, and mean fluid velocity, $\overline{u}$, from Eq. (E.12) as

$$q_r = \overline{u}A_{cs}\rho. \tag{E.39}$$

E.3 Results and discussion

The torque transfer and flow calculations on the contact region of the friction lining are strongly dependent on the surface roughness. The surface roughness of the friction lining is quite high, as shown by measurement of friction lining surface in Fig E.4.

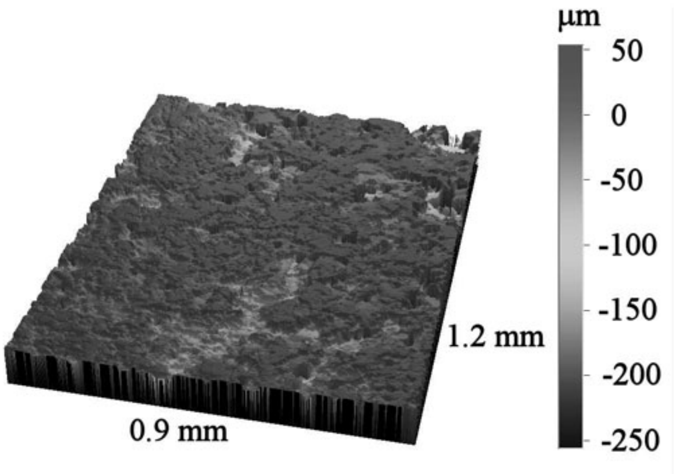

Figure E.4: Surface roughness measurement of friction material of sintered bronze. Ra= 18.7 μm, Rt= 308 μm, Rsk= -1.26

The simulation model was validated to measurements made in a wet clutch test rig which is suitable for measurements of limited slip behavior of wet clutches. The test rig is described in detail by Mäki et al. in [10]. The input data for solids and fluid which were used in measurements and simulations are presented in Table E.1.

Table E.1: Input parameters

Parameter	**Value**
ρ_{cd}	7860 kg/m^3
c_{pcd}	500 J/kgK
k_{cd}	48 W/mK
ρ_{fl}	5000 kg/m^3
c_{pfl}	471 J/kgK
k_{fl}	15.7 W/mK
ρ_{sd}	7860 kg/m^3
c_{psd}	500 J/kgK
k_{sd}	48 W/mK
ρ_{fluid}	855 kg/m^3 (at 40°C)
c_{pfluid}	2190 J/kgK
k_{fluid}	0.131 W/mK
η	0.0296 Pas (at 40°C)
ε	$6.5 \cdot 10^{-4}$ 1/K;
α_z	2500 W/m^{2}K
α_r	2000 W/m^{2}K
r_{min}	$38 \cdot 10^{-3}$ m
r_{max}	$56.5 \cdot 10^{-3}$ m
z_{cd}	$1.8 \cdot 10^{-3}$ m
z_{fl}	$0.6 \cdot 10^{-3}$ m
z_{sd}	$1.6 \cdot 10^{-3}$ m
θ_d	$\pi/32$

The test used for validation was a test sequence where rotational speed was increased linearly from 0 to 100 rpm in 10 seconds with a constant axial load. During the test the generated heat in the sliding interface increases the temperature of the clutch in such extent that transmitted torque decreases due to the decreasing friction coefficient. Figure E.5 shows measured and simulated temperature during the linear increase in rotational speed at two different axial loads, 10 and 20 kN. The temperature is measured in the separator disc on the side opposite to the friction interface, *i.e.* on the separator disc surface shown in Fig. E.1. This is also the temperature visualized in Fig. E.5 from the sim-

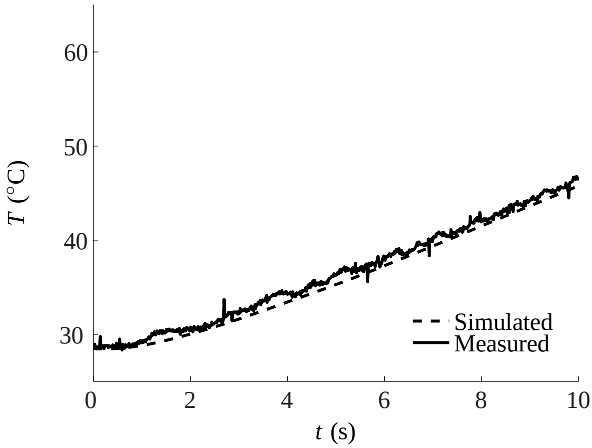

(a) Axial force = 10 kN.

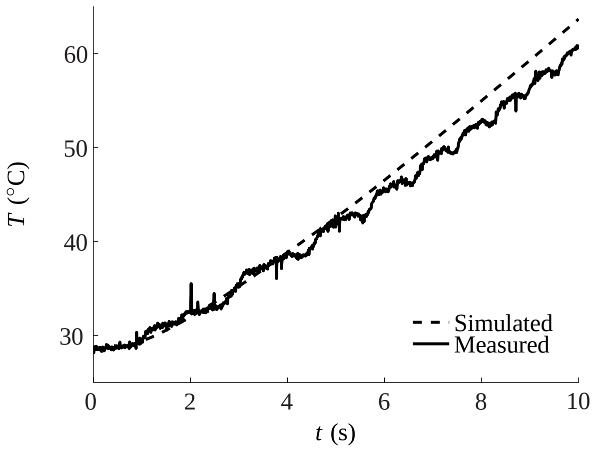

(b) Axial force = 20 kN.

Figure E.5: Comparison between simulated and measured temperature at two different axial forces. Temperature is measured on the side of the separator disc opposite to the sliding interface.

ulation model. When comparing simulated and measured temperature the difference between them is not very large. The largest difference is for the higher load, 20kN, which has a difference of maximum 3°C between simulated and measured temperature after ten seconds, see Fig E.5(b). For the higher load the increase in temperature is somewhat higher in the simulations compared to the measured temperature. One explanation for this difference is due to the boundary conditions in z-direction, see section E.2.1.1. In the test rig the heat transfer over the external boundaries in z-direction is governed by conduction into a complex system of pistons, bearing, lubricant, etc, whilst in the simulation model it is approximated with a heat transfer function. However, the small difference in temperature between simulation and measurement after ten seconds, a normal test sequence in the test rig, is not of large importance. This temperature difference does not influence the temperature dependent boundary lubrication friction coefficient [57] much and additionally the measured boundary friction is governed by the temperature in the sliding interface and not the temperature shown in Fig. E.5. Figure E.6 shows the temperature distribution in the friction disc after 4 seconds of engagement with an axial load of 20 kN. The figure shows an advantage with the 3D temperature model since the temperature on the nominal contact areas are obviously higher than in the grooves, which is not possible to estimate in a 2D axisymmetrical model. Since the boundary lubrication friction forces are only applied on the nominal contact areas that temperature is of most interest for the boundary lubrication torque calculations. The friction coefficient is measured for a friction mate-

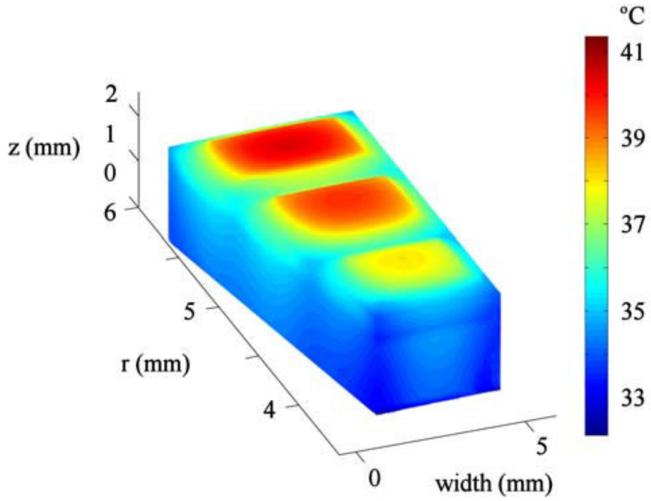

Figure E.6: Temperature distribution in simulated friction disc domain after 4 seconds of engagement with an axial load of 20 kN.

rial with a normal permeability for a limited slip differential application since is was shown by Marklund et al. [58] that the boundary lubrication friction coefficient can be dependent on the permeability of the material.

The transfered torque from both simulations and measurements are shown in Fig E.7 and a good correlation between them are obtained.

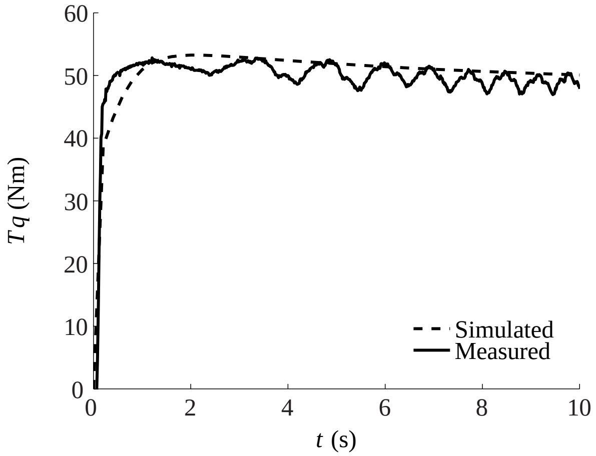

(a) Axial force = 10 kN.

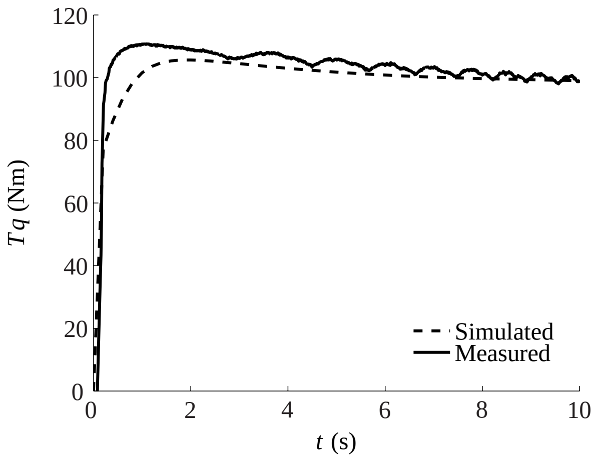

(b) Axial force = 20 kN.

Figure E.7: Comparison between simulated and measured torque for two different axial forces

In the measured transfered torque there are obvious fluctuations with a maximum amplitude of about 3%. These fluctuations are responses to a fluctuation in axial load in the test rig of the same order of magnitude. This implies that the measured torque should be smoother than shown here if the test rig had had a better regulation of the axial load. However, the mean axial load is very close to that specified, hence the simulated torque may be compared to the measured torque in defiance of the measured fluctuations.

From the simulation it is possible to divide the total torque into boundary lubrication torque and hydrodynamic torque, which is shown in Fig. E.8 for an axial load of 10 kN. The hydrodynamic torque is at most 1.5 Nm at the

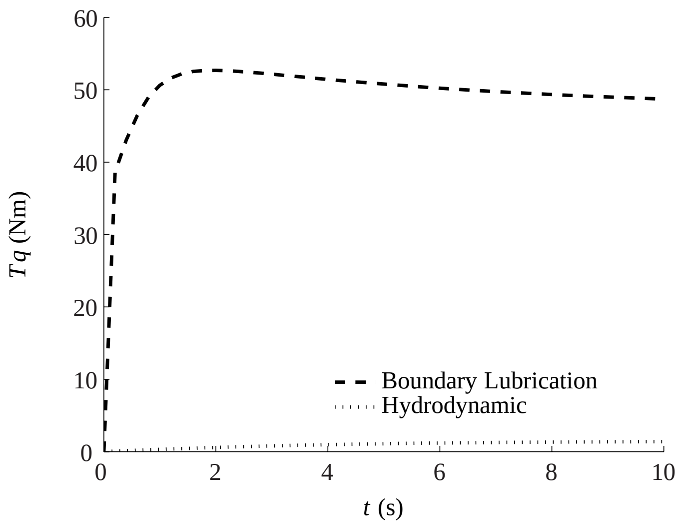

Figure E.8: Simulated torque for an axial load of 10 kN. Contribution from boundary lubrication and hydrodynamic lubrication.

highest rotational speed of 100 rpm. This is less than 3% of the total transferred torque of the clutch and for lower rotational speeds the hydrodynamic torqe is even less significant. The hydrodynamic torque is also less significant for simulations with higher axial loads. For lower temperatures of the lubricant, and thus higher viscosity, the hydrodynamic torque can, however, be a larger part of the total transferred torque.

E.4 Conclusions

Good agreement between simulations and measurements is achieved, both regarding temperature and transferred torque.

The model is shown to predict torque and temperatures for wet clutches working under limited slip conditions and can be a good tool to use when designing new limited slip wet clutch systems.

The hydrodynamic torque is shown to be less than 3% of the total transferred torque at the highest investigated rotational speed and the smallest investigated axial load. This implies that a good approximation of the total transfered torque can be achieved for the investigated running conditions even if the hydrodynamic torque transfer is neglected in the computations. A temperature dependent friction coefficient is, however, necessary to include in the model.

E.5 Acknowledgments

The authors would like to thank their colleagues at Haldex Traction Systems, Statoil Lubricants and Luleå University of Technology for their contributions to this work. The measurements from the wet clutch test rig used for validation of the simulation model were made by Kim Berglund and his help is very much appreciated. Thanks are also due to the Program Board for Automotive Research (PFF) and the Swedish Foundation for Strategic Research (ProViking) for financial support.

Bibliography

[1] P. H. Jost. Lubrication (tribology) - a report on the present position and industy's needs. *England, Department of Education and Science, H. M. Stationery Office*, 1966.

[2] G.W. Stachowiak and Bachelor A.W. *Engineering tribology*. Butterworth-Heinemann, Boston, 2001.

[3] R. Stribeck. Die wesentlichen eigenschaften der gleit- und rollenlager. *Zeitschrift des vereines deutcher ingenieure*, 46:1341–1349, 1902.

[4] O. Reynolds. On the theory of lubrication and its application to mr. beauchamp tower's experiments including on experimental determination of the viscosity of olive oil. *Trans. Royal Society of London*, 177:157–235, 1886.

[5] C. L. M. H. Navier. Memoire sur les du mouvement des fluides. *Mem. Acad. Sci. Inst. France*, 6:389–416, 1823.

[6] G. G. Stokes. On the theories of the internal friction of fluids in motion, and of the equilibrium and motion of elastic solids. *Trans. Cambridge Philosophical Society*, 8:287–341, 1845.

[7] *Oxford English Dictionary*, volume E. Oxford University Press, 2006.

[8] Y. Kato and T. Shibayama. Mechanisms of automatic transmissions and their requirements for wet clutches and brakes. *Japanese Journal of Tribology*, 39(12):1427–1437, 1994.

[9] B. Ganemi, R. Olsson, and B. Lundström. Durability and friction characteristics of a novel high performance four wheel drive automotive transmission fluid. *SAE Technical Papers*, (2000-01-2907), 2000.

[10] R. Mäki, B. Ganemi, R. Olsson, and B. Lundström. Limited slip wet clutch transmission fluid for AWD differentials; part 1: System requirements and evaluation methods. *SAE Technical Papers*, (SAE 2003-01-1980, JSAE 20030119), 2003.

[11] R. Mäki, B. Ganemi, and R. Olsson. Wet clutch transmission fluids for AWD differentials: base fluid influence on friction characteristics. *Tribotest*, 12:47–56, 2006.

[12] S. Shirahama. Adsorption of additives on wet friction pairs and their frictional characteristics. *Japanese Journal of Tribology*, 39(12):1479–1486, 1994.

[13] T. Ichihashi. Recent development in lubricating oils for wet clutches and wet brakes. *Japanese Journal of Tribology*, 39(12):1461–1470, 1994.

[14] S.Q.A. Rizvi. History of automotive lubrication. *SAE Technical Papers*, (961949), 1996.

[15] Y. Arakawa, R. Yauchibara, and Y. Murakami. Development of a multi-purpose ATF meeting DEXRON III, MERCON and JASO M315 specifications. *SAE Technical Papers*, (2003-01-1984), 2003.

[16] R. Mäki. *Wet clutch tribology- friction characteristics in limited slip differentials*. PhD thesis, Luleå University of Technology, Sweden, 2005.

[17] S. Kitahara and T. Matsumoto. Present and future trends in wet friction materials. *Japanese Journal of Tribology*, 39(12):1451–1459, 1994.

[18] S. Ohkawa, T. Kuse, N. Kawasaki, A. Shibata, and M. Yamashita. Elasticity- an important factor of wet friction materials. *SAE Technical Papers*, (911775), 1991.

[19] E. J. Berger, F. Sadeghi, and C. M. Krousgrill. Finite element modeling of engagement of rough and grooved wet clutches. *Journal of Tribology*, 118:137 – 146, 1996.

[20] E. J. Berger, F. Sadeghi, and C. M. Krousgrill. Torque transmission characteristics of automatic transmission wet clutches: Experimental results and numerical comparison. *Tribology Transactions*, 40(4):539 – 548, 1997.

[21] J. Y. Jang and M. M. Khonsari. Thermal characteristics of a wet clutch. *Journal of Tribology, Transactions of the ASME*, 121(3):610 – 617, 1999.

[22] S. Natsumeda and T. Miyoshi. Numerical simulation of engagement of paper based wet clutch facing. *Journal of Tribology, Transactions of the ASME*, 116(2):232 – 237, 1994.

[23] H. Gao and G.C. Barber. Engagement of a rough, lubricated and grooved disk clutch with a porous deformable paper-based friction material. *Tribology Transactions*, 45(4):464 – 470, 2002.

[24] H. Gao, G.C. Barber, and M. Shillor. Numerical simulation of engagement of a wet clutch with skewed surface roughness. *Journal of Tribology*, 124(2):305 – 312, 2002.

[25] H. Zhao, A. Neville, A. Morina, J. Durham, and R. Vickerman. A new method to evaluate the overall anti-shudder property of automatic transmission fluids - multiple parameters spider chart evaluation. *Proceedings of the Institution of Mechanical Engineers, Part J: Journal of Engineering Tribology*, 222(3):459 – 469, 2008.

[26] R. Mäki, P. Nyman, B. Ganemi, and R. Olsson. Measurement and characterization of anti-shudder properties in wet clutch applications. *SAE Technical Papers*, (2005-01-0878), 2005.

[27] H. Kitabayashi, C.Y. Li, and H. Hiraki. Analysis of the various factors affecting drag torque in multiple-plate wet clutches. *SAE Technical Papers*, (2003-01-1973), 2003.

[28] C.R. Aphale, Jinhyun Cho, W.W. Schultz, S.L. Ceccio, T. Yoshioka, and H. Hiraki. Modeling and parametric study of torque in open clutch plates. *Transactions of the ASME. Journal of Tribology*, 128(2):422 – 430, 2006.

[29] Y. Yuan, E.A. Liu, J. Hill, and Q. Zou. An improved hydrodynamic model for open wet transmission clutches. *Transactions of the ASME. Journal of Fluids Engineering*, 129(3):333 – 337, 2007.

[30] W. Ost, P. De Baets, and J. Degrieck. The tribological behaviour of paper friction plates for wet clutch application investigated on SAE 2 and pin-on-disk test rigs. *Wear*, 249:361–371, 2001.

[31] E. J. Berger, F. Sadeghi, and C. M. Krousgrill. Analytical and numerical modeling of engagement of rough, permeable, grooved wet clutches. *Journal of Tribology*, 119:143–148, 1997.

[32] J. Y. Jang and M. M. Khonsari. Thermal characteristics of a wet clutch. *Journal of Tribology, Transactions of the ASME*, 121:610–617, 1999.

[33] Y. Yang, R. C. Lam, and T. Fujii. Prediction of torque response during the engagement of wet friction clutch. *SAE Technical Papers*, (981097), 1998.

[34] P. Marklund and R. Larsson. Wet clutch under limited slip conditions - simplified testing and simulation. *Proceedings of the Institution of Mechanical Engineers, Part J: Journal of Engineering Tribology*, 221(5):545 – 551, 2007.

[35] T. S. Lundstrom, S. Toll, and J. M. Hakanson. Measurement of the permeability tensor of compressed fibre beds. *Transport in Porous Media*, 47(3):363 – 380, 2002.

[36] C. L. Davis, F. Sadeghi, and C.M. Krousgrill. A simplified approach to modeling thermal effects in wet clutch engagement: Analytical and experimental comparison. *Journal of Tribology*, 122:110–118, 2000.

[37] T. Almqvist, S.B. Glavatskikh, and R. Larsson. Thd analysis of tilting pad thrust bearings - comparison between theory and experiments. *Journal of Tribology, Transactions of the ASME*, 122(2):412 – 417, 2000.

[38] F. Sahlin. *Lubrication, contact mechanics and leakage between rough surfaces*. PhD thesis, Luleå University of Technology, Sweden, 2008.

[39] N. Patir and H. S. Cheng. Average flow model for determining effects of three-dimensional roughness on partial hydrodynamic lubrication. *Journal of Lubrication Technology*, 100(1):12–17, 1978.

[40] Y. Yang, R. C. Lam, and Y. F. Chen. Modeling of heat transfer and fluid hydrodynamics for a multidisc wet clutch. *SAE Technical Papers*, (950898), 1995.

[41] P. Zagrodzki. Numerical analysis of temperature fields and thermal stresses in the friction discs of a multidisc wet clutch. *Wear*, 101(3):255–271, 1985.

[42] S. Andersson, A. Söderberg, and S. Björklund. Friction models for sliding dry, boundary and mixed lubricated contacts. *Proceedings, NordTrib 2004, Norway*, 2004.

[43] H. Wu. An analysis of the engagement of wet-clutch plates. *Wear*, 24:23–33, 1973.

[44] P. Zagrodzki and S.A. Truncone. Generation of hot spots in a wet multi-disk clutch during short-term engagement. *Wear*, 254:474–491, 2003.

[45] P. Marklund, R. Mäki, J. Jang, M. M. Khonsari, R. Larsson, and E. Höglund. Thermal influence on torque transfer of wet clutches in limited slip differential applications. *Tribology International*, 40(5):876 – 884, 2007.

[46] J. Bear. *Dynamics of fluids in porous media*. Dover Publications Inc., 1972.

[47] S. H. Ahn, W. I. Lee, and G. S. Springer. Measurement of the three-dimensional permeability of fiber preforms using embedded fiber optic sensors. *Journal of Composite Materials*, 29(6):714 – 733, 1995.

[48] B. R. Gebart and P. Lidström. Measurement of in-plane permeability of anisotropic fiber reinforcements. *Polymer Composites*, 17(1):43 – 51, 1996.

[49] J. D. Lindsay. The anisotropic permeability of paper. *Tappi Journal*, pages 223 – 229, 1990.

[50] B. Chavdar. A permeameter measuring normal and lateral permeability and an investigation on wet friction materials. *International SAMPE Symposium and Exhibition (Proceedings)*, 47 I:253 – 266, 2002.

[51] G. S. Beavers and D. D. Joseph. Boundary conditions at a naturally permeable wall. *Journal of fluid mechanics*, 30:197 – 207, 1967.

[52] A. Cameron. *Basic lubrication theory*, volume 2. Chichester, 1976.

[53] P. Marklund, R.Larsson, and T.S. Lundström. Permeability of sinter bronze friction material for wet clutches. *Tribology Transactions*, 51, issue 3:303–309, 2008.

[54] P. R. K. Murti. Lubrication of finite porous journal bearings. *Wear*, 26(1):95 – 104, 1973.

[55] C. Cusano. Effect of variable permeability and rotation on the performance characteristics of porous bearings. *Wear*, 23(1):55 – 62, 1973.

[56] Y.X Quan and P.M Wang. Theoretical analysis and experimental investigation of a porous metal bearing. *Tribology International*.

[57] P. Marklund and R. Larsson. Wet clutch friction characteristics obtained from simplified pin on disc test. *Tribology International*, 41, issues 9-10, Nordtrib 2006:824–830, 2008.

[58] P. Marklund, K. Berglund, and R. Larsson. The influence on boundary friction of the permeability of sintered bronze. *Tribology Letters*, 31(1):1 – 8, 2008.

[59] R. Mäki, B. Ganemi, and R. Olsson. Wet clutch transmission fluid for awd differentials: Base fluid influence on friction characteristics. *TriboTest*, 12(1):47–56, 2006.

[60] F. Sahlin. *Lubrication, contact mechanics and leakage between rough surfaces*. PhD thesis, Luleå University of Technology, Sweden, 2008.

[61] H.J. Kim, P. Ehret, D. Dowson, and C.M. Taylor. Thermal elastohydrodynamic analysis of circular contacts: Part 1: Newtonian model. *Proceedings of the Institution of Mechanical Engineers, Part J: Journal of Engineering Tribology*, 215(4):339 – 352, 2001.

[62] P. Payvar. Laminar heat transfer in the oil groove of a wet clutch. *International Journal of Heat and Mass Transfer*, 34(7):1791–1798, 1991.

[63] P. Payvar, Y. N. Lee, and W. J. Minkowycz. Simulation of heat transfer to flow in radial grooves of friction pairs. *International Journal of Heat and Mass Transfer*, 37(2):313–319, 1994.

Index